1981

Mechanistic chemistry of some transition metal complexes

Garry Wayne Kirker
Iowa State University

KIRKER, GARRY WAYNE

MECHANISTIC CHEMISTRY OF SOME TRANSITION METAL COMPLEXES

Iowa State University PH.D. 1981

Mechanistic chemistry of some transition metal complexes

by

Garry Wayne Kirker

A Dissertation Submitted to the

Graduate Faculty in Partial Fulfillment of the

Requirements for the Degree of

DOCTOR OF PHILOSOPHY

Department: Chemistry
Major: Inorganic Chemistry

Approved:

Signature was redacted for privacy.

In Charge of Major Work

Signature was redacted for privacy.

For the Major Department

Signature was redacted for privacy.

For the Graduate College

Iowa State University
Ames, Iowa

1981

TABLE OF CONTENTS

LIST OF TABLES

LIST OF FIGURES

SYMBOLS AND CONVENTIONS

Certain symbols which appear throughout this thesis are defined as follows:

D	Absorbance
D_t	Absorbance at time t
D_∞	Absorbance at the end of a reaction
ε	Extinction coefficient (M^{-1} cm^{-1})
ℓ	Pathlength of an optical cell
M	Molarity (moles/liter)
[ ]	Concentration (M)
λ	Wavelength (nm)
nm	Nanometer
R	Gas constant (8.314 J mol^{-1} K^{-1})
T	Temperature
t	Time
s	Second
N	Avogadro's number (6.02×10^{23} molecules mol^{-1})
h	Planck's constant (6.62×10^{-34} J s)
σ^*	Taft polar substituent parameter

INTRODUCTION

This thesis has been divided into two parts as indicated by the title. The first part dealing with α-hydroxyalkylchromium(III) complexes is further subdivided into two subsections. The first subsection discusses the investigation of acidolysis and homolysis reactions. The second subsection deals with the reactions of Fe^{3+} and Cu^{2+} with these complexes. Part II was based on a study of some cobalt complexes of binucleating Schiff-base ligands which has already been published (1).

PART I. REACTIONS OF α-HYDROXYALKYLCHROMIUM(III) COMPLEXES

A. ACIDOLYSIS AND HOMOLYSIS

INTRODUCTION

General

Interest in metal carbon bonds has been especially keen since vitamin B_{12} was found by a crystal structure determination to contain a cobalt-carbon bond (2). Today, even more interest in metal-carbon bonds may be attributed to the study of homogeneous and heterogeneous catalysis (3,4). Although a thorough understanding of metal-carbon bond reactivity would seem to be essential to the creation of more efficient catalysts, few systematic studies are available (3). Indeed, the rapid growth in the field of homogeneous catalysis has already gone far beyond our mechanistic understanding of the molecular processes (4,5). It was with these points in mind that we sought a broader understanding of chromium-carbon bond reactivity and thus undertook the study of a homologous series of complexes.

The objective of this thesis was to investigate systematically the reactivity of the chromium-carbon bond in a homologous series of complexes of the type $(H_2O)_5CrC(R^1R^2)OR^{2+}$. The reactivity of these complexes was studied to obtain a quantitative estimate of the chromium-carbon bond strength as well as an understanding of the relative effect of substitution on chemical reactivity.

A better understanding of metal-carbon bond strengths would allow further insight into the question of reactivity of organometallic species. More a priori knowledge of metal-carbon bond strengths might also be useful in predicting stabilities of previously unknown

complexes. As already alluded to, this understanding could also be applied to catalysis research dealing with metal-alkyl species especially relating to homogeneous systems.

All of the complexes studied in this thesis have the general structure shown below. The chromium is formally considered to be in the

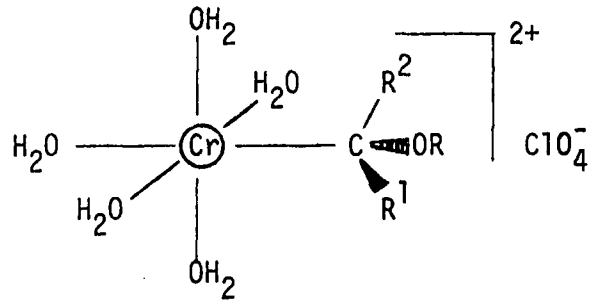

plus three oxidation state and the alkyl group is counted as a carbanion. Throughout the remainder of this thesis, the structural formulae of these complexes will be abbreviated as $CrC(R^1R^2)OR^{2+}$. The remaining five coordination sites around the chromium are occupied by water molecules and are usually not indicated henceforth.

Historical

The first reported synthesis of organochromium complexes of the form $(H_2O)_5CrR^{2+}$ was in 1957 by Anet and LeBlanc (6). They synthesized the complexes by addition of $Cr(ClO_4)_2$ to benzyl and substituted benzyl halides. The reaction was shown to obey the following stoichiometry. Several different routes to benzylchromium dications have subsequently been developed.

$$2Cr^{2+} + ClCH_2C_6H_5 \longrightarrow CrCl^{2+} + CrCH_2C_6H_5^{2+} \qquad (I\text{-}1)$$

A more general route to organochromium complexes was developed through the use of hydroperoxides.

Scheme I-1

$$R\text{-}OOH + Cr^{2+} \xrightarrow{H^+} R\text{-}O^{\cdot} + Cr(III) \qquad (I\text{-}2)$$

$$R\text{-}O^{\cdot} \longrightarrow R^{\cdot} + (CH_3)_2C{=}O \qquad (I\text{-}3)$$

$$R^{\cdot} + Cr^{2+} \longrightarrow CrR^{2+} \qquad (I\text{-}4)$$

This preparation was initially used for benzylpentaaquochromium^{2+} (7), and methylpentaaquochromium^{2+} (8-10). Leslie and Espenson have subsequently used this method to prepare a series of alkylchromium dications including: Cr-R^{2+} where R = ($-CH_3$, $-C_2H_5$, n-C_3H_7, i-C_3H_7, $(CH_3)_3CCH_2$-, sec-C_4H_9, t-C_4H_9) (11). A third method of forming pentaaquoorganochromium dications involves the radiolytic generation of organic radicals in the presence of $Cr(ClO_4)_2$. This method has been used to prepare a wide variety of organochromium species including: Cr-R^{2+} where R = ($-CH_2OH$, $-CH_2CHO$, $-CH(CH_3)OH$, $-CH(CH_3)OC_2H_5$, $-CH_2COOH$) (12,13). All of these preparative methods have one feature in common, i.e., the generation of an organic radical in the presence of an inorganic radical (Cr^{2+}).

We have used a different method which we will refer to as a modified Fenton's reagent (MFR) preparation. This method was first used by Schmidt, Swinehart and Taube for the generation of α-hydroxyalkylchromium^{2+} complexes (9). Their proposed mechanism was a follows, using the case of the formation of α-hydroxymethylchromium^{2+} for illustration:

Scheme I-2

$$Cr^{2+} + H_2O_2 \longrightarrow Cr^{3+} + \dot{O}H + H_2O \qquad (I\text{-}5)$$

$$\dot{O}H + CH_3OH \longrightarrow \dot{C}H_2OH + H_2O \qquad (I\text{-}6)$$

$$Cr^{2+} + \dot{C}H_2OH \longrightarrow CrCH_2OH^{2+} \qquad (I\text{-}7)$$

Under optimum conditions, these reactions yield the organochromium complex in a yield ∿80% of the theoretical, the latter being one-half of the initial quantity of Cr^{2+}, considering the 2:1 stoichiometry of Cr^{2+} to H_2O_2. This method allows a certain degree of flexibility by choice of RH and other reaction conditions and is the method of choice for preparing the α-hydroxyalkylchromium^{2+} ions for the kinetic analysis undertaken in this thesis. Their results and ours clearly show that under appropriate conditions of concentrations, the reaction of Cr^{2+} with the radical competes very favorably with the competing dimerization of the organic radical. These organochromium complexes have characteristic u.v.-visible absorption spectra which are similar to the absorption spectra of the simple alkylchromium^{2+} complexes (10). Cohen and Meyerstein have discussed the electronic spectra of these complexes (13).

Cohen and Meyerstein have also studied the rates of reaction for a number of radiolytically generated α-hydroxyalkyl radicals combining with Cr^{2+} (13). Their results show that the radicals combine with Cr^{2+}, equation I-7, with second order rate constants of 10^7-10^8 $M^{-1}s^{-1}$ depending on the particular radical. These values are significantly lower than diffusion controlled, but because of the large excess of

$[Cr^{2+}]$ over $[\dot{R}]$, the Cr^{2+} capture of the radical competes quite favorably with radical coupling reactions. Some of the reactions which the α-hydroxyalkylchromium^{2+} complexes undergo are typical of other organochromium complexes, namely acidolysis and homolysis reactions. Schmidt et al. (9) and Cohen and Meyerstein (13) have previously examined acidolysis of a number of these and related complexes. We studied both reactions with an interest in the effect of substitution on Cr-C bond reactivity as noted earlier. Other work with α-alkoxyalkylchromium(III) complexes has recently included: reactions with Hg^{2+}, VO^{2+}, Fe^{3+} and Cu^{2+} (14-16). The homolysis reaction of organochromium complexes has previously been discussed only for aralkylchromium(III) complexes (17-23) and this aspect of the work, therefore, was markedly different from what previous investigators had reported (9,13).

Nohr and Espenson studied the mechanism of oxidative cleavage for the reaction of benzylchromium^{2+} and substituted analogs (17). Remarkably, the rate of reaction of the benzylchromium^{2+} with a variety of oxidants (Fe^{3+}, Cu^{2+}, O_2, H_2O_2, $Co(NH_3)_5Br^{2+}$ and $Co(NH_3)_5Cl^{2+}$), was independent of both the nature and concentration of the oxidant. They proposed a scheme which involved the unimolecular homolytic cleavage of the chromium-carbon bond. The example shown below illustrates the reaction when Fe^{3+} is used as the oxidant.

Scheme I-3

$$PhCH_2Cr^{2+} \longrightarrow Ph\dot{C}H_2 + Cr^{2+} \qquad (I\text{-}8)$$

Scheme I-3 (Continued)

$$Cr^{2+} + Fe^{3+} \longrightarrow Cr^{3+} + Fe^{2+} \qquad (I\text{-}9)$$

$$H_2O + PhCH_2^{\cdot} + Fe^{3+} \longrightarrow PhCH_2OH + H^+ + Fe^{2+} \qquad (I\text{-}10)$$

Product analyses showed that the inert Cr^{3+} products formed were the same as those obtained from reactions of Cr^{2+} with the given oxidant used. The organic products also depended upon the given oxidant, with Fe^{3+} and Cu^{2+} forming $PhCH_2OH$ (24), but bibenzyl was formed when $Co(NH_3)_5Cl^{2+}$ was used as the oxidant. These results pointed to the S_H1 unimolecular homolysis mechanism depicted in Scheme I-3.

The first step depicted in Scheme I-3 is, in fact, the microscopic reverse of the formation reaction between a benzyl radical and Cr^{2+}. It is not surprising, therefore, that homolytic cleavage should be an important pathway for reaction of benzyl-like organochromium complexes. Indeed, the homolysis pathway was also observed by Marty and Espenson (18) for dichromium complexes such as $(CrCH_2C_6H_4)_2O^{4+}$ and Pohl and Espenson (19) for a variety of difunctional aralkylchromium(III)$^{4+}$ species including $[CrCH_2C_6H_4CH_2Cr]^{4+}$ and $[CrCH_2C_6H_4(CH_2)_nC_6H_4CH_2Cr]^{4+}$, further substantiating the homolytic pathway. The homolysis reaction in the latter system was also supported by both kinetic data and product analyses (18,19).

As previously stated, a common feature of the preparative routes to organochromium(III) complexes CrR^{2+} has involved the coupling of two radicals, Cr^{2+} and R•, in the formation step, Equation I-4. As

stated, Schmidt et al. utilized this knowledge by generating $\cdot C(R^1R^2)OH$ radicals in the presence of Cr^{2+} using a modified Fenton's (25) reagent consisting of Cr^{2+} and H_2O_2 (9). It had previously been known that Cr^{2+} as well as Fe^{2+}, Ti(III) (26,27) and V(II) would react with H_2O_2 to generate $\dot{O}H$ (12). In some cases, ESR evidence showed that with a suitable organic substrate in solution, an organic radical would be generated by hydrogen abstraction as in equation I-11.

$$\cdot OH + H\text{-}C(R^1R^2)OR \longrightarrow H_2O + \cdot C(R^1R^2)OR \qquad (I\text{-}11)$$

Other $M\text{-}C(R^1R^2)OH^{n+}$ species have previously either been proposed as reactive intermediates or very unstable complexes in solution (28-32). Although the α-hydroxyalkyl radicals are very strong one electron reducing agents (12, 33-37), typically the reaction which forms the organometallic species, at least formally, must be considered a one electron oxidation of the metal (38). Thus, Ni(I) reacted with $\cdot CH_2OH$ forms $Ni^{II}\text{-}CH_2OH$. Also, Cr^{2+} is considered to be oxidized to the Cr(III) oxidation state upon reaction with $\cdot C(R^1R^2)OH$ as in equation I-12.

$$Cr^{II} + \cdot C(R^1R^2)OH \longrightarrow Cr^{III}\text{-}C(R^1R^2)OH \qquad (I\text{-}12)$$

Of all the presently known α-hydroxyalkyl complexes, those of Cr(III) are the most kinetically stable. This may in part be ascribed to the substitution inertness of Cr(III) complexes (39). Although substitutional inertness (or lability) is certainly important, it cannot be the only factor stabilizing these organometallic complexes.

Indeed, the comparatively substitutionally inert organocobalt(III)-(macrocycle)[1] analogs have been studied and were found to be quite unstable (40,41). Some decomposed by an internal redox reaction between the organic group and Co(III) resulting in heterolytic cleavage of the Co-C bond, Equation I-13 (40). This pathway towards decomposition is much less favorable for the organochromium complexes because the Cr(I) oxidation state would be expected to be much less accessible than the Co^{I}(macrocycle) oxidation state. Thus, the α-hydroxyalkylchromium(III)

$$L_5CoCH_2OH \longrightarrow L_5Co^{I-} + HCHO + H^{+} \qquad (I\text{-}13)$$

complexes provide a rather rare example in which the organocobalt (macrocycle) analogs are actually less stable, as the reverse has invariably been found for alkyls and other organometallic compounds.

Recently, interest in α-hydroxyalkyl-metal complexes has been attributed to the possible role of these species as intermediates in the reductive polymerization of carbon monoxide commonly referred to as the Fischer-Tropsch reaction (42-44). Only a few examples of these species appear in the literature (45-47). Very recently, the reaction of some α-hydroxyalkylchromium(III) complexes, including $Cr\text{-}R^{2+}$ where R = ($-CH_2OH$, $-CH(CH_3)OH$, $-C(CH_3)_2OH$, $-CH(CH_3)OC_2H_5$, $-CH(CF_3)OH$), with Fe^{3+} and Cu^{2+} was reported (46). The more highly substituted analogs of α-hydroxyalkylchromium(III) complexes studied here, including $Cr\text{-}R^{2+}$

---

[1](Macrocycle) = Me_6[14]diene N_4; the complex $RCo(N_4mac)$ is abbreviated as L_5CoR.

where R = ($-C(CH_3)(C_2H_5)OH$, $-C(C_2H_5)_2OH$, $-C(CH_3)(i\text{-}C_3H_7)OH$, $-C(CH_3)_2OCH(CH_3)_2$), allowed further insight into the mechanisms of these reactions.

EXPERIMENTAL

Materials

Reagents

Organochromium complexes The complexes $CrCH_2OH^{2+}$, $CrCH_2OCH_3^{2+}$ and $CrCH(CH_3)OC_2H_5^{2+}$ can be isolated pure by ion-exchange chromatography because they are the most stable complexes of the series. It was found that the more highly substituted analogs, which were the main focus of this study, are much less stable toward decomposition, even at reduced temperatures and could not be chromatographically isolated in pure form. It should be noted, however, that previous workers had already encountered this problem and studied reactions of their complexes in the unseparated reaction solution (9). It has also been shown that the rates of reaction of $CrCH_2OH^{2+}$ toward acidolysis, Cu^{2+} or Fe^{3+} (9,48) are identical whether the complex is purified by ion-exchange chromatography or not.

The reaction forming the basis of the preparative procedure used for all of the complexes is the MFR method shown in Equations I-14 to I-16. All of the complexes were prepared in 1 M alcohol or ether,

$$Cr^{2+} + H_2O_2 \xrightarrow{H^+} Cr^{3+} + H_2O + \dot{O}H \qquad \text{(I-14)}$$

$$\dot{O}H + HC(R^1R^2)OR \longrightarrow \cdot C(R^1R^2)OR + H_2O \qquad \text{(I-15)}$$

$$Cr^{2+} + \cdot C(R^1R^2)OR \longrightarrow CrC(R^1R^2)OR \qquad \text{(I-16)}$$

aqueous perchloric acid solutions except in cases in which the alcohol or ether are not soluble to the 1 M level. In those cases, the alcohol

or ether was typically 0.01 to 0.1 M and no differences were noted. Because the highly substituted analogs were quite unstable, they were used immediately after preparation or were prepared and studied in situ. The complexes were prepared by mixing excess Cr^{2+} (typically 1.5-5.0 mM) with H_2O_2 (0.5-1.0 mM) in presence of the desired co-solvent alcohol or ether at 1 M concentration or lower.

Cr(II) perchlorate solutions The chromium(II) perchlorate solutions were prepared by two methods and all results were found to be independent of the method chosen. In the first method, chromium pellets (Apache Chemicals Inc.; 99.999%) were dissolved in $HClO_4$ (49). In a typical preparation, chromium metal (~1 g) was dissolved in $HClO_4$ (40 mL, 1 M). The chromium metal was activated with HCl (4 M) just prior to dissolution in the N_2 purged $HClO_4$. Dissolution of the pellets required one or two days after which the solution was transferred off any remaining metal and stored under oxygen-free conditions.

Solutions of chromium(II) perchlorate were also prepared by electrochemical reduction of $Cr(ClO_4)_3 \cdot nH_2O$. Crystals of the $Cr(ClO_4)_3$-hydrate were prepared by a reduction of chromium trioxide by hydrogen peroxide. Pure $Cr(ClO_4)_3 \cdot nH_2O$ was dissolved in $HClO_4$ (0.2-0.3 M) to an approximate concentration of 0.25 to 0.3 M. These deep blue solutions were reduced over a mercury pool cathode at 8-9 volts for one to two hours under a constant stream of N_2. The Cr^{2+} solutions obtained were typically 97-98% Cr^{2+}.

Other inorganic reagents The perchlorate salts of halopentaamminecobalt(III) complexes were prepared by dissolution of $[Co(NH_3)_5Br]Br_2$ (50) or $[Co(NH_3)_5Cl]Cl_2$ (51,52) in $HClO_4$ (1.5, 0.2 M) at 35°C. After the solution was filtered to remove any undissolved material, concentrated $HClO_4$ (~300 mL) was added and the solution was gradually cooled. Precipitates were recrystallized twice from dilute $HClO_4$ and finally washed several times with cold 95% ethanol and ether. The u.v.-visible spectra matched values reported in the literature (53).

Lithium perchlorate was prepared by neutralization of Li_2CO_3 (Baker, reagent) with $HClO_4$ and was typically recrystallized three times. Other inorganic reagents were used as received.

Organic reagents Most of the organic reagents used in this study were simple aliphatic alcohols; in one case, a dialkyl ether was also used. The organic reagents used are summarized in Table I-1. All of the alcohols were commercially available and the cases of n-propanol, 2-propanol and 3-pentanol were used as received. In the remaining cases, the alcohols were fractionally distilled at atmospheric pressure with only a middle cut from the distillation being used for experimental purposes. For isopropyl ether, there has been sufficient documentation of its propensity to form peroxides (54) that it was pretreated with several washings with Cr^{2+} solutions prior to being distilled. To reduce the chance of a peroxide explosion, the distilling pot was never allowed to approach dryness.

Table I-1. Purification of organic reagents

Alcohol/Ether	Source	b.p. (Lit.)	b.p. (°C)	Checked by
n-Propanol	Mallinckrodt	97.4	---	---[a]
2-Propanol	Fischer Scientific	82.4	---	---[a]
2-Butanol	Eastman Chemicals	99.5	98-99[b]	^{1}H nmr[c]
3-Methyl-2-butanol	Aldrich (98%)	112.9	112[b]	---
3,3-Dimethyl-2-butanol	Aldrich (99%)	120.4	119[b]	^{1}H nmr[c]
3-Pentanol	Aldrich (99+%)	116.1	---	---[a]
Isopropyl ether	Aldrich (99%)	68.0	68-68.5[d]	g.c./^{1}H nmr[c]

[a]Used as received.

[b]Doubly distilled with only middle fraction used.

[c]Ref. 55.

[d]Double distilled from Cr^{2+} and used immediately; stored under N_2.

Methods

Analyses

Reagents The concentration of Cr^{2+} solutions was calculated from the absorbance of a solution at 713 nm (ϵ = 4.9 M^{-1} cm^{-1}). The total amount of chromium present in a solution was determined by Haupt's method (56). This method involved oxidizing all chromium species present to chromium(VI) in alkaline solution. After oxidation was complete, the absorbance at 372 nm (ϵ = 4830 M^{-1} cm^{-1}) was determined and the concentration was calculated. The concentration of $HClO_4$ in $Cr(ClO_4)_2$ solutions was determined by a difference method. Aliquots of $Cr(ClO_4)_2$ solutions were placed on Dowex 50W X-8 cation exchange resin in the H^+ form and eluted with water. The acidic eluent collected was titrated with standardized NaOH to a pink phenolphthalein endpoint. Using the known $[Cr^{2+}]$ and the total $[H^+]$ from the titration, the $[H^+]$ in the $Cr(ClO_4)_2$ solution was calculated. The concentration of Li^+ was determined by titrating the H^+ released after aliquots were passed through a column of Dowex 50W X-8 cation exchange resin in the H^+ form.

Hydrogen peroxide solutions were analyzed using the iodometric method of Kolthoff and Sandell (57). In a typical analysis, an aliquot of H_2O_2 (2 mL) was pipetted into a 50 mL erlenmeyer flask, KI ($\sim$0.2 g) was added and three drops of a neutral ammonium molybdate catalyst was added after the solution was acidified with H_2SO_4 (2 mL; 4 M). The solution was titrated to a sharp endpoint with sodium thiosulfate using starch indicator.

Reaction products The organic products of some reactions were determined by g.l.c. analyses. The analytical services department of the Ames Laboratory performed all of the g.l.c. analyses.

In some cases, preseparation and concentration of the samples to be analyzed by extraction into CH_2Cl_2 was necessary. In one case, the organic product(s) from the homolysis reaction of $CrC(CH_3)(C_2H_5)OH^{2+}$ were separated in the following manner: the $CrC(CH_3)(C_2H_5)OH^{2+}$ was prepared by reacting Cr^{2+} (2.5 mM); $HClO_4$ (0.10 M); 2-butanol (50 mM); H_2O_2 (1 mM) in a 100 mL total volume. The initial concentration of $CrC(CH_3)(C_2H_5)OH^{2+}$ was estimated from the absorbance of a cold solution at 400 nm to be ~0.5 mM. After addition of $Co(NH_3)_5Cl^{2+}$ (3.5 mM), the cold solutions (~4°C) were extracted with CH_2Cl_2 (seven 10 mL washings), the CH_2Cl_2 extracts were washed twice with $HClO_4$ (0.1 M; 5 mL), and the volume of CH_2Cl_2 reduced to 10 mL.

The only organic product of $CrC(CH_3)(C_2H_5)OH^{2+}$ homolysis was found to be 2-butanone and it was formed quantitatively. A blank experiment in which the $Co(NH_3)Cl^{2+}$ was added prior to the H_2O_2 so that the Cr^{2+} was converted to $CrCl^{2+}$ indicated no 2-butanone was formed.

Kinetics

The decomposition of the α-hydroxyalkylchromium(III) complexes was followed spectrophotometrically at a convenient wavelength, usually the absorption maximum for these complexes near 400 nm. The experiments were carried out under an atmosphere of Cr^{2+}-scrubbed nitrogen using standard syringe/septa techniques. A constant

temperature was maintained by a circulating water bath and a jacketed cell-holder for experiments of conventional time scales.

Conventional time scale experiments were performed on a Cary 219 spectrophotometer. Most kinetic measurements were made by introducing solutions containing H_2O_2, alcohol (or ether), perchloric acid and lithium perchlorate in 2 cm cylindrical quartz cells. After thermostating the cell, Cr^{2+} was injected, producing the alkylchromium; its formation was readily apparent visually from the yellow color. For acidolysis experiments, this one injection was all that was needed since acid was already present. Therefore, after injection of the Cr^{2+} and shaking the cell to mix the solution, the absorbance was recorded as a function of time at a constant wavelength. Typically for acidolysis experiments, in which an excess of Cr^{2+} over $CrROR^{2+}$ was desired, the Cr^{2+} was 1-3 mM, at least three times the $[CrROR^{2+}]$.

A few homolysis experiments were performed on the Cary 219, especially the low temperature experiments with $CrC(CH_3)(C_2H_5)OH^{2+}$. The method used for these experiments was identical to the method just described for acidolysis experiments, except that once the organochromium was produced, an additional injection of halopentaammine-cobalt(III) was made. In order to study faster reactions ($t_{1/2} \lesssim 7$ sec), the stopped-flow technique was used. A Durrum-Gibson D-110 stopped-flow instrument with a D-132 multi-mixing accessory was used. The multi-mixing apparatus was necessitated by several experimental considerations. The major consideration was the very fast acidolysis rates of the more highly substituted α-hydroxyalkylchromium(III)

complexes. This intrinsic acidolysis decomposition tended to decompose the organochromium(III) complexes so fast that they could not be thermostated for the kinetic measurements of other fast reactions they undergo. The multi-mixing apparatus circumvented these difficulties since it first mixes two solutions, and then rapidly mixes that with a third. It thus allowed the formation of the organochromium(III) complexes *in situ* for reaction with other reagents. More details of the D-132 multi-mixing operation are presented in the Instrumentation section.

All of the reactions were performed under conditions which gave pseudo-first-order plots of $\ln(D_t-D_\infty)$ *versus* time which were linear for greater than three half-lives. For most stopped-flow experiments, the data were automatically transferred to a PDP-15 computer for immediate calculation of rate constants using a least-squares analysis. Graphical analysis was also used as a check in some cases.

Activation parameters

Activation parameters were obtained for both acidolysis and homolysis reactions of some of the complexes. Values of $\Delta H^{\ddagger}$ and $\Delta S^{\ddagger}$ were evaluated by collecting kinetic data at various temperatures and using the Eyring relation shown in Equation I-17. In all cases

$$k = \frac{RT}{Nh} e^{(\Delta S^{\ddagger}/R)} e^{(-\Delta H^{\ddagger}/RT)} \qquad \text{(I-17)}$$

where activation parameters were determined, a least-squares analysis of the data was utilized. In a few cases, the overall temperature

range studied was rather narrow and the values obtained from these results are probably less accurate than for wider temperature ranges (see Results section).

Instrumentation

For conventional kinetic studies, a Varian Instruments Cary 219 u.v.-visible spectrophotometer equipped with a thermostated cell holder was used. A modified Durrum-Gibson D-110 stopped-flow spectrophotometer equipped with a D-132 multi-mixing accessory (58) was used for all reactions which were too fast to be studied by conventional techniques. A schematic of this device is shown in Figure I-1. In principle and in practice, the D-132 allows the formation of unstable intermediates which, once formed, may then be reacted with other reagents. The D-132 accessory itself consists of standard hardware including a syringe block and cuvette which literally may be bolted onto the D-110 frame and an electronic control unit which controls a number of variables including: drive time (the time the pneumatic piston rams the drive syringes); age time (the delay between the first ramming for initial mixing and second ramming); purge time (the time period which the purge valve is open); collect time (the time period which the collect valve is open). All of these parameters must be adjusted in order to optimize the operation of the multi-mixing device. In fact, there are other parameters which also determine the flow rate of solution through the solvent pathways. These include the pressure which is driving the pneumatic piston and the viscosity of the solvent

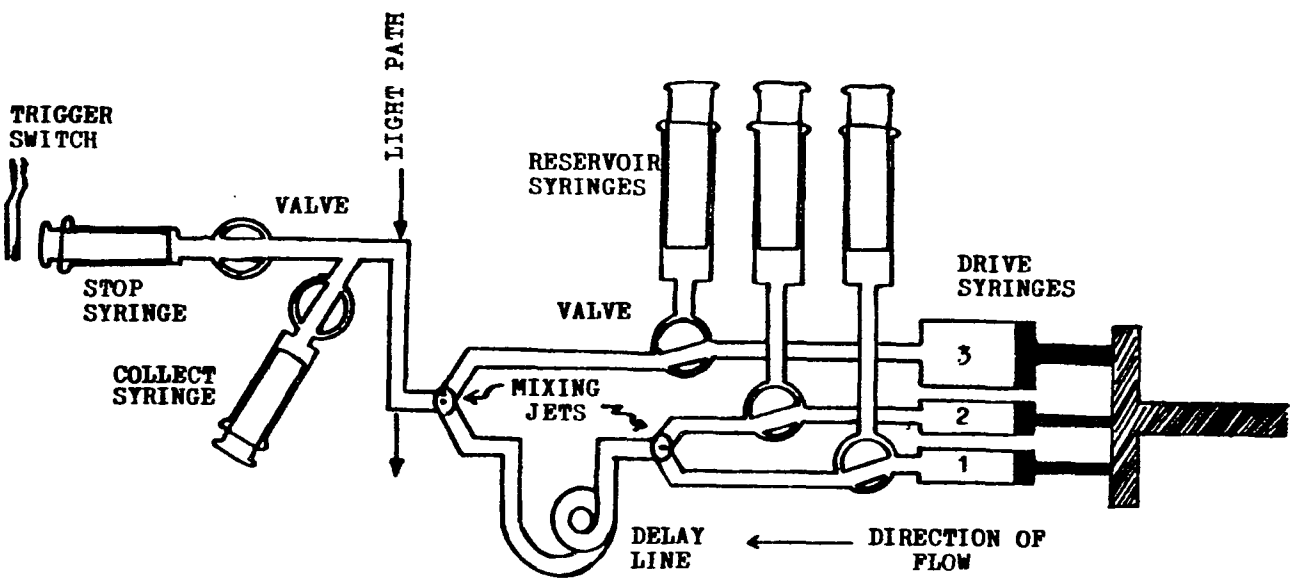

Figure I-1. Schematic diagram of the D-132 multi-mixing system

being used. Optimization of these conditions involved varying several parameters until satisfactory results were obtained.

Photochemical generation of $CrC(R^1R^2)OH^{2+}$

A photochemical method was also used to generate α-hydroxyalkylchromium(III) complexes. The photochemical experiments were carried out using fast-extinguishing Xenon-arc flash lamps in the Xenon Corporation Model 710 system. The experiments were performed in quartz cells using unfiltered u.v. radiation. Typically, 300 J energies were used. The experiments were usually performed by exposing a solution of Cr^{2+} ((1.9 to 15) x 10^{-3} M) and ketone (acetone or 2-butanone) 1-3 M, in dilute aqueous perchloric acid (1 x 10^{-4} to 1 M). In some cases, a complementary alcohol such as 2-propanol was also added (10^{-3} M to 1 M). Most experiments were carried out at 24±1°C. In a typical experiment, a pale blue solution of Cr^{2+}, 2 to 15 x 10^{-3} M, was added to a deaerated mixed ketone/aqueous $HClO_4$ solution. This solution was exposed up to five times with 300 J pulses of light to produce a substantial amount of α-hydroxyalkylchromium(III) (see Results section).

RESULTS

Characterization and Reactivity

Identification of organochromium complexes

The complexes which were the focus of this study were analogs of complexes which have been previously studied and characterized (9,13, 14,42). Some of the evidence for the formation of these complexes is based upon their u.v.-visible absorption spectra. In some cases, although the absorption spectrum was not measured, the intense absorption band around 400 nm, characteristic of the organochromium complexes, was qualitatively observed during kinetic determinations.

The u.v.-visible spectrum of $CrC(CH_3)(C_2H_5)OH^{2+}$ was recorded between 450 and 280 nm (Figure I-2) at ∿4°C to minimize the decomposition of the complex. The extinction coefficients were determined to be 500±100 M^{-1} cm^{-1} at 405±5 nm and ∿2000 M^{-1} cm^{-1} at ∿310 nm. These values must be regarded as lower limits because of some decomposition of the complex due to acidolysis even at ∿4°C. These values are quite similar to the known values for $CrC(CH_3)_2OH^{2+}$ (ε = 700 M^{-1} cm^{-1} at 407 nm; 2500 M^{-1} cm^{-1} at 311 nm) (13).

The reactivity of these complexes was also taken as another indication of their identity. Thus, all of these complexes were found to undergo reactions typical of other known α-hydroxyalkylchromium(III) complexes. These reactions included acidolysis, homolysis, and Fe^{3+} or Cu^{2+} reactions, which are treated in the next part. This pattern of

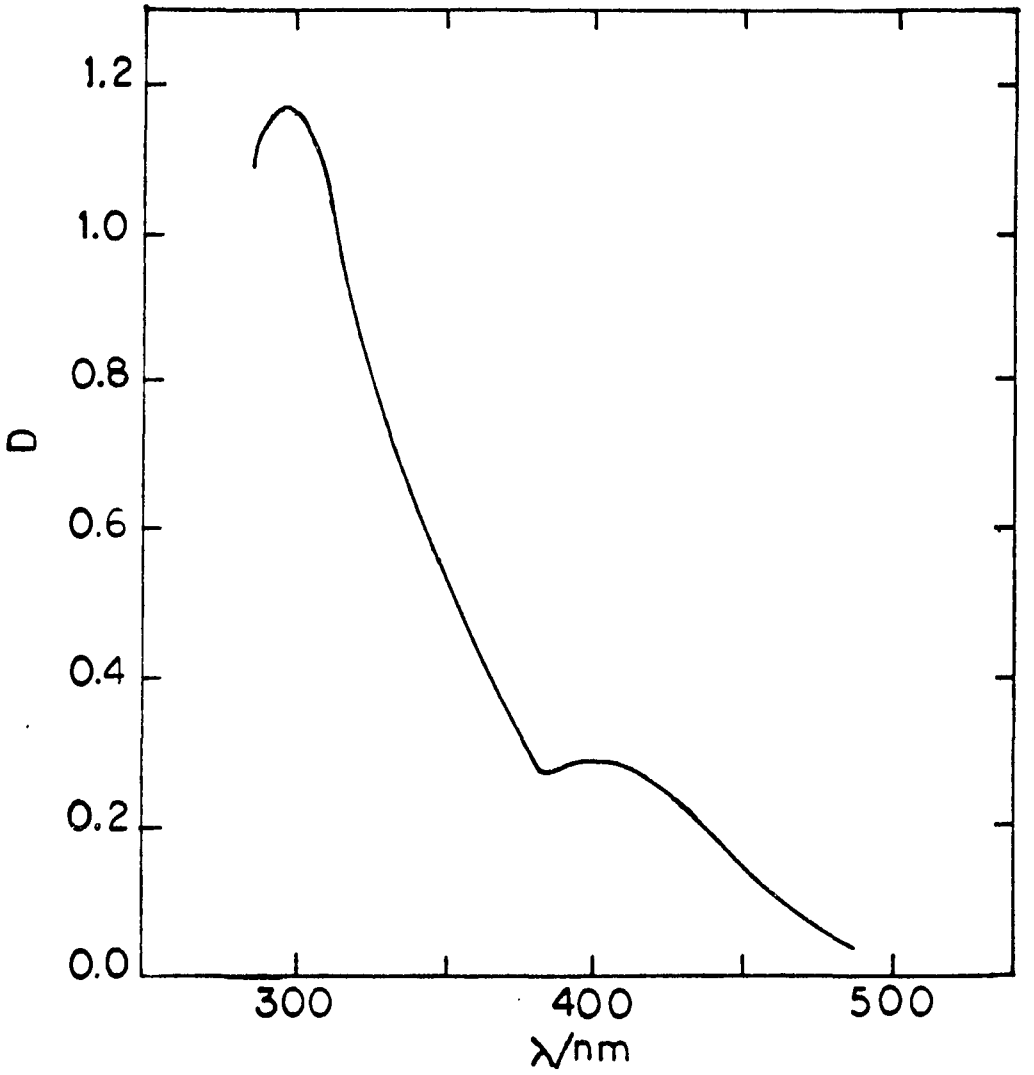

Figure I-2. Electronic spectrum of $(H_2O)_5CrC(CH_3)(C_2H_5)OH^{2+}$, ($\ell$ = 1 cm), $\sim x10^{-4}$ M

reactivity has been previously shown for other α-hydroxyalkylchromium(III) complexes (42,48). Finally, the products of various reactions were consistent with the schemes which are presented in this thesis. Thus, homolysis of α-hydroxy-2-butylchromium(III) produced 2-butanone quantitatively. The final absorption spectra after reaction also indicated that $Cr(H_2O)_6^{3+}$ was formed by acidolysis. Thus, the sum total of various observations and experiments indicated that the spectra and reactivity patterns of these complexes were those of α-hydroxyalkylchromium(III) species.

Reaction selection

The two reactions of α-hydroxyalkylchromium(III) complexes which were focused on in this study were acidolysis and homolysis reactions. By careful selection of reaction conditions, the reaction of interest could be studied. In order to focus on the acidolysis reaction, the homolysis reaction pathway was suppressed by having an excess of Cr^{2+} present in solution. The excess of Cr^{2+} prevented the loss of organochromium to radical coupling reactions because Cr^{2+} recombines with any carbon-centered radicals formed by homolysis. Radical coupling reactions would lead to the production of pinacols at the expense of organochromium complex as shown in Scheme I-4 (59).

Scheme I-4

$$CrC(R^1R^2)OR^{2+} \rightleftarrows Cr^{2+} + \cdot C(R^1R^2)OR \qquad (I\text{-}18)$$

$$2\ \cdot C(R^1R^2)OR \rightarrow RO(R^1R^2)C\text{-}C(R^1R^2)OR \qquad (I\text{-}19)$$

The steady-state concentration of $\cdot C(R^1R^2)OR$ may be estimated from Equation I-20. This equation may be simplified by assuming that

$$[\cdot C(R^1R^2)OR]_{ss} = \frac{k_{18}[CrC(R^1R^2)OR^{2+}]}{k_{-18}[Cr^{2+}] + 2k_{19}[\cdot C(R^1R^2)OR]} \qquad (I\text{-}20)$$

$k_{-18}[Cr^{2+}] > 2k_{19}[C(R^1R^2)OR]_{ss}$. Under typical acidolysis conditions, the $[\cdot C(R^1R^2)OR]_{ss}$ concentrations were estimated to be $\sim 10^{-7}$ M or lower. Once formed, the radicals would either couple with each other or with a Cr^{2+} species (59). With the $[Cr^{2+}]$ at least 1000 times greater than $[\cdot C(R^1,R^2)OR]_{ss}$, the competitive process favored recoupling with Cr^{2+} to reform the organochromium. Except for the two complexes with the fastest homolysis rates, the radical dimerization process was easily suppressed by a five-fold excess of Cr^{2+} over the $CrC(R^1R^2)OR^{2+}$ concentration. Based upon these calculations, some radical coupling may have contributed to the observed acidolysis rates for $CrC(CH_3)(i\text{-}C_3H_7)OH^{2+}$, although under most acidolysis conditions it was probably less than 10%. Radical coupling processes may have been very important in the decomposition of $CrC(CH_3)(t\text{-}C_4H_9)OH^{2+}$, but this complex was only briefly examined under acidolysis conditions and found to decompose with a k_{obs} of ~ 10 sec^{-1} at 25.0°C. Since this decomposition rate was much lower than the homolysis rates observed, it was not studied further. An estimate of the steady-state radical concentrations and the percent of reaction which may proceed with radical coupling is presented in Table I-2. A large concentration excess of Cr^{2+} over the steady-state concentration of radicals favored

Table I-2. Estimation of steady-state radical concentrations under some acidolysis conditions

Complex	k_{hom}/s^{-1}	$[R\cdot]_{ss}/M^a$	Maximum % Coupling[b]
$CrC(CH_3)(i\text{-}C_3H_7)OH^{2+}$	21.6	$\sim 3.5 \times 10^{-7}$	7.0
$CrC(C_2H_5)_2OH^{2+}$	8.4	1.6×10^{-7}	1.6
$CrC(CH_3)_2OCH(CH_2)_2^{2+}$	5.8	6.0×10^{-8}	0.4
$CrC(CH_3)(C_2H_5)OH^{2+}$	0.92	1.8×10^{-8}	0.07
$CrCH(C_2H_5)OH^{2+}$	1.0×10^{-3}	4.0×10^{-9}	0.01

[a]Calculated as $[R\cdot]_{ss} = k_{hom}[CrROH^{2+}]/(k_{18}[Cr^{2+}] + 2k_{19}[R\cdot])$ with $k_{-18} \sim 10^7\ M^{-1}\ s^{-1}$, as given in Table I-4; $k_{19} = 10^9\ M^{-1}\ s^{-1}$ by successive approximation; $[Cr^{2+}]_0 = 0.5$ mM; $[CrR^{2+}]_0 = 0.1$ mM; T = 25.0°C; μ = 1.0 M ($LiClO_4$).

[b]Calculated from $100(k_{19}[\cdot C(R^1,R^2)OR]_{ss}/(k_{-18}[Cr^{2+}] + k_{19}[\cdot C(R^1,R^2)OR]_{ss}))$; these values were calculated under "worst-case conditions."

the recombination of the radicals with Cr^{2+} and allowed the acidolysis rates to be determined without any interfering side reactions.

Another reaction which was of interest was the homolytic cleavage of the chromium-carbon bond. This reaction was studied by scavenging either Cr^{2+} or the radical, or both. This reaction will be subsequently referred to as simply the homolysis reaction. Because Cr^{2+} and the radicals are both very good one-electron reducing agents, oxidants were used as "trapping" or scavenging reagents. The scheme showing how the homolysis reaction was selected is presented in Scheme I-5. As indicated in the scheme, the acidolysis reaction of the

Scheme I-5

$$CrC(R^1,R^2)OR^{2+} \underset{k_f}{\overset{k_{hom}}{\rightleftharpoons}} Cr^{2+} + \cdot C(R^1,R^2)OR$$

$$\downarrow k_A \qquad \text{fast} \downarrow OX \qquad \text{fast} \downarrow OX$$

acidolysis products $\qquad Cr^{III}$ prod. $\qquad$ organic product(s) + 2 red

organochromium(III) species still occurred while the rate of the homolysis reaction was measured, but in general, it was a small percentage of the overall reaction. The observed rate constant under homolysis conditions was defined as:

$$k_{obs} = k_A + k_{hom} \qquad \text{(I-21)}$$

or $$k_{obs} = (k_1 + k_2[H^+]) + k_{hom} \qquad \text{(I-22)}$$

Under homolysis conditions, the rate limiting step becomes homolytic cleavage of the Cr-C bond because the subsequent reactions of Cr^{2+}

and the radicals with the various oxidants are very fast as shown by the following data taken from the literature:

Oxidant	$k_{Cr^{2+}}/M^{-1}\ s^{-1}$	Ref	$k_{\cdot C(CH_3)_2OH}/M^{-1}\ s^{-1}$	Ref
$Co(NH_3)_5Cl^{2+}$	2.4×10^6	60	4.0×10^7	61
$Co(NH_3)_5Br^{2+}$	6.0×10^6	62	3.0×10^8	61
H_2O_2	$(2.8\pm0.7) \times 10^4$	63		

Acidolysis reactions

The acidolysis reactions of the following α-alkoxyalkylchromium(III) complexes were studied: $CrCH(C_2H_5)OH^{2+}$, $CrC(CH_3)(C_2H_5)OH^{2+}$, $CrC(CH_3)(i\text{-}C_3H_7)OH^{2+}$, $CrC(C_2H_5)_2OH^{2+}$ and $CrC(CH_3)_2OCH(CH_3)_2^{2+}$. Plots of $\ln(D_t-D_\infty)$ versus time were linear for three or more half-lives (Figures I-3 and I-4). The acidolysis reactions were studied over a range of acid concentrations at a constant ionic strength of 1.00 M. Plots of the observed rate constants versus acid concentration are linear for each complex (Figures I-5 through I-8). The following rate law is thus obeyed by the acidolysis reactions:

$$-d\frac{[CrC(R^1R^2)OR]^{2+}}{dt} = (k_1 + k_2[H^+])[CrC(R^1R^2)OR]^{2+} \qquad (I\text{-}23)$$

The values of k_1 and k_2 determined from the intercept and slope of plots of k_A versus $[H^+]$ and are summarized in Table I-3 along with the literature values for analogous complexes. The last three entries in the table represent some α-alkoxyalkylchromium(III) complexes which

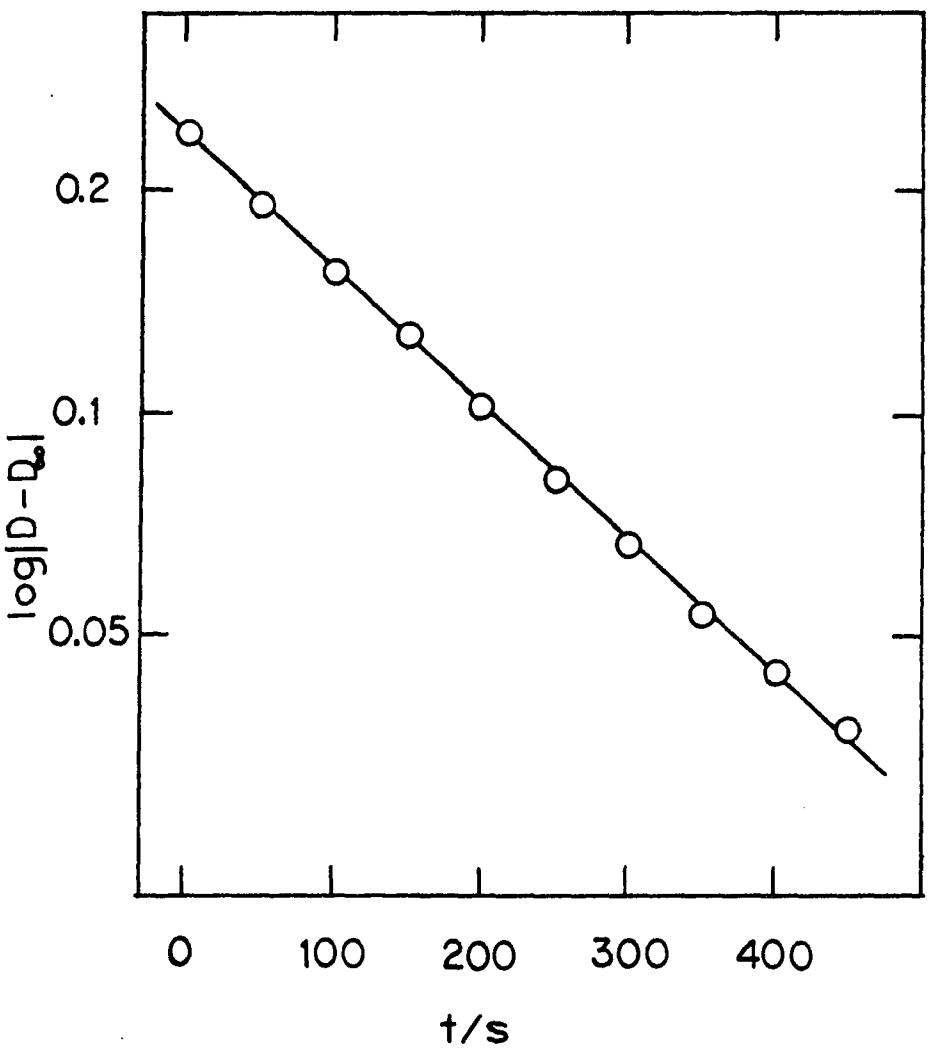

Figure I-3. Plot of log $|D-D_\infty|$ *versus* time for decomposition of $CrCH(C_2H_5)OH^{2+}$ under acidolysis conditions at 0.5 M $HClO_4$, 25°C, μ = 1.00 M ($LiClO_4$)

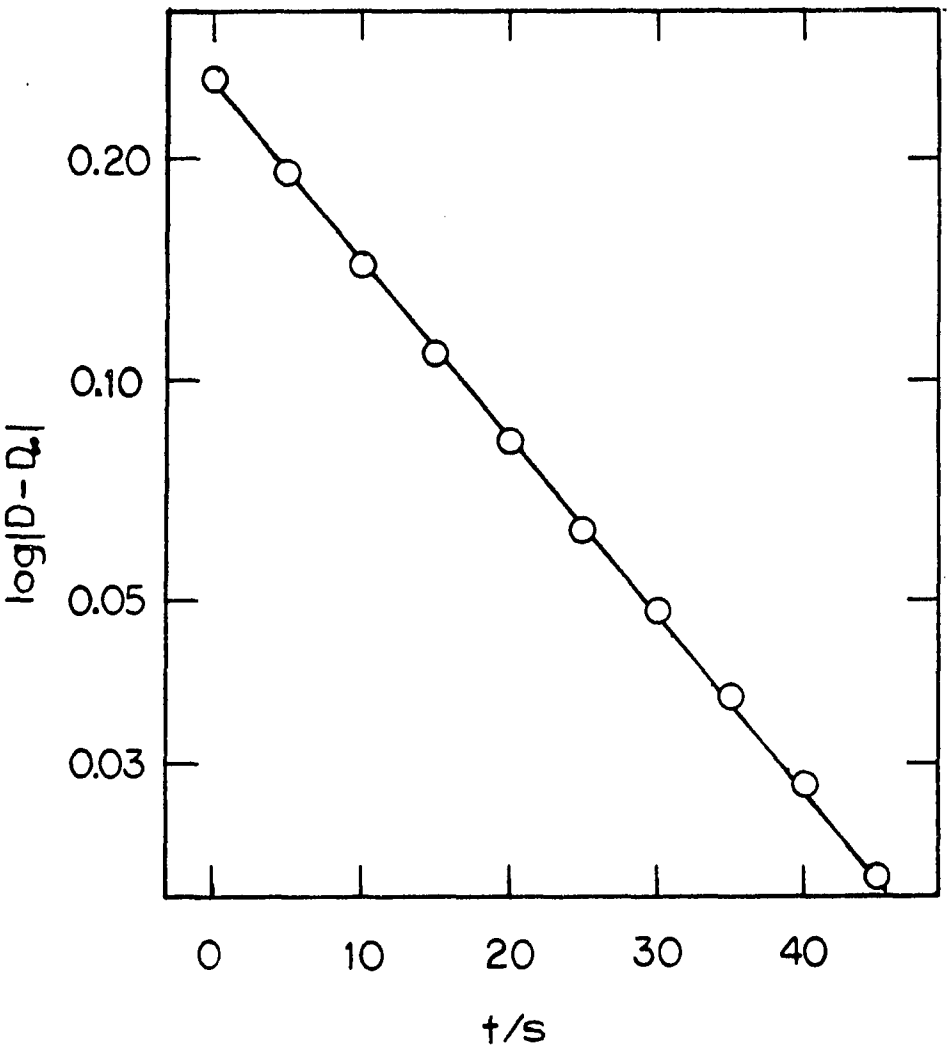

Figure I-4. Plot of log $|D-D_\infty|$ *versus* time for decomposition of $CrC(CH_3)(C_2H_5)OH^{2+}$ under acidolysis conditions at 0.098 M $HClO_4$, 25.0°C, μ = 1.00 M ($LiClO_4$)

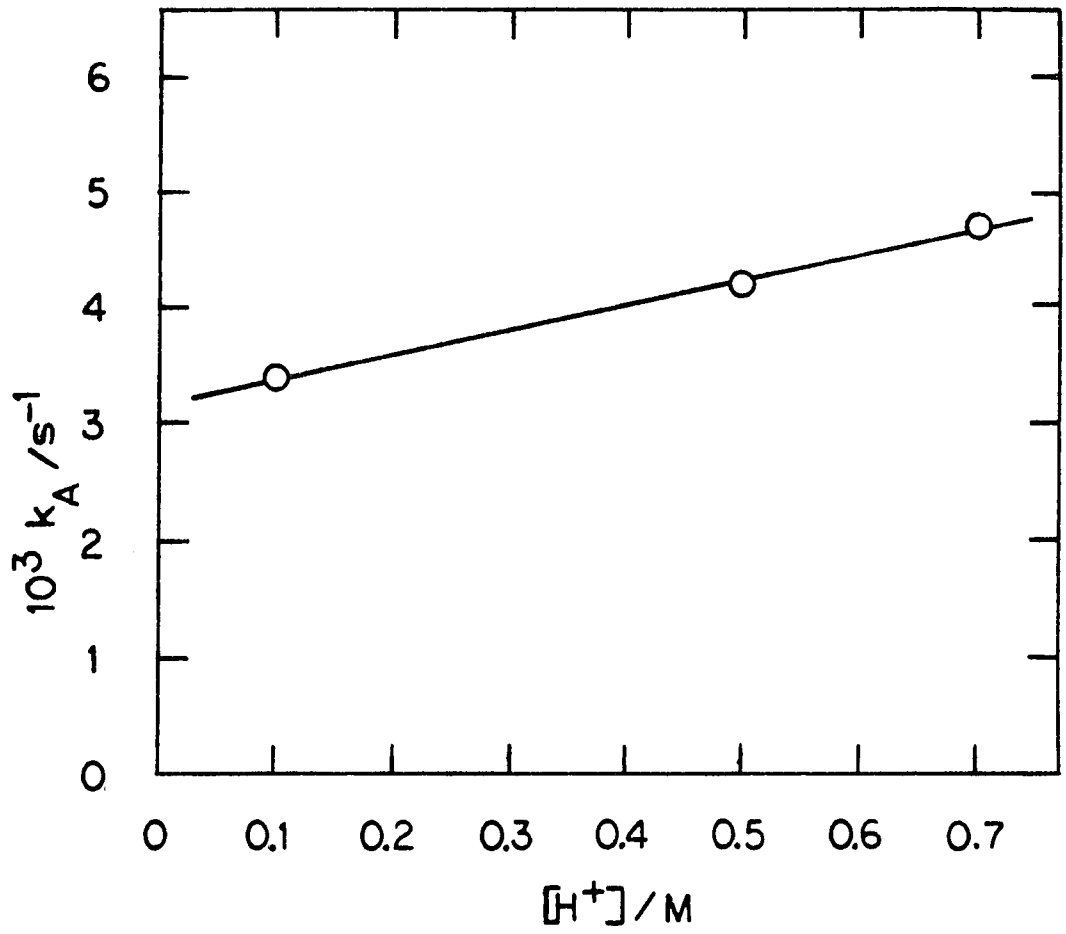

Figure I-5. Plot of k_A *versus* $[H^+]$ for acidolysis reactions of $CrCH(C_2H_5)OH^{2+}$ at 25°C, μ = 1.00 M ($LiClO_4$)

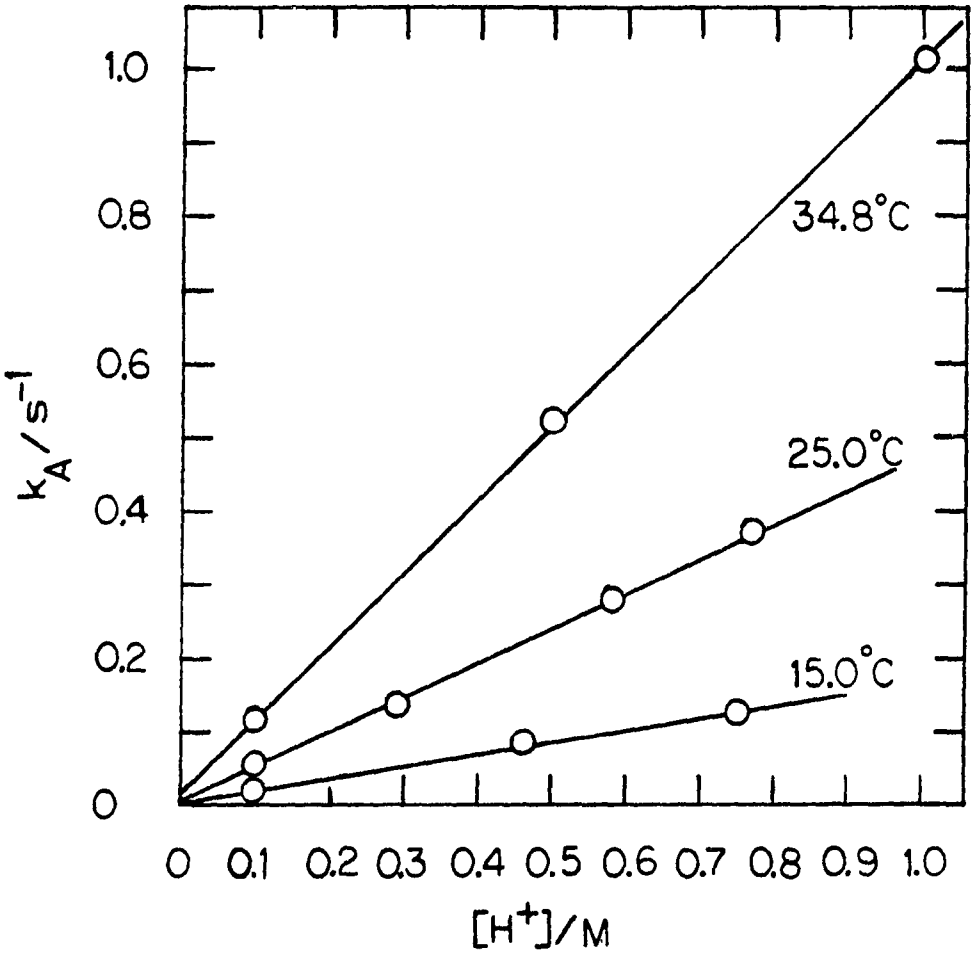

Figure I-6. Plot of k_A <u>versus</u> $[H^+]$ for acidolysis reactions of $CrC(CH_3)(C_2H_5)OH^{2+}$ at 15.0, 25.0 and 34.8°C, μ = 1.00 M ($LiClO_4$)

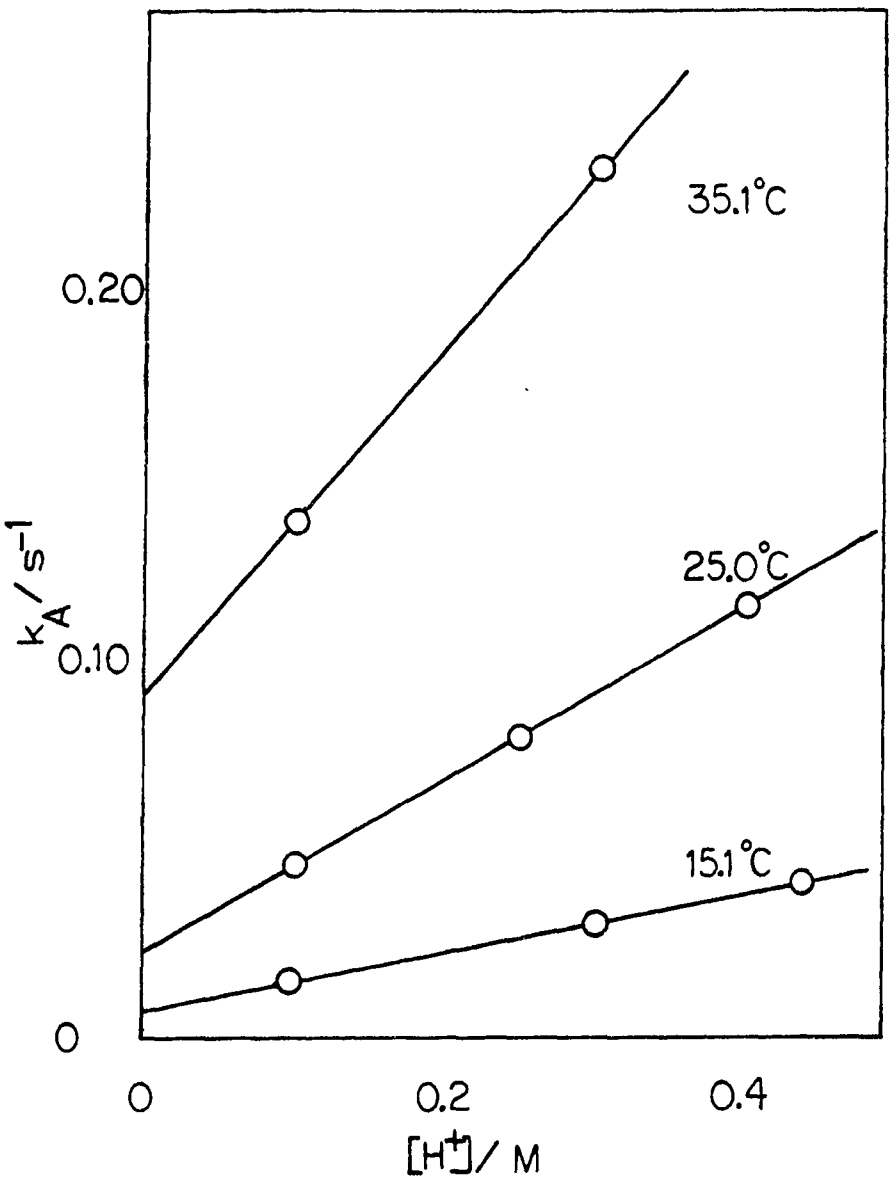

Figure I-7. Plot of k_A versus $[H^+]$ for acidolysis reactions of $CrC(CH_3)(i\text{-}C_3H_7)OH^{2+}$ at 15.1, 25.0 and 35.1°C, μ = 1.00 M ($LiClO_4$)

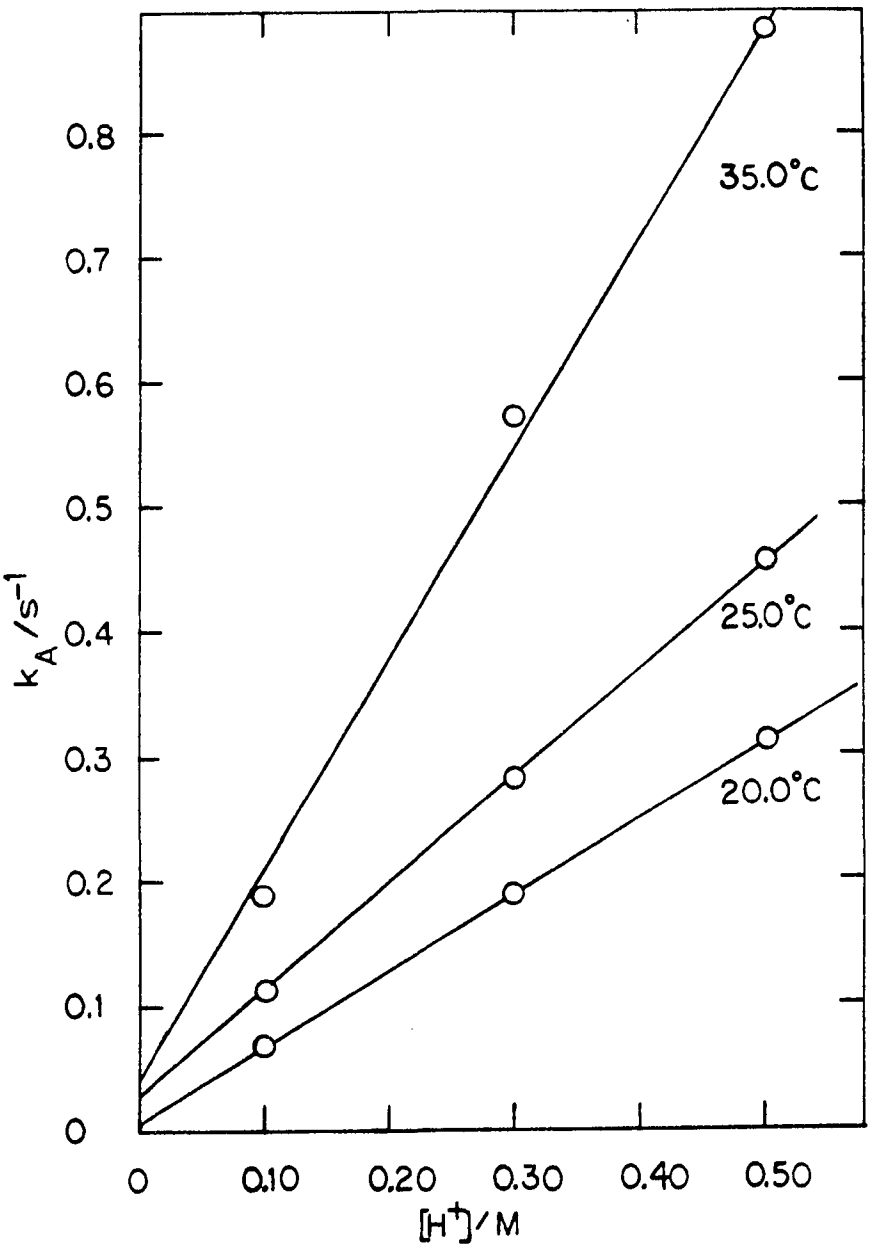

Figure I-8. Plot of k_A *versus* $[H^+]$ for acidolysis reactions of $CrC(C_2H_5)_2OH^{2+}$ at 20.0, 25.0 and 35.0°C, μ = 1.00 M ($LiClO_4$)

Table I-3. Summary of acidolysis values at 25.0°C

Complex	k_1/s^{-1}	$k_2/M^{-1}\ s^{-1}$	Reference
$Cr\text{-}CH_2OH^{2+}$	0.66×10^{-3}	0.465×10^{-3}	64
$Cr\text{-}CH(CH_3)OH^{2+}$	1.97×10^{-3}	9.54×10^{-4}	9
$Cr\text{-}CH(C_2H_5)OH^{2+}$	3.17×10^{-3}	2.14×10^{-3}	This work[a]
$Cr\text{-}C(CH_3)_2OH^{2+}$	3.3×10^{-3}	4.7×10^{-3}	9, 48[a]
$Cr\text{-}C(CH_3)(C_2H_5)OH^{2+}$	8.0×10^{-3}	0.469	This work[a]
$Cr\text{-}C(CH_3)(i\text{-}C_3H_7)OH^{2+*}$	0.024	0.231	This work[a]
$Cr\text{-}C(C_2H_5)_2OH^{2+*}$	0.027	0.858	This work[a]
$CrC(CH_3)(t\text{-}C_4H_9)OH^{2+*}$	$\sim 10\ sec^{-1}$ at 0.10 M H^+		This work[a]
$CrCH_2OCH_3^{2+*}$	very slow	$<<10^{-6}\ sec^{-1}$	48[a]
$CrCH(CH_3)OC_2H_5^{2+*}$	$\leq 5.0 \times 10^{-7}$	3.8×10^{-5}	9[a]
$CrC(CH_3)_2OCH(CH_3)_2^{2+*}$	$(3.6 \pm 0.2) \times 10^{-3}$	$(4.7 \pm 0.4) \times 10^{-3}$	This work[a,b]

[a]The ionic strength was maintained at 1.0 M ($LiClO_4$), co-solvent was 1 M alcohol or ether, except for entries denoted with (*), in which cases saturated solutions were used.

[b]This complex rearranges to $CrC(CH_3)_2OH^{2+}$ under acidolysis conditions.

have also been investigated. The unusually high reactivity of the complex from isopropyl ether (the last entry) was due to its rapid conversion to α-hydroxy-2-propylchromium(III) in acid and will be discussed later. The kinetic data for the acidolysis reactions of individual complexes are summarized in Tables I-5 through I-8. In order to further characterize the acidolysis reaction, it was also studied at several temperatures for each complex and Eyring plots of ln(k/T) versus 1/T were made (Figure I-9). Using this relationship, the activation parameters $\Delta H^{\ddagger}$ and $\Delta S^{\ddagger}$ were calculated. These activation parameters are listed in Table I-4 for several of the complexes. In some of the cases, the activation parameters for the acid-independent term were not evaluated as it was a minor term under the range of H^+ concentration which was studied. The activation parameters for the acid dependent k_2 term compare quite favorably with the values obtained by Schmidt et al. (9). The products of acidolysis are the organic alcohol (9,48) and $Cr(H_2O)_6^{3+}$, the latter identified by its visible spectrum.

Homolysis reactions

All of the complexes studied were found to undergo a facile homolysis reaction (Equation I-24). The homolysis of the chromium-

$$CrC(R^1R^2)OR^{2+} \underset{}{\overset{k_{hom}}{\rightleftharpoons}} Cr^{2+} + \cdot C(R^1R^2)OR \qquad \text{(I-24)}$$

carbon bond was followed at the absorption maximum characteristic of these complexes. The observed rate constants of decomposition under homolysis conditions obey clean first-order kinetics. Plots of

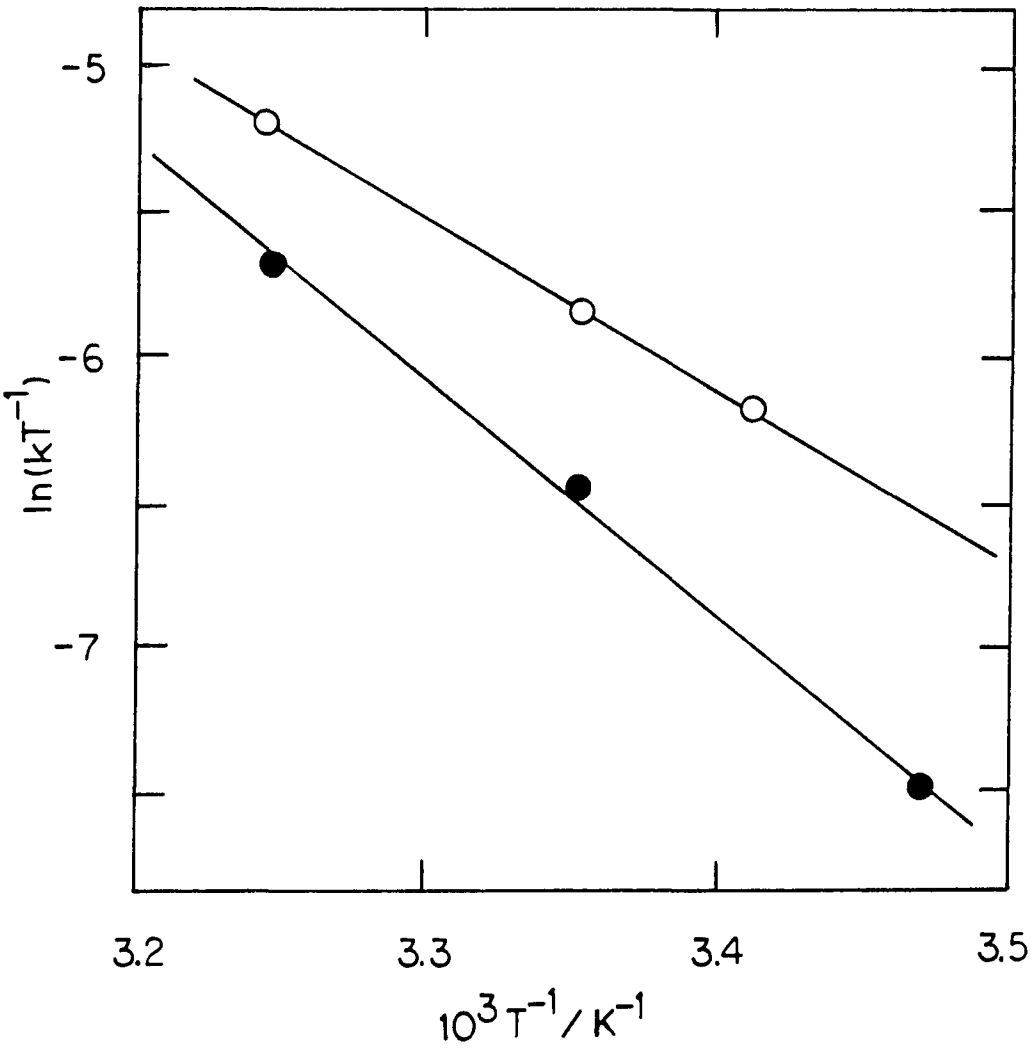

Figure I-9. Eyring plots for the decomposition of $CrC(CH_3)(C_2H_5)OH^{2+}$ (•) and $CrC(C_2H_5)_2OH^{2+}$ (o) under acidolysis conditions at 1 M $HClO_4$

Table I-4. Summary of activation parameters for acidolysis of $CrC(R,R^1)OH^{2+}$ complexes[a]

Complex	k_1		k_2	
	$\Delta S_1^{\ddagger}$/e.u.	$\Delta H_1^{\ddagger}$/kcal mol^{-1}	$\Delta S_2^{\ddagger}$/e.u.	$\Delta H_2^{\ddagger}$/kcal mol^{-1}
$CrC(CH_3)_2OH^{2+}$[b]	-11±2	17.1±0.7	-5±2	19.4±0.8
$CrC(CH_3)(C_2H_5)OH^{2+}$[c,d]	---	---	-8±4	15.6±1.7
$CrC(CH_3)(i\text{-}C_3H_7)OH^{2+}$[c,e]	0.5±7.5	19.1±2.2	-10±6	15.4±1.7
$CrC(C_2H_5)_2OH^{2+}$[c,e]	-27±31	11.7±9.4	-18.3±0.45	12.1±0.13

[a] 1 M ionic strength ($LiClO_4$).

[b] Reference 9.

[c] This work.

[d] 1 M 2-butanol.

[e] 0.02-0.05 M alcohol.

Table I-5. The kinetics of reaction of $CrC(CH_3)(C_2H_5)OH^{2+}$ under acidolysis conditions[a]

T/°C	$[H^+]$/M	k_{obs}/s^{-1}	
15.0	0.10	0.022	(3)
15.0	0.46	0.083	(3)
15.0	0.75	0.128	(3)
25.0	0.003	0.011	(3)
25.0	0.098	0.055	(3)
25.0	0.29	0.139	(3)
25.0	0.48	0.234 ± 0.001	(4)
25.0	0.58	0.280 ± 0.008	(8)
25.0	0.77	0.37	(4)
34.8	0.10	0.113	(5)
34.8	0.50	0.520	(6)
34.8	1.0	1.01	(6)

[a] μ = 1.0 M ($LiClO_4$)' $[Cr^{2+}]$ was varied between (1-3) x 10^{-3} M. $[CrC(CH_3)(C_2H_5)OH^{2+}]$ was estimated (0.1-0.4) x 10^{-3} M depending on the run; all values were in 1 M 2-butanol. The numbers in parentheses represent the number of replicate determinations.

Table I-6. The kinetics of reaction of $CrC(C_2H_5)_2OH^{2+}$ under acidolysis conditions[a]

T/°C	$[H^+]$/M	k_{obs}/s^{-1}
15.4	0.50	0.214 ± 0.004
15.7	0.30	0.136 ± 0.003
20.0	0.50	0.310 ± 0.005
20.0	0.30	0.190 ± 0.002
20.0	0.10	0.069 ± 0.0005
25.0	0.50	0.457 ± 0.01
25.0	0.30	0.283 ± 0.004
25.0	0.10	0.114 ± 0.002
35.0	0.50	0.884 ± 0.015
35.0	0.30	0.574 ± 0.01
35.0	0.10	0.190 ± 0.014

[a]Ionic strength was 1.0 M ($LiClO_4$); $[Cr^{2+}]_0 \sim 2.5 \times 10^{-3}$M; $[H_2O_2]_0 = 0.5 \times 10^{-3}$ M; saturated 3-pentanol in the aqueous acid were estimated between 50-100 x 10^{-3} M.

Table I-7. The kinetics of reaction of $CrC(CH_3)(i\text{-}C_3H_7)OH^{2+}$ under acidolysis conditions[a]

T/°C	$[H^+]$/M	k_{obs}/s^{-1}
15.1	0.10	0.0151
15.1	0.30	0.0317
15.1	0.437	0.0411
25.0	0.10	0.0468
25.0	0.25	0.0808
25.0	0.40	0.116
35.1	0.10	0.138
35.1	0.30	0.232

[a]Ionic strength was 1.0 M ($LiClO_4$); $[Cr^{2+}]_0 \sim (1.5\text{-}3.0) \times 10^{-3}$ M; $[H_2O_2]_0 = (0.5\text{-}0.75) \times 10^{-3}$ M. Saturated solutions of the alcohol were estimated to be ~0.02 - 0.04 M.

Table I-8. Summary of acidolysis and homolysis rate constants for $CrCH(C_2H_5)OH^{2+a}$

T/°C	$[H^+]$/M	$k_A + k_{hom}$ $(10^3)/s^{-1}$	k_A[b] $(10^3)/s^{-1}$	k_{hom}[c] $(10^3)/s^{-1}$
25.0	0.10	4.41 ± 0.02[d]	3.40	1.01
	0.50	---	4.20	---
	0.70	---	4.70	---
35.0	0.10	14.7 ± 0.3[d]	8.5 ± 0.2	6.2 ± 0.5

[a]Constant ionic strength of 1.0 M ($LiClO_4$).

[b]$[Cr^{2+}]_0$ varied between 2-4 x 10^{-3} M; estimated $CrCH(C_2H_5)OH^{2+}$ ∿(0.1-0.3) x 10^{-3} M.

[c]Calculated as the difference $(k_A + k_{hom}) - k_A$.

[d]In these experiments ∿3 mM $Co(NH_3)_5Br^{2+}$ was used.

$\ln(D_t-D_\infty)$ *versus* time were linear for at least three half-lives. In all cases, the homolysis data were in accord with the rate expression:

$$\frac{-d[CrC(R^1R^2)OR^{2+}]}{dt} = k_{hom}[CrC(R^1R^2)OR^{2+}] \qquad (I\text{-}25)$$

The kinetic data for the reaction shown in Equation I-24 are summarized in Table I-9. The results for analogous complexes are also included in this table. The second-order rate constants for the formation reaction between Cr^{2+} and the organic radical were included for those entries for which they were available.

Although in most of the cases studied here, the homolysis reaction was much faster than acidolysis, such was not the case for $CrCH(C_2H_5)OH^{2+}$. For this complex, the acidolysis and homolysis reactions were of comparable magnitude and the homolysis rate constants were determined by subtracting a substantial acidolysis component (Table I-8). For this particular complex, the acidolysis rate constant had been previously measured (9) and the value determined here was in reasonable agreement with the literature value. This check increased the confidence with which the homolysis rate could be measured and added support to our identification of these complexes and their reactions.

The rate constants for the homolysis of the remaining complexes are much higher than that for homolysis of $CrCH(C_2H_5)OH^{2+}$ (1.01×10^{-3} s^{-1} at 25.0°C) and, in general, the correction for acidolysis was small. Nevertheless, to be accurate the observed rate constants under homolysis conditions (see Reaction Selection)

Table I-9. Rate constants for homolysis of $CrC(R^1R^2)OR^{2+}$ complexes[a]

Complex	k_{hom}/s^{-1}	Reference
$Cr\text{-}CH_2OH^{2+}$	3.7×10^{-5}	48
$Cr\text{-}CH(CH_3)OH^{2+}$	$(8.5\pm0.3) \times 10^{-4}$	48
$CrCH(C_2H_5)OH^{2+}$	$(1.01\pm0.04) \times 10^{-3}$	This work
$CrC(CH_3)_2OH^{2+}$	0.127 ± 0.003	48, This work
$CrC(CH_3)(C_2H_5)OH^{2+}$	0.92 ± 0.03	This work
$CrC(C_2H_5)_2OH^{2+}$	8.39 ± 0.09	This work
$CrC(CH_3)(i\text{-}C_3H_7)OH^{2+}$	21.6 ± 0.1	This work
$CrC(CH_3)(t\text{-}C_4H_9)OH^{2+}$	≥ 300	This work[b]
$CrCH_2OCH_3^{2+}$	$< 10^{-6}$	48[c]
$CrCH(CH_3)OC_2H_5^{2+}$	2.04×10^{-3}	48
$CrC(CH_3)_2OCH(CH_3)_2^{2+}$	5.77 ± 0.15	This work

[a]At 25.0°C and 1 M ionic strength ($LiClO_4$).

[b]Calculated from values at a lower temperature.

[c]Estimated.

were corrected for the small, but well-known, contribution from acidolysis.

The homolysis reactions were studied over a range of temperatures in order to determine activation parameters. The values of activation parameters for reaction I-24 are summarized in Table I-10. Table I-11 shows the independence of the homolysis rate constant on the oxidant nature and concentration. In most cases, the temperature range studied was limited to ∿20°C due to experimental considerations. However, two of the complexes studied had homolysis rates in a particularly convenient range so that their homolysis rates could be determined by both stopped-flow and conventional techniques. The variable temperature data for these two complexes are listed in Tables I-12 and I-13. These data were also used to construct Eyring plots which showed a linear relation between ln(k/T) against 1/T over the entire temperature range studied (Figures I-10 and I-11). In Figure I-12, the independence of the homolysis rate on oxidant is shown for $CrC(CH_3)(C_2H_5)OH^{2+}$.

The other complexes studied were examined over a more limited temperature range. The homolysis rate constants for the complex derived from 3-pentanol co-solvent, $CrC(C_2H_5)_2OH^{2+}$, are summarized in Table I-14. For this complex, with a homolysis rate of 8.39 s^{-1} at 25°C, the homolysis reaction greatly dominates over the acidolysis reaction and only a small correction for acidolysis was necessary. As with the other complexes, the homolysis rate is independent of the oxidant concentration (Figure I-13). The Eyring plot from the variable temperature data (Table I-15) was linear over the temperature range studied (Figure I-14).

Table I-10. Summary of the activation parameters for the homolysis reaction

Complex	$\Delta S^{\ddagger}$/cal mol^{-1} K^{-1}	$\Delta H^{\ddagger}$/kcal mol^{-1}	Reference
$CrCH(C_2H_5)OH^{2+}$	37.0	32.5	This work
$CrC(CH_3)_2OH^{2+}$	29.4 ± 0.4	27.4 ± 0.1	48
	28.6 ± 0.3	27.2 ± 0.1	---[a]
$CrC(CH_3)(C_2H_5)OH^{2+}$	27.9 ± 1.8	25.9 ± 0.5	This work
$CrC(C_2H_5)_2OH^{2+}$	23.6 ± 1.6	23.2 ± 0.5	This work
$CrC(CH_3)(i\text{-}C_3H_7)OH^{2+}$	20.1 ± 1.2	21.6 ± 0.4	This work
$CrC(CH_3)(t\text{-}C_4H_9)OH^{2+}$	27.0 ± 12.0	22.0 ± 3.0	This work
$CrCH(CH_3)OC_2H_5^{2+}$	30.2 ± 0.3	30.1 ± 0.1	48
$CrC(CH_3)_2OCH(CH_3)_2^{2+}$	25.0 ± 2.0	23.9 ± 0.7	This work

[a]This value represents a combined value from all of the data available from both this work and Reference 48.

Table I-11. Range of oxidants used to study the homolysis reaction of $CrC(CH_3)(C_2H_5)OH^{2+}$[a]

Oxidant	10^3 [oxidant]/M	k_{hom}/s^{-1}[b]
H_2O_2	5 - 50	0.90 (0.07)[c]
$Co(NH_3)_5Cl$	2 - 11	0.90 (0.02)
$Co(NH_3)_5Br$	1 - 12.5	0.94 (0.03)
Cu^{2+}	20 - 100	0.96 (0.05)[d]
Fe^{3+}	24 - 69	0.97 (0.01)[d]

[a]All experiments were in 1 M 2-butanol aqueous $HClO_4$ solutions with $[H^+]$ = 0.10 M, except for $Co(NH_3)_5Br^{2+}$ experiments which were in 0.408 M $HClO_4$ (see Table I-1); μ = 1.0 M.

[b]All values have been corrected for acidolysis; 0.055 s^{-1} at 0.10 M H^+.

[c]At much higher H_2O_2 there seemed to be a slight dependence on $[H_2O_2]$; at 0.48 M H_2O_2 k_{obs} was $\sim$1.5 s^{-1}.

[d]These values were determined from the intercepts of the k_{obs} vs [oxidant] plots; these reactions are discussed in Part I.B of the thesis.

Table I-12. Variation of k_{hom} with temperature for $CrC(CH_3)_2OH^{2+}$

Temp/°C	k_{hom}/s^{-1} [a,b]	k_{obs} [c]/s^{-1}
4.4 [d]	0.00396	
8.2 [d]	0.00757	
14 9 [d]	0.0243	
15.0 [d]	0.0252	
24.8 [d]	0.126	0.137 ± 0.006 (3) [e]
25.0 [d]	0.127	0.16 (2) [f]
29.6 [c]	0.254	
33.5 [c]	0.46	
37.3 [c]	0.83	

[a] These homolysis rate constants were corrected for acidolysis at each temperature.

[b] All values in 1 M, 2-propanol.

[c] This work; $[Cr^{2+}]_o$ = 1-2 x 10^{-3} M; $[H_2O_2]$ = 0.4 x 10^{-3} M; $[Co(NH_3)_5Br^{2+}$ = 3 x 10^{-3} M.

[d] Values from Reference 48.

[e] This $CrC(CH_3)_2OH^{2+}$ was generated photochemically in 1 M acetone; $[Cr^{2+}]_o$ = 1.9 x 10^{-3} M; $[Co(NH_3)_2Cl^{2+}]$ = (2.3 - 4.6) x 10^{-3} M; T = 24.5 ± 0.5°C; μ = 1 M ($NaClO_4$); 0.1 M $HClO_4$.

[f] Identical experiment as (e) except $Co(NH_2)_5Br^{2+}$ (2.1 - 2.3 x 10^{-3} M) was used; $[H^+]$ = 1 M.

Table I-13. Variation of k_{hom} for $CrC(CH_3)(C_2H_5)OH^{2+}$ as a function of temperature[a]

Temp/°C	°K	1/T °K^{-1} (x10^3)	k_{hom}/s^{-1}	ℓn k	ℓn $\frac{k}{T}$
3.0	276.2	3.621	0.0205 ± 0.004	-3.89	-9.51
5.1	278.3	3.593	0.033 ± 0.003	-3.41	-9.04
10.0	283.2	3.531	0.081 ± 0.01	-2.51	-8.16
∿11.2[b]	284.4	3.516	0.148 ± 0.002	-1.91	-7.56
∿15.3[b]	288.5	3.466	0.286 ± 0.02	-1.25	-6.92
∿15.9[b]	289.1	3.459	0.298 ± 0.01	-1.21	-6.88
20.1	293.3	3.409	0.432 ± 0.014	-0.839	-6.52
20.3	293.5	3.407	0.482 ± 0.009	-0.73	-6.41
24.8	298.0	3.356	0.935 ± 0.02	-0.067	-5.76
25.0	298.2	3.353	0.92 ± 0.03	-0.073	-5.77
29.9	303.1	3.299	1.74 ± 0.05	0.554	-5.16
30.3	303.5	3.295	1.80 ± 0.05	0.588	-5.12
32.7	305.9	3.269	2.58 ± 0.1	0.948	-4.78
34.6	307.8	3.249	2.75 ± 0.18	1.01	-4.72
36.8	310.0	3.226	4.26 ± 0.3	1.45	-4.29

[a]All values were measured in 0.10 M $HClO_4$; 1 M ionic strength ($LiClO_4$) and 1 M 2-butanol; the known values were corrected for a small acidolysis contribution.

[b]These temperatures were approximate and are probably too low.

Table I-14. Range of oxidants used to study the homolysis reaction of $CrC(C_2H_5)_2OH^{2+}$

Oxidant	10^3 [oxidant]/M	k_{hom}/s^{-1} [a]
$Co(NH_3)_5Cl^{2+}$	2.5 - 7.5	8.40 ± 0.09
Cu^{2+}	22 - 149	8.45 ± 0.17 [b]
Fe^{3+}	23 - 73	8.70 ± 0.3 [b]

[a] These values represent the homolysis rate constants corrected for acidolysis.

[b] These values were obtained from the intercepts of k_{obs} vs [ox] plots and are corrected for acidolysis; $[CrC(C_2H_5)_2OH^{2+}]$ estimated $\lesssim 0.1 \times 10^{-3}$ M.

Table I-15. Homolysis data for $CrC(C_2H_5)_2OH^{2+}$ [a]

T (°C)	T (°K)	k_{obs} (s^{-1})	$(10^3)1/T$ ($°K^{-1}$)	k_A (s^{-1})	k_{hom} (s^{-1})	$\ell n \left(\frac{k}{T}\right)$
14.5	287.7	2.18 ± 0.07	3.476	0.05	2.13	-4.91
20.1	293.3	4.5 ± 0.1	3.409	0.07	4.43	-4.19
25.0	298.2	8.5	3.353	0.11	8.39	-3.57
30.0	303.2	16.5 ± 0.14	3 298	0.14	16.36	-2.92
33.2	306.4	24.8	3.264	0.18	24.6	-2.52
34.0	307.2	28.6 ± 0.5	3.255	0.185	28.4	-2.38
38.0	311.2	51.0 ± 4.0	3.213	0.24	51.0	-1.81

[a] Oxidant used for these values was $Co(NH_3)_5Cl^{2+}$; experiments were performed in 0.1 M $HClO_4$; μ = 1.0 M ($LiClO_4$); aqueous solutions saturated with 3-pentanol were used.

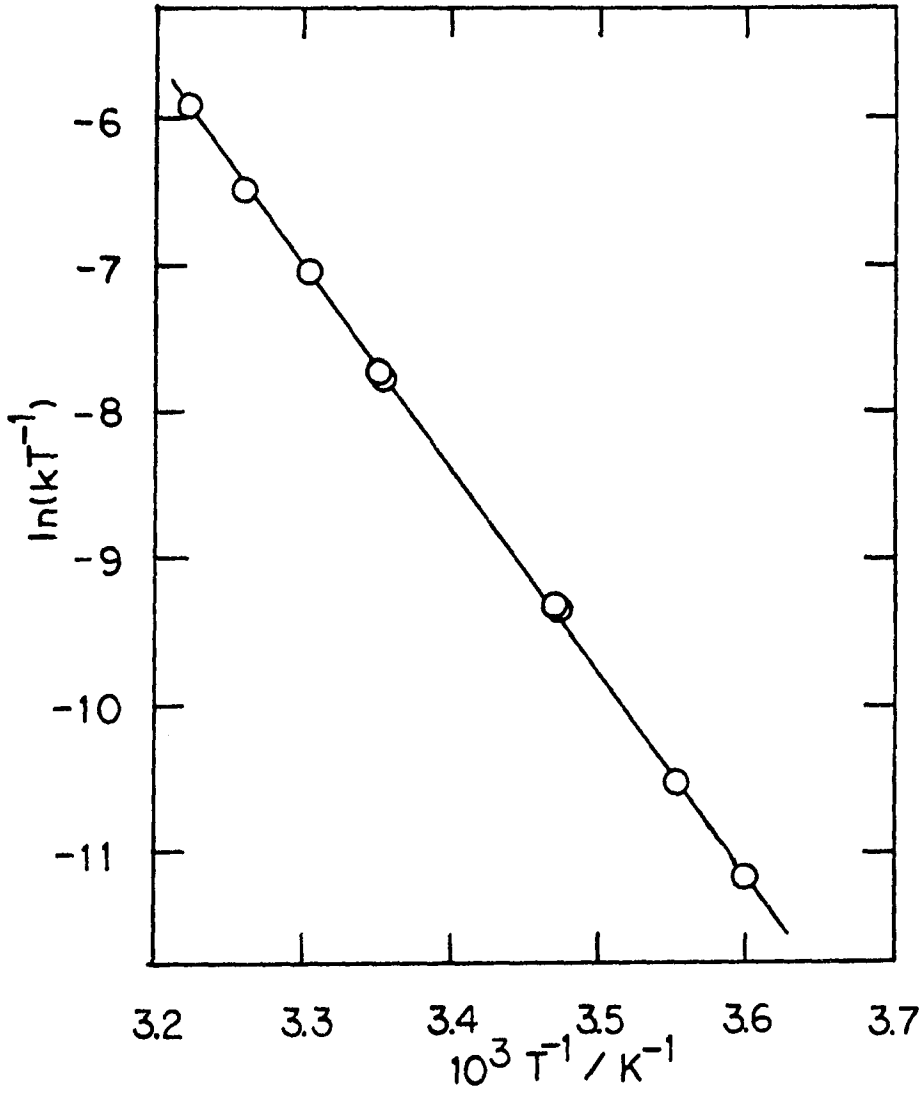

Figure I-10. Eyring plot for the decomposition of $CrC(CH_3)_2OH^{2+}$ under homolysis conditions

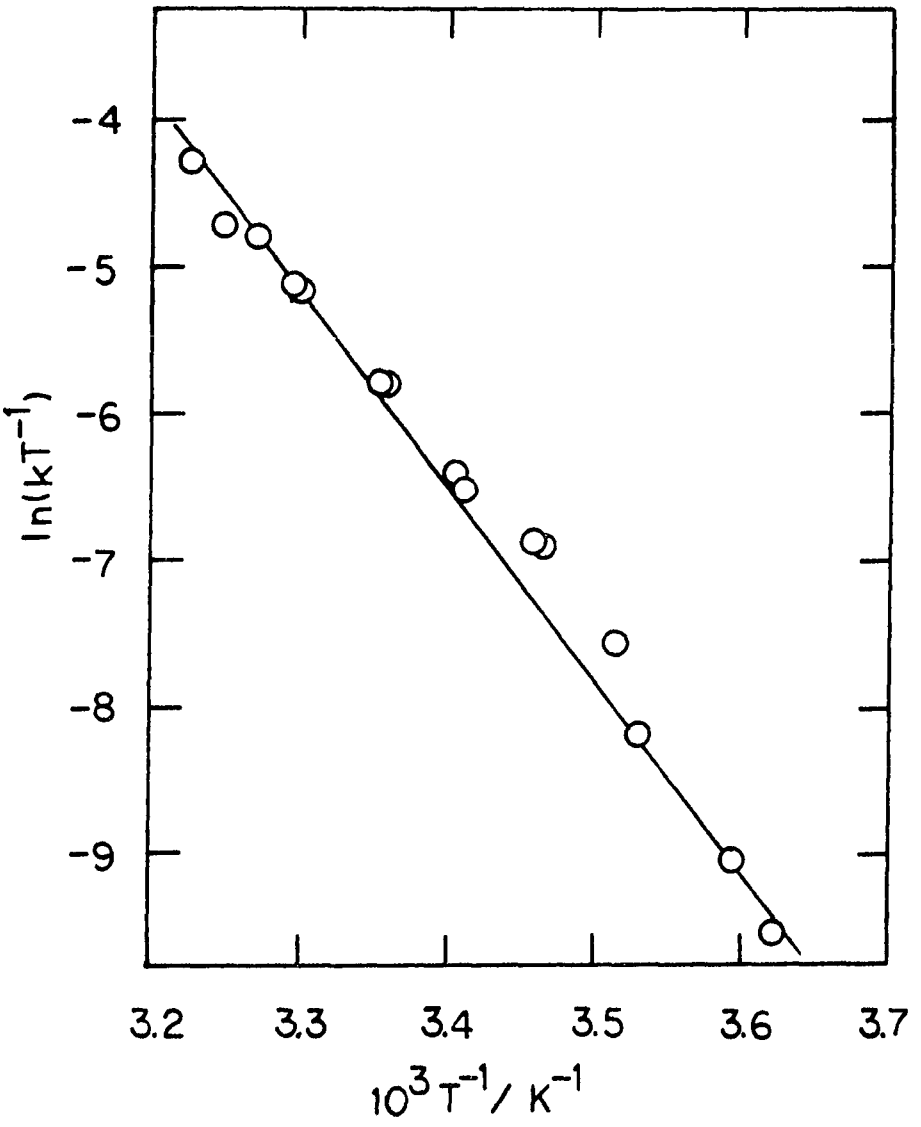

Figure I-11. Eyring plot for the decomposition of $CrC(CH_3)(C_2H_5)OH^{2+}$ under homolysis conditions

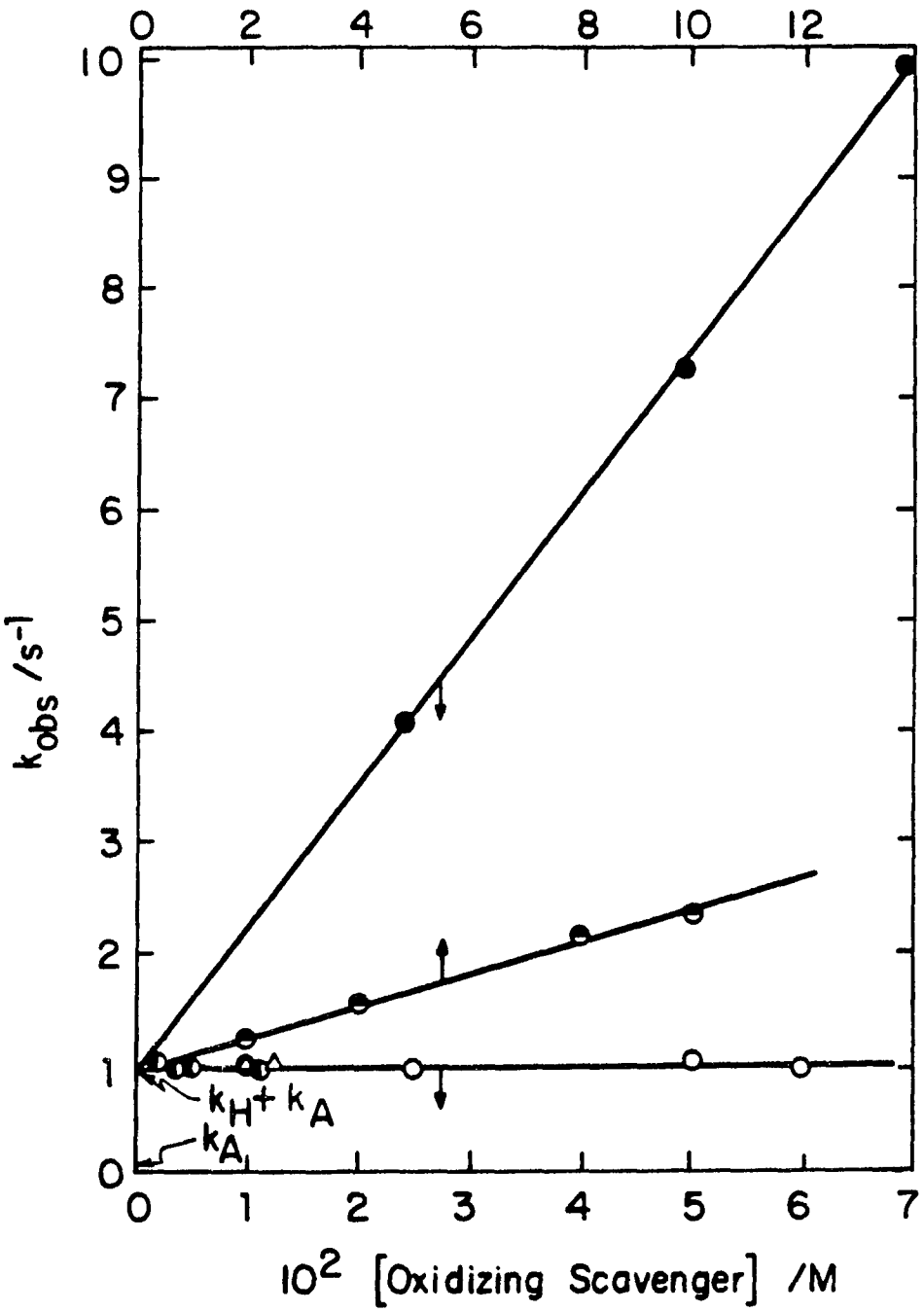

Figure I-12. Plot of k_{obs} versus [Oxidizing Scavenger] for reactions of $CrC(CH_3)(C_2H_5)OH^{2+}$ with the oxidants: Fe^{3+} (●), Cu^{2+} (●), H_2O_2 (o), $Co(NH_3)_5Cl^{2+}$ (●), and $Co(NH_3)_5Br^{2+}$ (Δ)

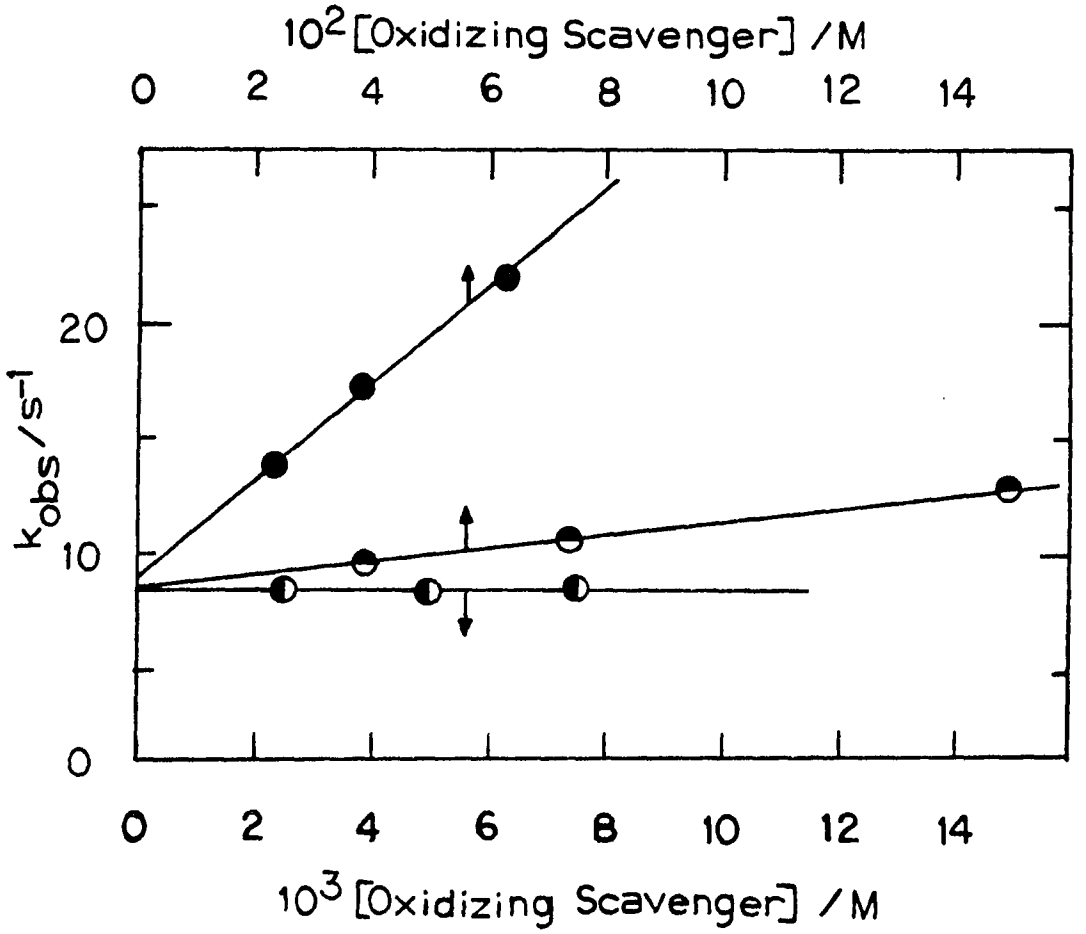

Figure I-13. Plot of k_{obs} <u>versus</u> [Oxidizing Scavenger] for the reactions of $CrC(C_2H_5)_2OH^{2+}$ with the oxidants: Fe^{3+} (●), Cu^{2+} (◐) and $Co(NH_3)_5Cl^{2+}$ (◑)

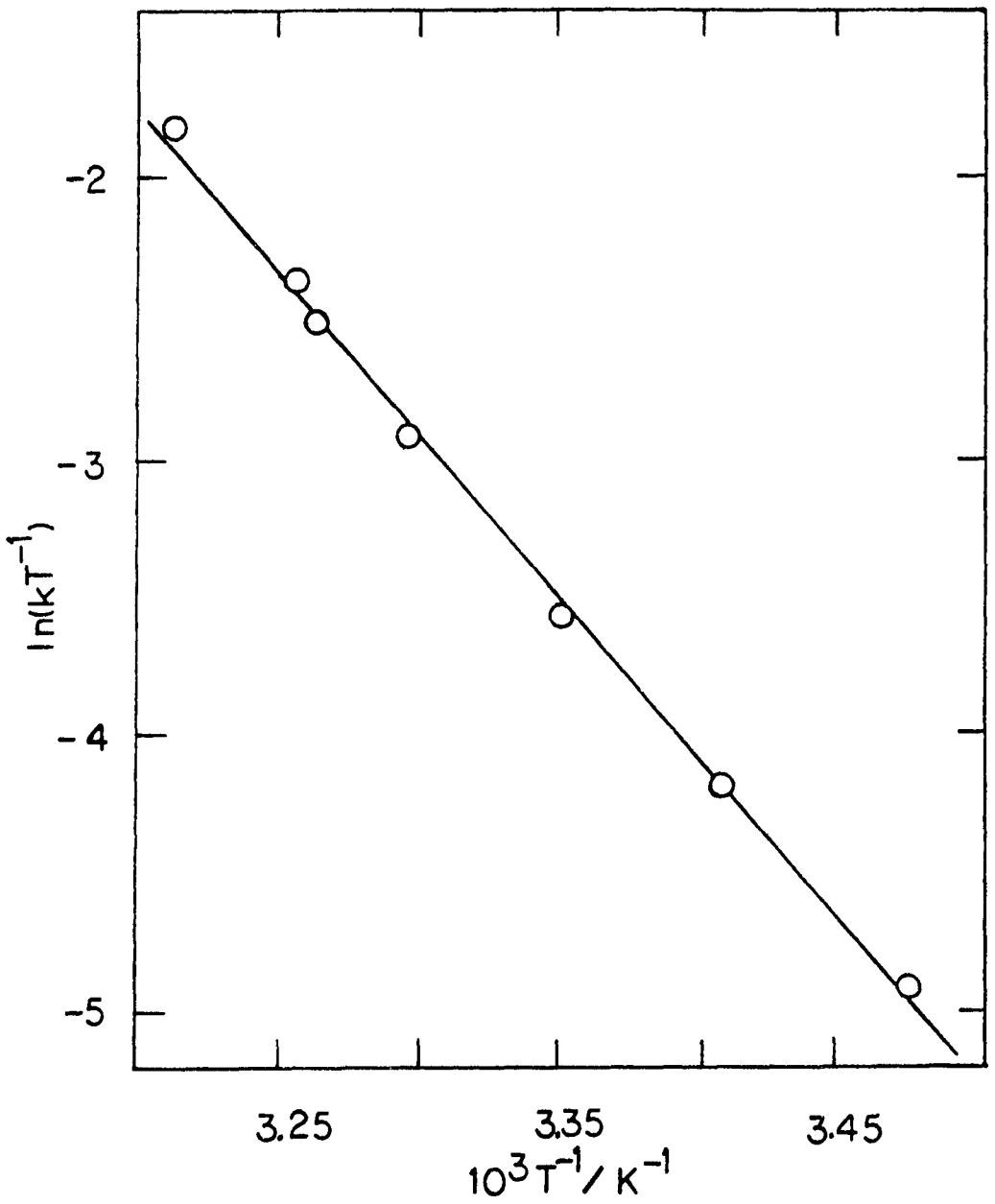

Figure I-14. Eyring plot for the decomposition of $CrC(C_2H_5)_2OH^{2+}$ under homolysis conditions

The two complexes with the fastest homolysis rates were $CrC(CH_3)(i\text{-}C_3H_7)OH^{2+}$ (Table I-16) and $CrC(CH_3)(t\text{-}C_4H_9)OH^{2+}$. The typical plots of k_{obs} versus oxidant and ln(k/T) versus 1/T(°K) for the homolysis reaction of $CrC(CH_3)(i\text{-}C_3H_7)OH^{2+}$ are shown in Figures I-15 and I-16. The results for the complex derived from 3,3-dimethyl-2-butanol deserve special comment: the experiments with this complex were difficult because of the very fast reaction observed. The rate constants were near the upper-limit of the stopped-flow range even at 20°C (Table I-17). Due to these complications, a very limited temperature range was studied and the Eyring plot shown in Figure I-17 suffers from this limitation. Despite this difficulty, the reactions of $CrC(CH_3)(t\text{-}C_4H_9)OH^{2+}$ were very much the same as for the other complexes, just faster. This means that the rate of homolysis was still independent of oxidant concentration and without added oxidant a much slower acidolysis-like reaction occurred. Because the reaction rates of $CrC(CH_3)(t\text{-}C_4H_9)OH^{2+}$ were so high, it was not studied in as much detail as the other complexes.

The homolysis reactions of $CrC(CH_3)_2OCH(CH_3)_2^{2+}$ were studied over a range of temperatures as with the other complexes (Table I-18). The homolysis rate was found to be independent of oxidant and oxidant concentration, in this case even Fe^{3+} and Cu^{2+} (Figure I-18). The Eyring plot yielded activation parameters very similar to the values determined for the α-hydroxalkylchromium(III) complexes (Figure I-19). The product analysis of the homolysis reactions were performed under conditions so that $CrC(CH_3)_2OCH(CH_3)_2^{2+}$ was not allowed to age in the

Table I-16. Range of oxidants used to study the homolysis reaction of $CrC(CH_3)(i\text{-}C_3H_7)OH^{2+}$

Oxidant	10^3[Oxidant]/M	k_{hom}/s^{-1}
$Co(NH_3)_5Cl^{2+}$	2.9 - 11	21.6 ± 0.1
Cu^{2+}	19 - 159	20.4 ± 0.9[a]
Fe^{3+}	14 - 50	22.4 ± 1.0[a]

[a]These values were obtained from the intercepts of k_{obs} *vs* [ox] plots at various $[H^+]$ at high $[H^+]$ a small acidolysis correction was applied.

Table I-17. Variation of k_{hom} with temperature for $CrC(CH_3)(t\text{-}C_4H_9)OH^{2+}$[a]

T/ °C	(°K)	$10^3\ T^{-1}/K^{-1}$	k^b_{obs}/s^{-1}	ℓn(k/T)
14.9	288.1	3.471	94 ± 9	-1.12
18.5	291.7	3.428	141 ± 24	-0.727
20.2	293.4	3.408	196 ± 53	-0.403

[a]All values were measured in 0.10 M $HClO_4$· 1 M ionic strength ($LiClO_4$) and solutions were saturated with 3,3-dimethyl-2-butanol.

[b]These values were not corrected for acidolysis which would be a very minor contribution.

Table I-18. Variation of k_{hom} with temperature for $CrC(CH_3)_2OCH(CH_3)_2^{2+}$[a]

T/°C	$10^3\ T^{-1}/°K^{-1}$	k_{hom}/s^{-1}	$\ell n(\frac{k}{T})$
13.9	3.483	1.28	-5.41
15.4	3.465	1.68	-5.15
20.5	3.405	2.98	-4.59
20.6	3.404	2.5	-4.77
20.8	3.401	3.2	-4.53
25.0	3.353	5.7	-3.99
29.9	3.299	13.1	-3.14
33.1	3.265	17.6	-2.86
35.2	3.243	23.8	-2.53
38.9	3.204	36.8	-2.14
39.0	3.203	37.2	-2.13

[a]At 1 M ionic strength ($LiClO_4$); H_2O_2 and $Co(NH_3)_5Cl^{2+}$ were used as oxidants; solutions were saturated with di-isopropyl ether and $[H^+]$ = 0.10 M in each experiment.

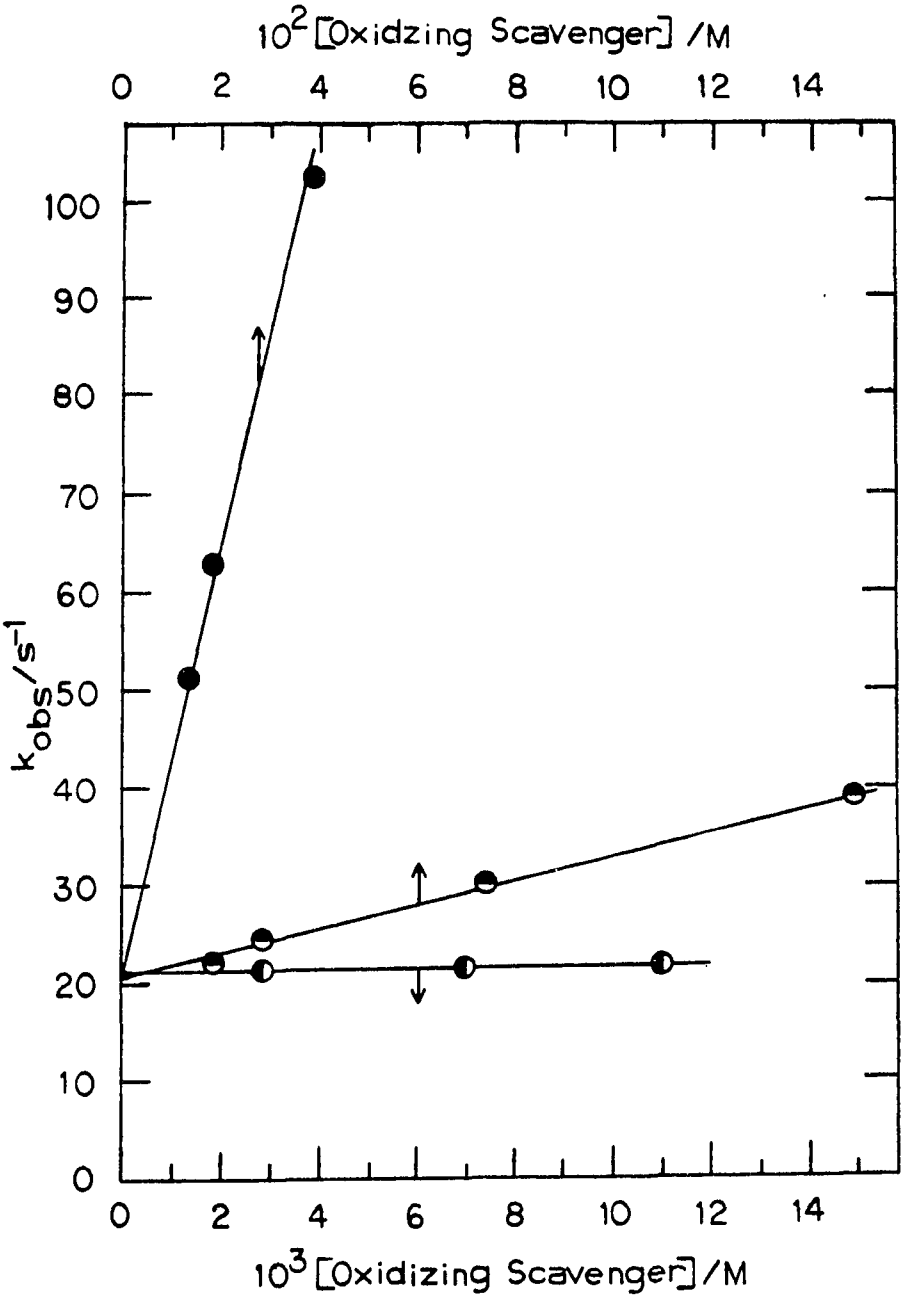

Figure I-15. Plot of k_{obs} versus [Oxidizing Scavenger] for the reactions of $CrC(CH_3)(i\text{-}C_3H_7)OH^{2+}$ with the oxidants: Fe^{3+} (●), Cu^{2+} (●) and $Co(NH_3)_5Cl^{2+}$ (●)

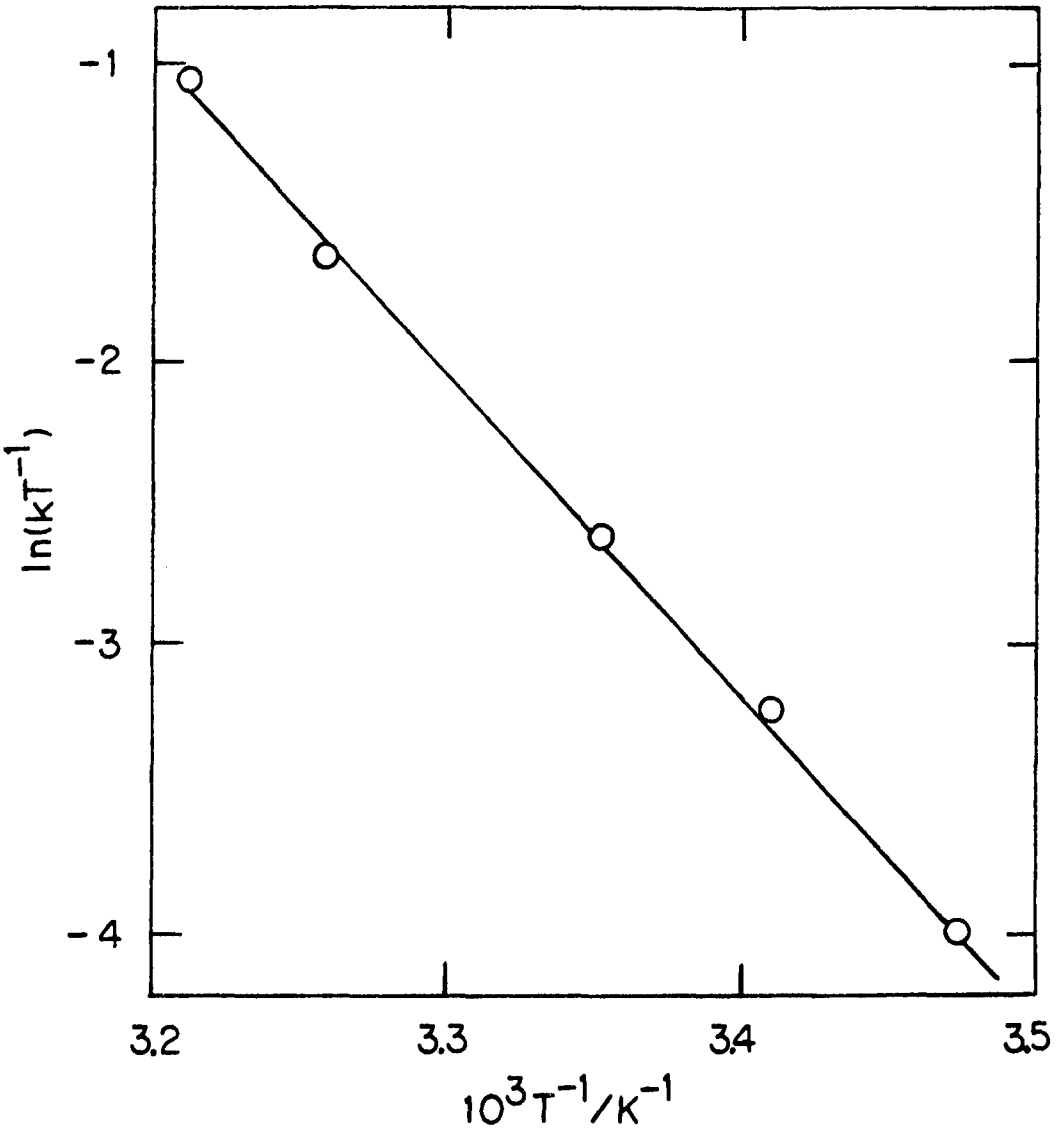

Figure I-16. Eyring plot for the decomposition of $CrC(CH_3)(i\text{-}C_3H_7)OH^{2+}$ under homolysis conditions

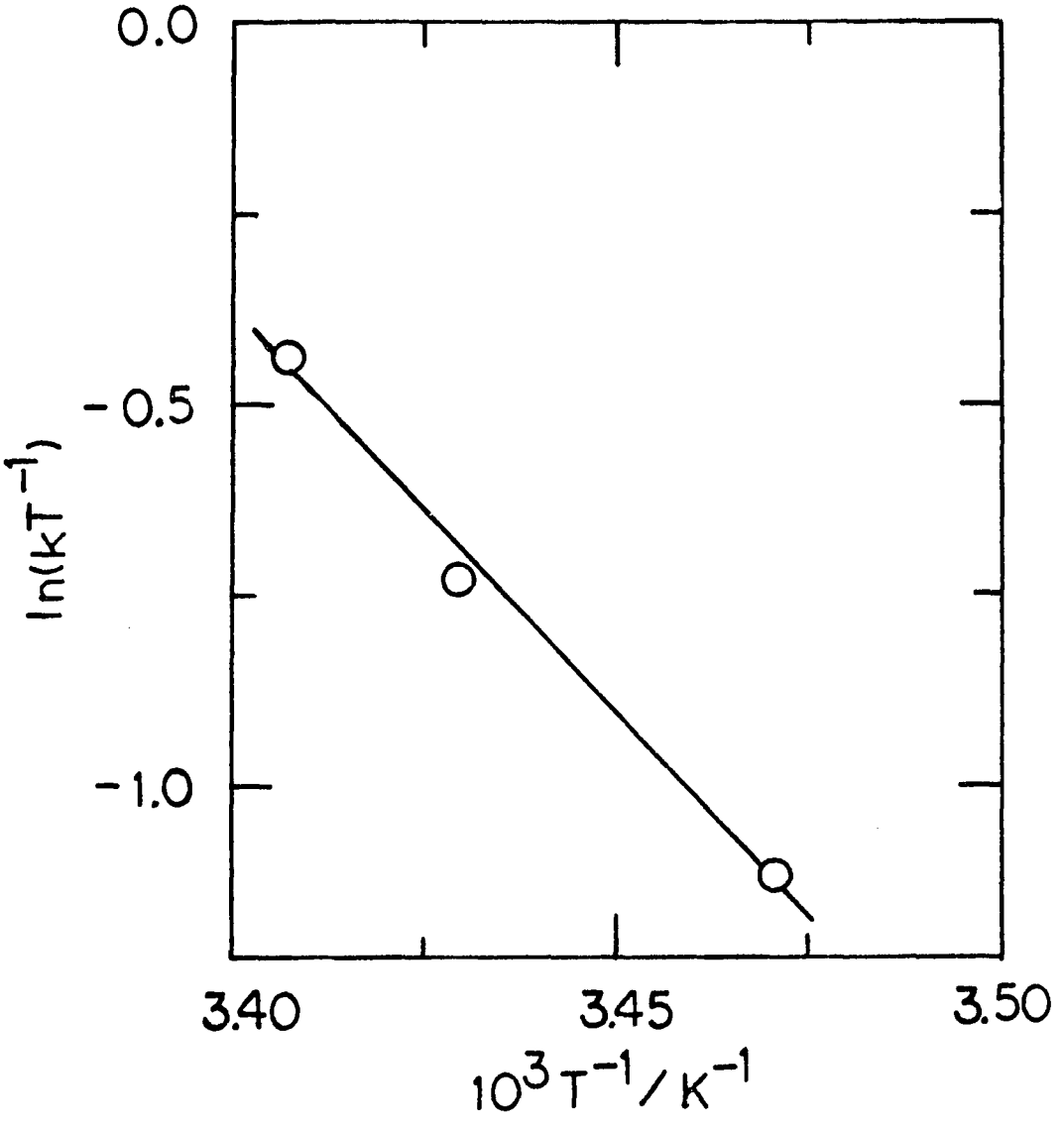

Figure I-17. Eyring plot for the decomposition of $CrC(CH_3)(t\text{-}C_4H_9)OH^{2+}$ under homolysis conditions

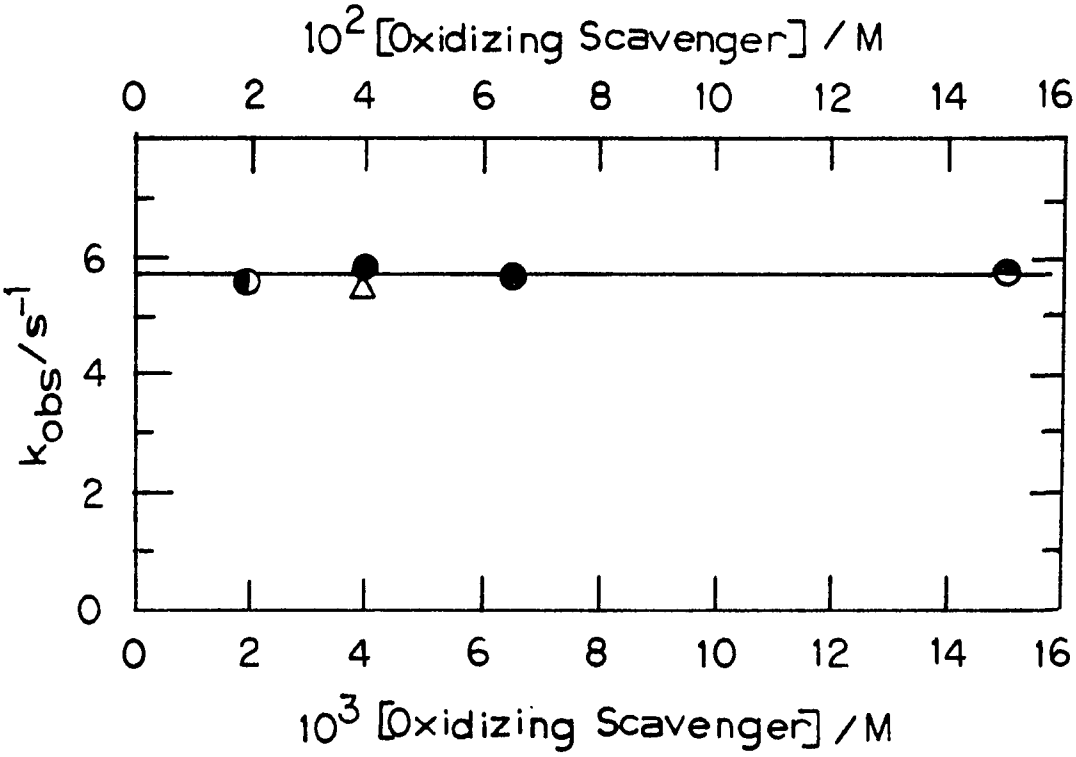

Figure I-18. Plot of k_{obs} <u>versus</u> [Oxidizing Scavenger] for the reactions of $CrC(CH_3)_2OCH(CH_3)_2^{2+}$ with the oxidants: Fe^{3+} (●), Cu^{2+} (●), $Co(NH_3)_5Cl^{2+}$ (●) and $Co(NH_3)_5Br^{2+}$ (△)

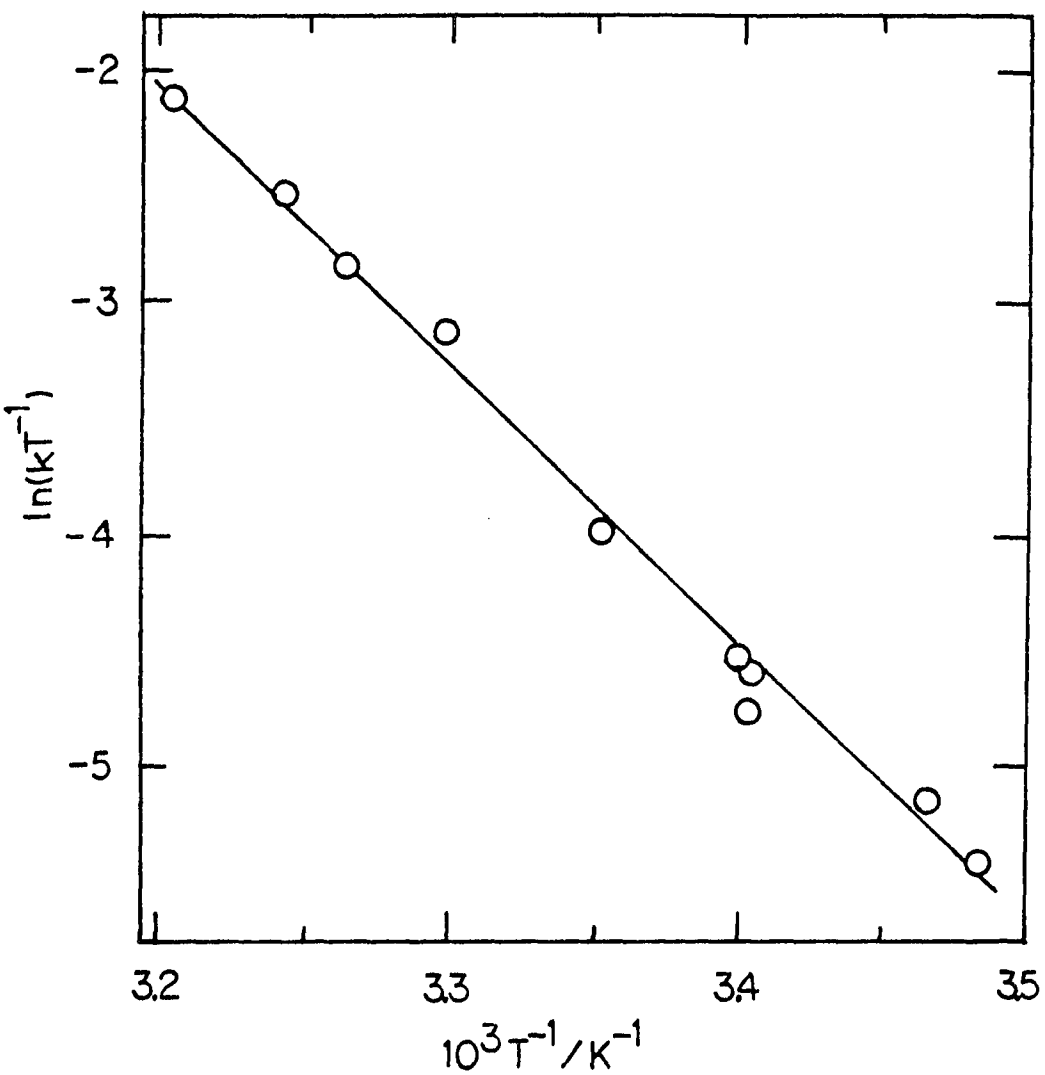

Figure I-19. Eyring plot for the decomposition of $CrC(CH_3)_2OCH(CH_3)_2^{2+}$ under homolysis conditions

$HClO_4$ solution and revealed approximately equal amounts of 2-propanone and 2-propanol were formed.

Photochemical generation of $CrC(R^1R^2)OH^{2+}$

In addition to producing α-hydroxyalkylchromium(III) complexes by the MFR method, a photochemical route was developed. We have found that aqueous acidic (10^{-3}-1 M $HClO_4$) solutions containing Cr^{2+} (2-15 mM) and acetone (1-3 M) with or without added 2-propanol produced α-hydroxy-2-propylchromium(III) when irradiated with uv radiation (65-69). The identity of the organochromium formed was confirmed by its rate constants for acidolysis and homolysis (Table I-12), in comparison with the same species prepared by chemical reactions. A spectrum of the product obtained by photolysing an acetone solution containing Cr^{2+} is shown in Figure I-20. Yields of up to ∿20% could be obtained by this route.

Similar results were obtained by flash photolysis of solutions containing 2-butanone/2-butanol mixtures in aqueous $HClO_4$ containing Cr^{2+}. These experiments also indicated $CrCH_2CH_3^{2+}$ was also formed in an appreciable yield. A very slow acidolysis rate was observed which was consistent with $CrCH_2CH_3^{2+}$. It was also found that addition of $Co(NH_3)_5Cl^{2+}$ did not increase the observed rate, again consistent with $CrCH_2CH_3^{2+}$ being the other species formed.

Acid rearrangement of $CrC(CH_3)_2OCH(CH_3)_2^{2+}$

The study of the acidolysis reaction of $CrC(CH_3)_2OCH(CH_3)_2^{2+}$ revealed an unexpected cleavage reaction of the bound ether ligand.

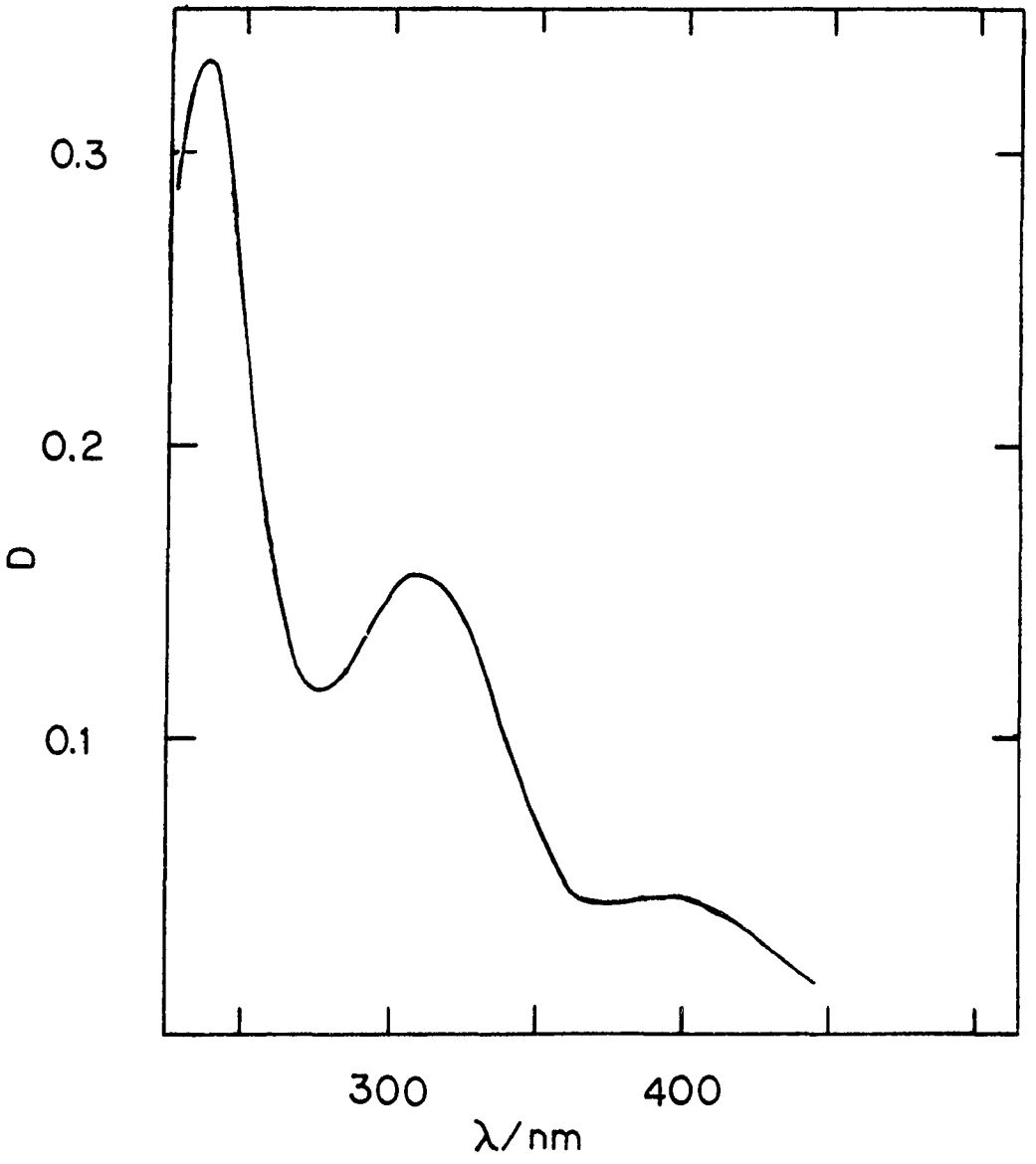

Figure I-20. Electronic spectrum of $(H_2O)_5CrC(CH_3)_2OH^{2+}$ generated photochemically from an aqueous acetone solution. Conditions: (ℓ = 1 cm) $[Cr^{2+}]_0 = 2 \times 10^{-3}$ M, $[acetone]_0$ = 0.02 M; 300 J unfiltered uv xenon flash of $\sim$30 μs duration. An identical cell which was not irradiated was used as a reference

The conclusion that this complex was undergoing a unique decomposition was supported by three main observations.[1] Each of these pieces of supporting evidence has been treated under a separate heading.

Effect of H^+ The decomposition of $CrC(CH_3)_2OCH(CH_3)_2^{2+}$ was found to occur at essentially the same rate as for $CrC(CH_3)_2OH^{2+}$ at 25.0°C (Tables I-3 and I-19). The acid-dependent term, k_2, was identical from the two kinetic studies ($k = 4.7 \times 10^{-3}\ M^{-1}\ s^{-1}$). This piece of evidence alone would not be sufficient to prove that $CrC(CH_3)_2OCH(CH_3)_2^{2+}$ decomposes by a unique mechanism among the ether-bound complexes, but it provided the first clue that something unusual was occurring.

Variation of homolysis conditions Experiments which were performed on the D-132 multi-mix system indicated that $CrC(CH_3)_2OCH(CH_3)_2^{2+}$ had a homolysis rate of $5.77 \pm 0.15\ sec^{-1}$ at 25.0°C (see Results, Homolysis Reactions). This rate was independent of both the nature and concentration of the oxidizing agent which has been shown to be true for other S_H1 mechanisms (17). Because of the indication from the acidolysis rate constants that $CrC(CH_3)_2OCH(CH_3)_2^{2+}$ might be converted to $CrC(CH_3)_2OH^{2+}$ some additional homolysis experiments were carried out. In these homolysis experiments, the $CrC(CH_3)_2OCH(CH_3)_2^{2+}$ was formed in a 2 cm quartz cell which had been carefully deoxygenated

---

[1] Product analyses (g.c.) also indicated that 2-propanol was produced as an organic product, providing additional evidence for ether-cleavage.

Table I-19. The kinetics of reaction of $CrC(CH_3)_2OCH(CH_3)_2^{2+}$ under acidolysis conditions[a]

$[H^+]$/M	10^3 k/s^{-1}
0.10	3.94 ± 0.07 (3)
0.30	4.94 ± 0.09 (2)
0.50	6.21 ± 0.13 (3)
0.89	7.66 ± 0.08 (5)

[a]At 25.0°C; μ = 1.0 M ($LiClO_4$); ~0.05 M isopropyl ether. The numbers in parentheses represent the number of replicate determinations.

by injecting a known amount of H_2O_2 into the cell which contained Cr^{2+}, isopropyl ether, $HClO_4$, and $LiClO_4$. The absorbance of the yellow solution was then recorded prior to injecting a known amount of $Co(NH_3)_5Cl^{2+}$ which was in excess over $2[Cr^{2+}]$. The result of this type of homolysis experiment was quite conclusive, a rate constant of $\sim$0.12 - 0.13 sec^{-1} was observed in each case at $\sim$25 0°C and the absorbance change observed accounted for 70-90% of the total absorbance change expected. This result indicated that $CrC(CH_3)_2OCH(CH_3)_2^{2+}$ which was first formed (as indicated by its unique homolysis rate of 5.77 sec^{-1}) was rapidly converted to $CrC(CH_3)_2OH^{2+}$ as indicated by the homolysis experiments performed on the Cary 219. One may estimate the boundary conditions for this conversion process to be slower than $\sim$1 sec^{-1} but faster than 0.05 sec^{-1} at 25.0°C, 0.1 M H^+ and 1.0 M ionic strength.

DISCUSSION

Acidolysis

The acidolysis reactions of the α-hydroxyalkylchromium(III) complexes which were the focus of this study were, in general, much faster than the reaction of the simpler analogs previously investigated (9). As far as can be determined from this study and previous work, the products of aquation are $Cr(H_2O)_6^{3+}$ and the co-solvent alcohol or ether $HC(R^1R^2)OH$. The acidolysis reaction may be viewed as a dissociation of a carbanion from the Cr(III) center. Clearly, formation of a free carbanion under the reaction conditions would not be favored, but it is useful to view the reaction in this manner. Formally then, protonation of the carbanion would ultimately lead to the observed products. This type of heterolytic cleavage of a metal alkyl bond resulting in loss of R- by reaction with a proton has been postulated for other alkyl metal systems important in catalysis (70).

In considering the intimate mechanism, one might argue that the pendant -OH group could play a special role in this reaction by hydrogen bonding to one of the incoming reactant molecules (H_2O). This would bring the reactant in close proximity to the reaction center thus presumably favorably increasing the likelihood of reaction. This may

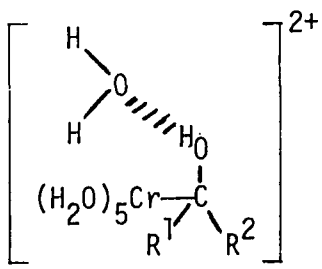

be viewed as shown after Schmidt et al. (9) and might serve as well as any figure for our conceptualization of what the activated complex must look like for the acid-independent pathway. It is important to note, however, that simple alkylchromium(III) complexes such as ethylpentaaquochromium(III) are also subject to acidolysis reactions which have two pathways, one zero order and one first order in acid concentration.

In order to separate polar and electronic contributions, three complexes which have ligands of very similar steric bulk have been listed in Table I-20. Using the Taft values cited, one would predict that $CrCH_2CH_3^{2+}$ should be much more susceptible to acidolysis than $CrCH_2OH^{2+}$, since the α-carbon in $CrCH_2CH_3^{2+}$ should have more electron density than in $CrCH_2OH^{2+}$ and $CrCH_2Cl^{2+}$. Also, $CrCH_2Cl^{2+}$ should be the most stable complex of the three. Only the latter statement holds true: $CrCH_2Cl^{2+}$ is the most stable towards acidolysis, but $CrCH_2OH^{2+}$ is about three times more susceptible to acidolysis than $CrCH_2CH_3^{2+}$. This may

Table I-20. Comparison of acidolysis rate constants for complexes of similar steric bulk

Complex	σ*[a]	Acidolysis rate constants	
		k_1/s^{-1}	$k_2/M^{-1}\ s^{-1}$
$CrCH_2Cl^{2+}$[b]	1.05	$< 10^{-7}$	$< 10^{-7}$
$CrCH_2OH^{2+}$[c]	0.55	6.6×10^{-4}	4.65×10^{-4}
$CrCH_2CH_3^{2+}$[c]	-0.10	2.2×10^{-4}	1.15×10^{-4}

[a]Values from Reference 71.

[b]Rate constants estimated; this complex may be kept for months at -10°C.

[c]Reference 64.

be due to hydrogen-bonding by the -OH group which assists in bringing an electrophile into proximity with the α-carbon.

Now turning to the complexes listed in Table I-3, it is apparent that for the series of α-hydroxyalkyl complexes the kinetic stability of these complexes to acidolysis decreases as the α-carbon becomes more electron-rich. In fact, as the steric crowding at the α-carbon increases, the acidolysis rates also increase. One might argue that there is even a steric acceleration of the reaction; (compare $CrC(CH_3)_2OH^{2+}$ $k_A = (3.3 \times 10^{-3} + 4.7 \times 10^{-3}\ [H^+])\ s^{-1}$ <u>versus</u> $CrC(CH_3)(C_2H_5)OH^{2+}$ $k_A = (8 \times 10^{-3} + 0.47\ [H^+])\ s^{-1}$). The steric acceleration seems to be most pronounced for the k_2 pathway. This very large enhancement of the k_2 term is observed for all of the complexes which have a β-CH_3 group with a quaternary α-carbon as in $CrC(CH_3)(C_2H_5)OH^{2+}$. It is not observed, however, when only a β-CH_3 group is present as in $CrCH(C_2H_5)OH^{2+}$ ($k_A = 3.17 \times 10^{-3} + 2.14 \times 10^{-3}\ [H^+]$). This steric enhancement may reflect the interactions between the β-CH_3 group(s) and water molecules which are coordinated to the chromium center and <u>cis</u> to the alkyl group. Space-filling models indicate that there is <u>much</u> more steric interaction with the $-C(CH_3)(C_2H_5)OH$ ligand as opposed to $-C(CH_3)_2OH$. Possibly, these interactions promote the formation of a preferred conformer which is more susceptible to attack by an incoming electrophile such as H_3O^+. Many arguments may be put forth to explain the large steric acceleration observed for β-CH_3 substituents, but there seems to be little justification for further speculation. At least all of the data clearly show

that the presence of a β-CH_3 group in the alkyl ligand (with a quaternary carbon) causes a very pronounced increase in the rate constant for the acid-dependent acidolysis pathway. Most likely, the steric acceleration is due to partial release, in the transition state, of steric compressions in the ground states of $CrC(CH_3)(C_2H_5)OH^{2+}$, $CrC(C_2H_5)_2OH^{2+}$ and $CrC(CH_3)(i\text{-}C_3H_7)OH^{2+}$ which could result from interaction between the β-CH_3 groups and <u>cis</u> water molecules bound to Cr^{III}.

Although the k_2 pathway is greatly influenced by the β-CH_3 substituents as presented in the preceding discussion, the k_1 acid-independent pathway seems only slightly influenced. This lack of steric acceleration may be due to the possibility that the k_1 pathway goes by transfer of a proton from a coordinated water as shown below. (This seems quite likely considering the proximity of the <u>cis</u> water molecules to the α-carbon and the greater acidity of coordinated water as opposed to bulk solvent water as shown below.) Thus, the internal pathway would probably not be as sensitive to the β-CH_3 substitution as a possible external pathway might be.

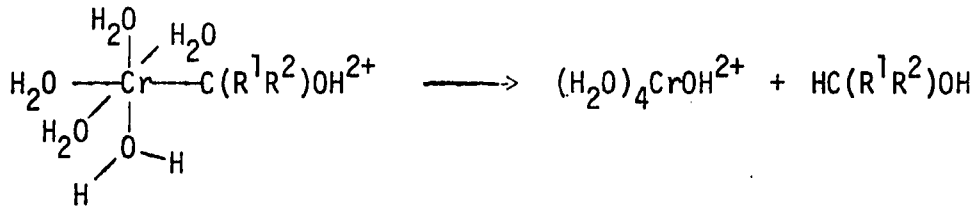

The study of $CrC(CH_3)_2OCH(CH_3)_2^{2+}$ under acidolysis conditions was found to have an unusual twist. This species was found to undergo a rearrangement to $CrC(CH_3)_2OH^{2+}$ in aqueous perchloric acid at room

temperature. A possible scheme for this cleavage mechanism is presented in Scheme 1.6. The acid-catalyzed cleavage of ethers which

Scheme 1-6

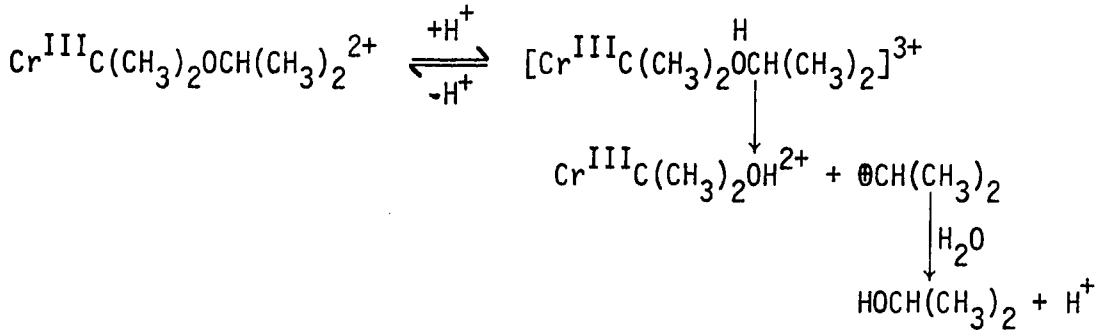

has been known for over a century (71,72), requires very vigorous conditions. One mechanism proposed the formation of a carbonium ion after protonation of the ether oxygen. The order of reactivity of dialkyl ethers is: $(CH_3)_2O < (C_2H_5)_2O < ((CH_3)_2CH)_2O < ((CH_3)_3C)_2O$, which reflects the ease with which the carbonium ion may be formed, $(CH_3)_3C^+$ being much more stable than $^+CH_3$ (73).

Other ether cleavage reactions have been noted. In a very strong acid medium (FSO_3H-SbF_5), the cleavage of ethers has been found to be very facile (73). Alkyl ethers which contain a tertiary group cleave readily even at -70°C in this strong acid medium, whereas n-alkyl ethers are stable at much higher temperatures for long periods of time (73). Similar observations have been made for some protonated alkyl carbonates, which also indicate that the ease of cleavage of the -C-O-C bond is very dependent on the nature of the carbocation formed (74).

The difference in reactivity between $CrC(CH_3)_2OCH(CH_3)_2^{2+}$ and $CrCH(CH_3)OC_2H_5^{2+}$ may thus be due to the lower stability of $^+CH_2CH_3$

compared to $^{+}CH(CH_3)_2$. It seems possible from the arguments presented here that preparation of $CrCH_2OC(CH_3)_3^{2+}$ from methyl-t-butyl ether should result in its facile conversion to the known $CrCH_2OH^{2+}$. This might be a good test of the hypothesis presented.

The k_2, acid-dependent, pathway for all of the complexes from this study have negative $\Delta S^{\ddagger}$ values similar to the literature value for $CrC(CH_3)_2OH^{2+}$ (Table I-4). If the $\Delta S^{\ddagger}$ is considered to be the change in disorder of the system in going from the ground state reactants to the transition state then the modest negative $\Delta S^{\ddagger}$ values found for these reactants indicate that more order is created in forming the transition state. This is exactly the situation expected for reaction between unipositive and dipositive ions reacting to create a tripositive transition state (75). This may be partially due to an increased ordering of solvent around the tripositive cation which is forming in the transition state.

The values of $\Delta H^{\ddagger}$ determined parallel the reactivity of the complex towards H_3O^{+}. Thus, the complex which is least stable towards acidolysis ($CrC(C_2H_5)_2OH^{2+}$) has the lowest enthalpy of activation (12.1 kcal/mol). This lower $\Delta H^{\ddagger}$ may be a reflection of the weaker chromium-carbon bond in the highly substituted complexes. This subject is dealt with more quantitatively in the Homolysis section.

Photochemical Syntheses

The photochemical generation of $CrC(CH_3)_2OH^{2+}$ and $CrC(CH_3)(C_2H_5)OH^{2+}$ from aqueous acetone and 2-butanone solutions probably occurs by the following scheme:

Scheme 1-7

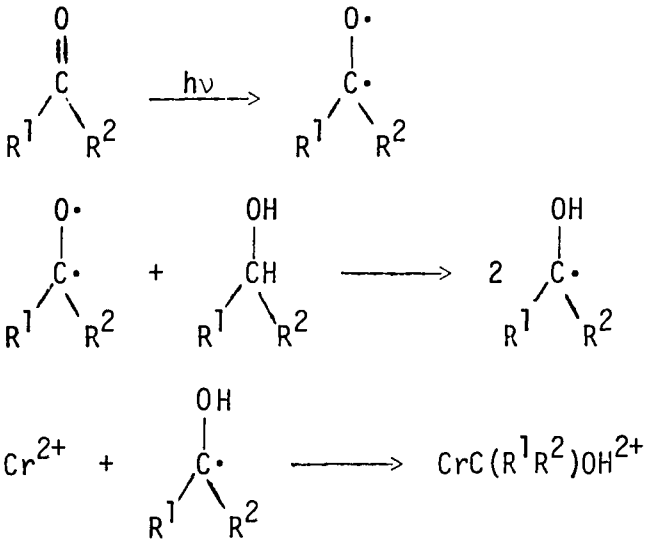

In Scheme 1-7, the first step corresponds to the excitation of the ketone to the triplet state (65-68), which may then abstract a hydrogen atom and combine with Cr^{2+} in the last step.

In some experiments in which no hydrogen donor was added to acetone solutions, it was likely that the acetone itself may act as a donor (68). Besides the chemistry shown in Scheme 1-7, a side reaction occurred in the experiments with 2-butanone to produce a species which reacted very much like $CrCH_2CH_3^{2+}$. This species was probably formed by the reaction of Cr^{2+} and ethyl radicals, the ethyl radicals presumably originating from the well-known α-cleavage of the excited-state triplet ketyl species (69).

Homolysis

Although a large number of pentaaquochromium(III) complexes have been characterized, the homolytic decomposition of these complexes has been previously investigated only for a variety of aralkyl complexes (17-24). We have found the homolysis of the chromium-carbon bond to be a general reaction of the α-hydroxyalkylchromium(III) and ether-derived complexes. In fact, the primary focus of this work was to study the homolysis reaction.

While researching the literature in preparation for this thesis, it became clear that many workers have previously recognized a need for more kinetic and thermodynamic data relating to metal-alkyl bonds (76, 77). The quantitative results of our kinetic study of the homolysis reaction allows a quantitative as well as qualitative discussion of chromium-carbon bond strengths to be made.

Using the homolysis rate constants in Table 1-5 and the k_{-1} values which were available in the literature (13), calculations of K_{eq} for the equilibrium shown in Equation I-26 were made (Table I-20).

$$Cr\text{-}C(R^1R^2)OH^{2+} \underset{k_{-1}}{\overset{k_{hom}}{\rightleftharpoons}} Cr^{2+} + \cdot C(R^1R^2)OR \qquad (I\text{-}26)$$

For those compounds for which k_{-1} has not been determined, an estimate was made based upon the degree of substitution on the α-carbon and a comparison with known k_{-1} values. These calculations of K_{eq} neglect a more detailed description of the homolysis reaction which would include a solvent-caged pair as a precursor to the free radical

formation. Usually solvent effects are less pronounced for radical-forming reactions than in analogous heterolytic reactions (78).

$$CrC(R,R')OR''^{2+} \underset{-1}{\overset{1}{\rightleftharpoons}} [Cr\cdots C(R,R')OR'']^{2+} \underset{-2}{\overset{2}{\rightleftharpoons}} Cr^{2+} + \cdot C(R,R')OR'' \qquad \text{(I-27)}$$

One must recognize, however, that involvement of the solvent in the transition state could be reflected in the activation barrier. If this caged intermediate were important in the homolysis of the Cr-C bond then by microscopic reversibility one would expect it to also be important in the formation of the Cr-C bond. This could possibly be tested by varying the viscosity of the solvent, but such experiments would probably not be very practical for experimental reasons with this series of complexes.

The values of the calculated equilibrium constants shown in Table I-21 indicate that for all of these complexes the equilibrium lies far to the left. This was not an unexpected result since the radical products of the decomposition of these complexes by chromium-carbon bond homolysis are less stable than the complexes themselves. These calculated equilibrium constants were used to make a linear free energy relationship (LFER) from a plot of log k_{hom} versus log K_{eq}. The plot yielded a satisfactory line with a slope of approximately 0.9 (Figure I-21). The fact that a straight line was obtained was not altogether surprising since we believe all of these complexes undergo homolysis in much the same way, by the S_H1 mechanism. Much more revealing perhaps was the slope of approximately unity. (One may also

Table I-21. Thermodynamic parameters for the homolysis reaction:

$$CrC(R^1R^2)OR^{2+} \underset{-1}{\overset{k_{hom}}{\rightleftharpoons}} Cr^{2+} + \cdot C(R^1R^2)OR$$

(#)	Complex	k^a_{hom}/s^{-1}	$k^b_{-1}/M^{-1}\ s^{-1}$	K_{eq}(calc)/M	$\Delta G^{\ddagger c}/kcal\ mol^{-1}$	$\Delta G^{\circ d}/kcal\ mol^{-1}$
	$Cr^{III}\text{-}R^{2+}$					
(1)	$CrCH_2OH^{2+}$	3.7×10^{-5}	1.6×10^{8}	2.3×10^{-13}	23.5	17.2
(2)	$CrCH(CH_3)OH^{2+}$	$(8.5 \pm 0.3) \times 10^{-4}$	7.9×10^{7}	1.1×10^{-11}	21.6	15.0
(3)	$CrCH(C_2H_5)OH^{2+}$	$(1.01 \pm 0.04) \times 10^{-3}$	$\sim 7.9 \times 10^{7*}$	1.3×10^{-11}	21.5	14.9
(4)	$CrC(CH_3)_2OH^{2+}$	0.127 ± 0.003	5.1×10^{7}	2.5×10^{-9}	18.7	11.7
(5)	$CrC(CH_3)(C_2H_5)OH^{2+}$	0.92 ± 0.03	$<5 \times 10^{7*}$	1.8×10^{-8}	17.5	10.6

[a] Values at 25.0°C.

[b] Reference 13; values at 22±2°C, (*) indicates estimated value.

[c] Values calculated from $\Delta G^{\ddagger} = -RT \ln k/6.21 \times 10^{12}\ s^{-1}$.

[d] Values calculated from $\Delta G^{\circ} = -RT \ln K_{eq}$.

Table I-21. (Continued)

(#)	Complex	k_{hom}^{a}/s^{-1}	$k_{-1}^{b}/M^{-1}\ s^{-1}$	K_{eq}(calc)/M	$\Delta G^{\ddagger c}$/kcal mol^{-1}	$\Delta G^{\circ d}$/kcal mol^{-1}
(6)	$CrC(C_2H_5)_2OH^{2+}$	8.39 ± 0.09	$<5 \times 10^{7*}$	1.7×10^{-7}	16.2	9.3
(7)	$CrC(CH_3)(i\text{-}C_3H_7)OH^{2+}$	21.6 ± 0.1	$<5 \times 10^{7*}$	4.3×10^{-7}	15.6	8.7
(8)	$Cr(CH_3)(t\text{-}C_4H_9)OH^{2+}$	≥ 300	$<5 \times 10^{7*}$	$\gtrsim 6 \times 10^{-6}$	~ 14.0	<7.2
(9)	$CrCH_2OCH_3^{2+}$	$\lesssim 10^{-6}$	$>3 \times 10^{7*}$	$\sim 10^{-14}$	$\gtrsim 25.6$	~ 19.0
(10)	$CrCH(CH_3)OC_2H_5^{2+}$	2.04×10^{-3}	3.4×10^{7}	6.0×10^{-11}	21.1	13.9
(11)	$CrC(CH_3)_2OCH(CH_3)_2^{2+}$	5.77 ± 0.15	$<3 \times 10^{7*}$	$\sim 2 \times 10^{-7}$	16.4	~ 9.0

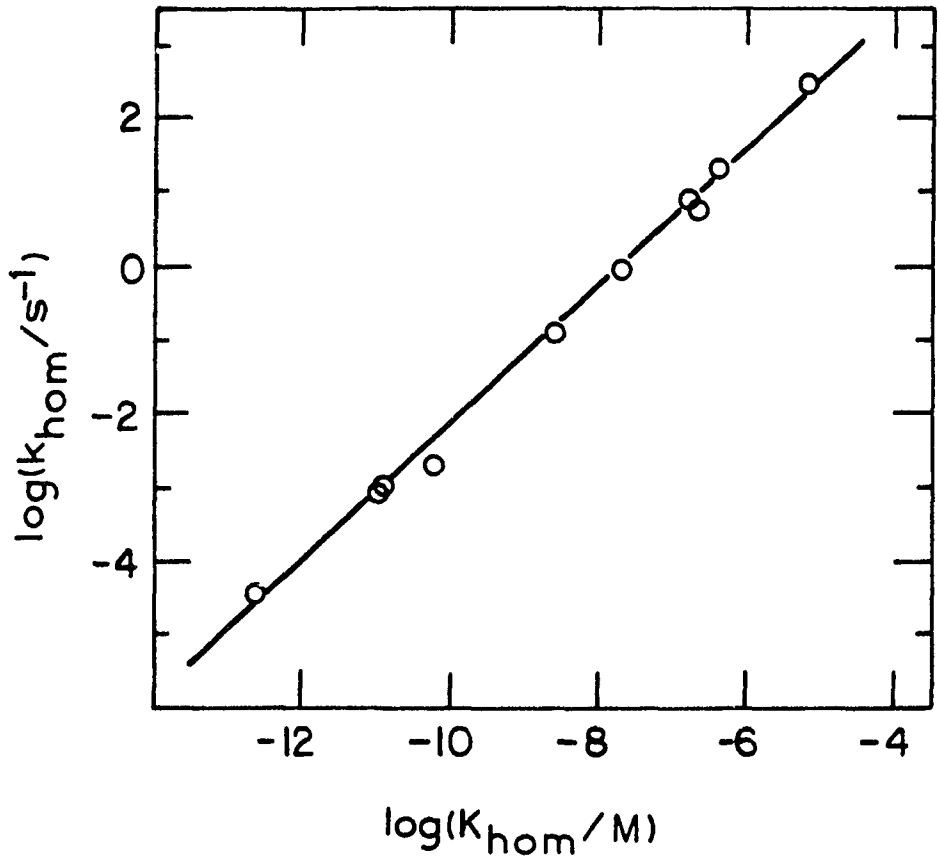

Figure I-21. Plot of log k versus log K for the homolysis reaction of the α-hydroxyalkylchromium(III) complexes

argue the linear fit with a slope of about one was required because of the small variation in k_{-1}.)

Langford made a similar plot for the results of various workers studying the aquation of $[Co(NH_3)X^{2+}]$ species (79) as in Equation I-28.

$$Co(NH_3)_5X^{2+} + H_2O \underset{k_{-28}}{\overset{k_{28}}{\rightleftharpoons}} Co(NH_3)_5H_2O^{3+} + X^- \qquad (I\text{-}28)$$

Langford reasoned that a plot of log k_{28} versus $K_{eq(28)}$ implied that the relationship shown in Equation I-29 must exist. The value of α is

$$\Delta\Delta G^{\ddagger} = \alpha \, \Delta\Delta G^{\circ} \qquad (I\text{-}29)$$

the slope of just such a plot and a value near one was proposed to indicate that the transition state should closely resemble the immediate products. In the case of the homolysis of the α-hydroxyalkylchromium(III) complexes, the value of α near unity suggests that the transition state closely resembles the products. The concept that the transition state for the chromium-carbon bond homolysis resembles Cr^{2+} and $\cdot R$ also is in harmony with Hammond's postulate. Hammond declared that for a highly endothermic reaction, such as a reaction producing free radicals, the transition state will closely resemble the products (80). It would seem that Hammond's postulate may be applied to the homolysis reaction as further support for the contention that the transition state closely resembles the products. One might view this transition state as being a loosely bound organic radical to a Cr(II)-like center.

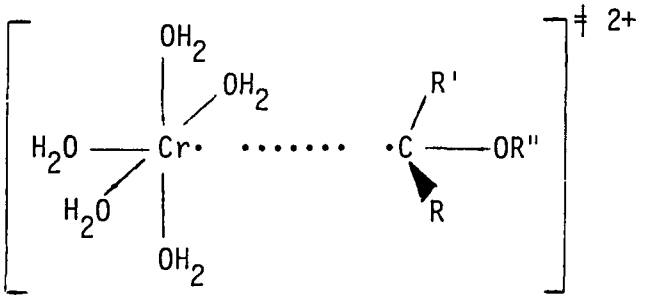

A further question, somewhat more subtle, concerns the possible role of an entering water ligand to complete the primary coordination sphere around the chromium(II) ion. Hammond (80) and Langford (79) both addressed this question. According to Hammond "...the entering group will be strongly bound in a transition state resembling the product only if the reaction is highly endothermic." Langford reasoned that for the aquation of the $[Co(NH_3)X^{2+}]$ complexes since $\Delta G^\circ \sim 0$, the entering water was at best only weakly bound in the transition state and thus favored a dissociative mechanism.

The values of ΔG° for the homolysis reactions of the α-hydroxyalkylchromium(III) complexes are greater than zero. If one considers these reactions "highly" endothermic in the sense meant by Hammond, the entering water ligand would have to be considered tightly bound in the transition state. Considering what is known about the system at hand, it seems likely that the entering water ligand is <u>not</u> tightly bound in the transition state. Several chemical facts speak to this point. First of all, the inorganic product of the homolysis reaction, Cr^{2+}, is a d^4 Jahn-Teller distorted ion in which two of the water molecules are weakly coordinated. The very fast water-exchange rate

of Cr^{2+} also points out how weakly bound the water ligands are. Secondly, one might expect the entering water ligand to favor a small or even negative entropy of activation as in the case of acidolysis (Table I-4), but all of the $\Delta S^{\ddagger}$ values measured for the homolysis reaction were highly positive. Finally, it may be concluded that an incoming water ligand would be only loosely bound due to steric constraints around the chromium-carbon bond (vide infra).

The activation parameters for the homolysis reactions of all of the complexes determined in this study are summarized in Table I-10. In general, these values have several rather interesting features. All of the complexes have a rather large, positive $\Delta S^{\ddagger}$. In simplest terms, this may be rationalized as resulting from a creation of greater disorder in forming the activated complex. This would seem to be consistent with the transition-state pictured on page 82. There also seems to be a trend to smaller absolute values of $\Delta S^{\ddagger}$ with the bulkier ligands. This may be due to an increase in the S° of the reactants in the ground state relative to the transition state, perhaps due to hydrophobic interactions with the solvent.

The enthalpies of activation, $\Delta H^{\ddagger}$, are also positive. This would be expected for a process involving the breaking of a metal-carbon bond. Furthermore, the magnitude of $\Delta H^{\ddagger}$ should be a reasonable estimate of the chromium-carbon bond strength. If the solvation of the organic radical and the entering of a sixth water molecule into the coordination sphere around Cr^{2+} do not contribute significantly to the $\Delta H^{\ddagger}$, and if the $\Delta H^{\ddagger}$ for the reverse process of Cr^{2+} and R· recombining

is estimated to be ∿0, then $\Delta H^{\ddagger}$ should indeed be a measure of the bond dissociation energy. We may view the reaction as proceeding along a reaction coordinate as shown in Figure I-22. Considering $\Delta H^{\ddagger}$ to be a good estimate of the strength of the chromium-carbon bond, it may be useful to consider the values we estimate from this study. The values of $\Delta H^{\ddagger}$ determined range from ∿32.0 to 21.6 kcal/mole. The next question seems obvious, are these reasonable bond energies? Although literature values seem scarce in the area of pentaaquoalkylchromium-(III) complexes, some other transition metal-carbon bond energies seem to fall into the same range. A few of these values are summarized below.

Complex	Estimated bond energy/kcal mol^{-1}
$(CO)_5MnCH_3$	∿30 (25.3 - 30.8) (Ref. 81,82)
$(CO)_5MnCH_2C_6H_5$	∿25 (Ref. 81)
$(CO)_5MnC(O)C_6H_5$	∿24 (Ref. 81)

Endicott et al. estimated the bond energies of cobalt-carbon bonds for a series of cobalt complexes of tetraaza macrocycles. Their estimates ranged from 33 to 47 kcal/mole, varying with the nature of the macrocycle (83). It would seem from these limited data that the bond strengths which we have estimated from our study are in reasonable agreement with some other first-row transition metal-carbon bonds.

The tremendous range of homolysis rates (∿10^8) prompted a consideration of the substituent effect on the homolysis rate. Substituent effects have been widely applied to organic reactions (84-86), but much less so for organometallic systems. One difficulty

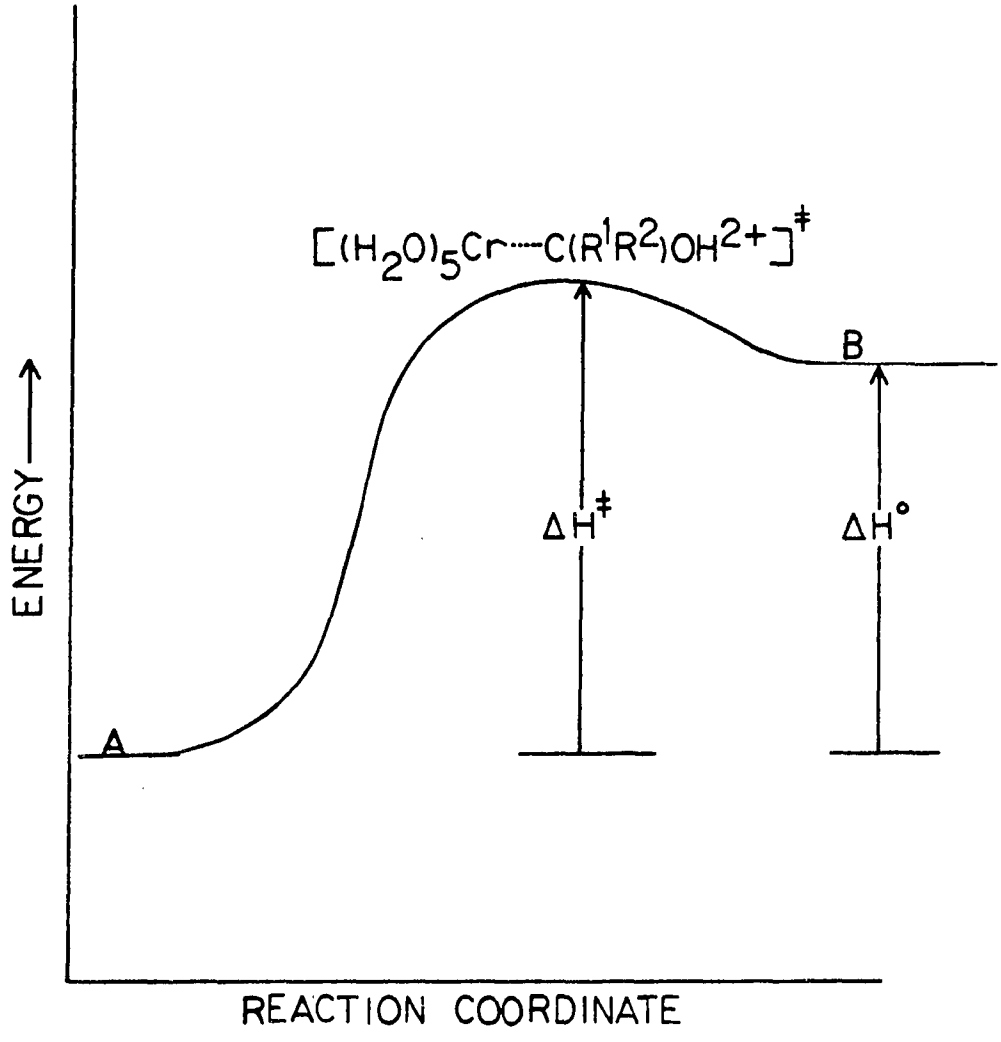

Figure I-22. Reaction coordinate diagram for the homolysis reactions; reactants at A, products at B

encountered in a consideration of substituent effects is a quantitative separation of the steric and electronic contributions. An attempt has been made to consider the substituent effects for homolysis of the Cr-C bond.

In a recent article, Rüchardt and Beckhaus reported a correlation between the free energy of activation for homolytic cleavage of C-C bonds and the strain enthalpy in the ground state (87). These workers were quite successful in sorting out the steric and electronic substituent effects for several homologous series of hydrocarbons. The strain enthalpy in the ground-state of the hydrocarbons was calculated by using force-field calculations (87). The strain enthalpy, H_{sp}, was defined as the difference between the standard enthalpy of formation in the gas phase and a calculated strain-free "normal heat of formation" (Ref. 87, p. 431). We have attempted to treat the homolytic cleavage of the Cr-C bond in an analogous manner to the Rüchardt and Beckhaus treatment of C-C homolytic cleavage. In order to treat the Cr-C system in an analogous manner, several assumptions had to be made. Because of the nature of the data available for the magnitude of the strain enthalpy in the ground state, it was necessary to assume that an -OH group was sterically similar to a $-CH_3$ group. This assumption is similar to one made by Rüchardt, wherein a -CN group was assumed to be sterically equivalent to a $-CH_3$ group (87).

A second assumption which was necessary involved the consideration of the inorganic portion of the complex. Since that portion of the complex (the Cr^{III} center and its five coordinated water molecules)

remains constant throughout the series, its contribution to the ground state strain enthalpy must be considered constant. This situation may be contrasted with the case of homolysis for the simply hydrocarbons which may be viewed as follows:

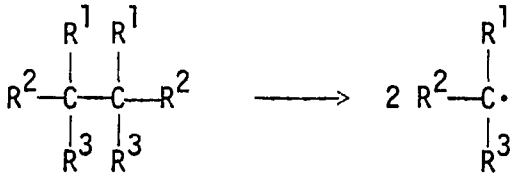

(I-29)

In this case, as the steric bulk of R^1, R^2 and R^3 increases, the bulk on <u>both</u> sides of the central C-C bond increases, whereas in the $CrC(R^1,R^2)OR^{2+}$ case, the inorganic portion of the complexes remains constant as R^1, R^2 and R^3 vary. To allow for this, the ground-

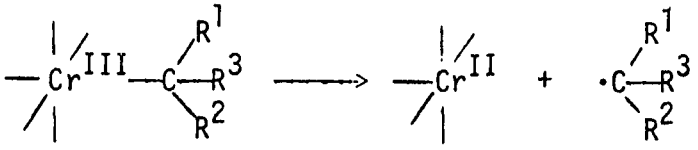

(I-30)

state strain enthalpy for the chromium(III) complexes is assumed to be proportional to the square-root of the ground-state strain enthalpy for the symmetrical hydrocarbons (Equation I-31). The values

$$\Delta G^{\ddagger}_{Cr\text{-}C} \propto \sqrt{H_{sp}} \qquad \text{(I-31)}$$

of $\Delta G^{\ddagger}$ and $\sqrt{H_{sp}}$ are summarized in Table I-22 and a plot of $\Delta G^{\ddagger}$ <u>versus</u> $\sqrt{H_{sp}}$ for the α-hydroxyalkylchromium(III) complexes has also been made (Figure I-23).

Table I-22. Estimation of the steric strain in $CrC(R^1,R^2)OR^{2+}$ complexes

Complex	R[a]	R^1	R^2	$\Delta G^{\ddagger}$ kcal/mol	$\sqrt{H_{sp}}$[b] $(kcal/mol)^{\frac{1}{2}}$
$CrCH_2OH^{2+}$	$-CH_3$	H	H	23.5	0
$CrCH(CH_3)OH^{2+}$	$-CH_3$	$-CH_3$	H	21.6	1.6
$CrCH(C_2H_5)OH^{2+}$	$-CH_3$	$-C_2H_5$	H	21.5	$\gtrsim$1.6
$CrC(CH_3)_2OH^{2+}$	$-CH_3$	$-CH_3$	$-CH_3$	18.7	2.6
$CrC(CH_3)(C_2H_5)OH^{2+}$	$-CH_3$	$-CH_3$	$-C_2H_5$	17.5	3.5
$CrC(C_2H_5)_2OH^{2+}$	$-CH_3$	$-C_2H_5$	$-C_2H_5$	16.2	4.5
$CrC(CH_3)(i\text{-}C_3H_7)OH^{2+}$	$-CH_3$	$-CH_3$	$i\text{-}C_3H_7$	15.6	4.7
$CrC(CH_3)(t\text{-}C_4H_9)OH^{2+}$	$-CH_3$	$-CH_3$	$t\text{-}C_4H_9$	$\sim$14.0	6.7
$CrCH_2OCH^{2+}$	$-C_2H_5$	-H	-H	$\sim$25.6	0.0
$CrCH(CH_3)OC_2H_5^{2+}$	$n\text{-}C_3H_7$	-H	$-CH_3$	21.1	$\gtrsim$1.6
$CrC(CH_3)OCH(CH_3)_2^{2+}$	$-CH_2CH(CH_3)_2$	$-CH_3$	$-CH_3$	16.4	4.15

[a] R is taken to be $-CH_3$ for an -OH group (see text DISCUSSION); for the ether complexes -OR is taken to be $-CH_2R$.

[b] These values were obtained by taking the square-root of the appropriate value in reference 87.

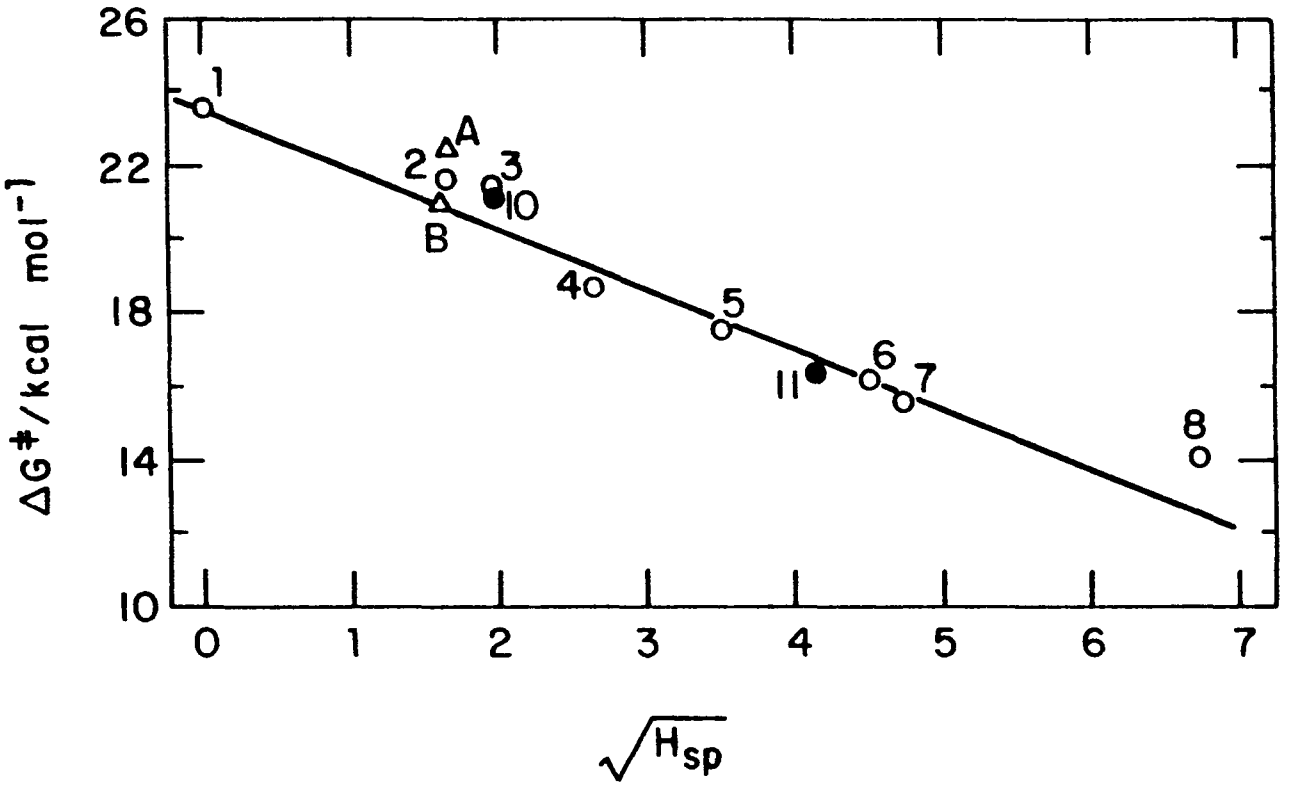

Figure I-23. Plot of $\Delta G^{\ddagger}$/kcal mol^{-1} versus $\sqrt{H_{sp}}$ for the homolysis reactions. The numbering scheme is from Table I-21; A refers to $CrCH(CH_3)_2^{2+}$, B refers to $CrCH_2C_6H_5^{2+}$

Although there is quite a degree of scatter in Figure I-23, there seems to be a good correlation between the $\sqrt{H_{sp}}$ and the $\Delta G^{\ddagger}$ for the homolysis of the Cr-C bond.

Because this analysis considers only the steric contributions of the organic ligand as the ligands become bulkier, it seems plausible that the steric substituent effects are dominant over electronic effects. This result seems rather surprising since one might expect that radical stabilities would also play a key role in determining the rate of homolysis. Clearly as the organic ligands become more bulky, the radical stabilities also increase due to increased delocalization of the odd electron. The presence of unpaired electrons on the oxygen atom also can be invoked in resonance structures which might help stabilize α-hydroxyalkyl radicals relative to simple alkyl radicals (88). If electronic effects also were important, one might expect a plot of log (k_1/k_0) versus Taft's σ* polar substituent parameter to be linear for the series of complexes studied here. In this equation,

$$\log \left(\frac{k}{k_o}\right) = \rho^*\sigma^* \qquad \text{(I-32)}$$

the σ* values are defined as Taft substituent constants for the electronic contribution of the substituents (89,90). The ρ* value may be evaluated from the slope of a plot of log (k/k_o) versus σ*. The significance of the ρ* value has been related to the mechanism of reactions (91).

Values of σ* were obtained from a recent compilation of substituent parameters (Table I-23) (92). A plot of log (k/k_o)

Table I-23. Taft substituent effect

Complex	σ^*[a]	k/s^{-1}	log (k/k_{CH_2OH})
Cr^{III}-CH_2OH	0.55 {+(0.51)}	3.7×10^{-5}	0.0
$-CH(CH_3)OH$	+0.46	8.5×10^{-4}	1.45
$-CH(C_2H_5)OH$	+0.45	1.0×10^{-3}	1.52
$-C(CH_3)_2OH$	+0.35 {(0.32)}	0.127	3.63
$-C(CH_3)(C_2H_5)OH$	+0.30	0.92	4.49
$-C(C_2H_5)_2OH$	+0.28	8.4	5.45
$-C(CH_3)(i\text{-}C_3H_7)OH$	+0.29	21.6	5.86
$-C(CH_3)(t\text{-}C_4H_9)OH$	+0.22	>300	7.0

[a] σ^* values from Ref. 92; numbers in parentheses indicate both values were listed.

versus σ^* is shown in Figure I-24. Although the data apparently correlate reasonably well with the Taft σ^* parameter, the value of ρ^* from the plot is calculated to be -25. This value is far from the range of normal ρ^* values, typically much less than 5. One might argue quite effectively that the correlation observed between log (k/k_o) and σ^* is mainly due to the fact that σ^* parallels the steric bulk of the substituents and, therefore, the correlation is

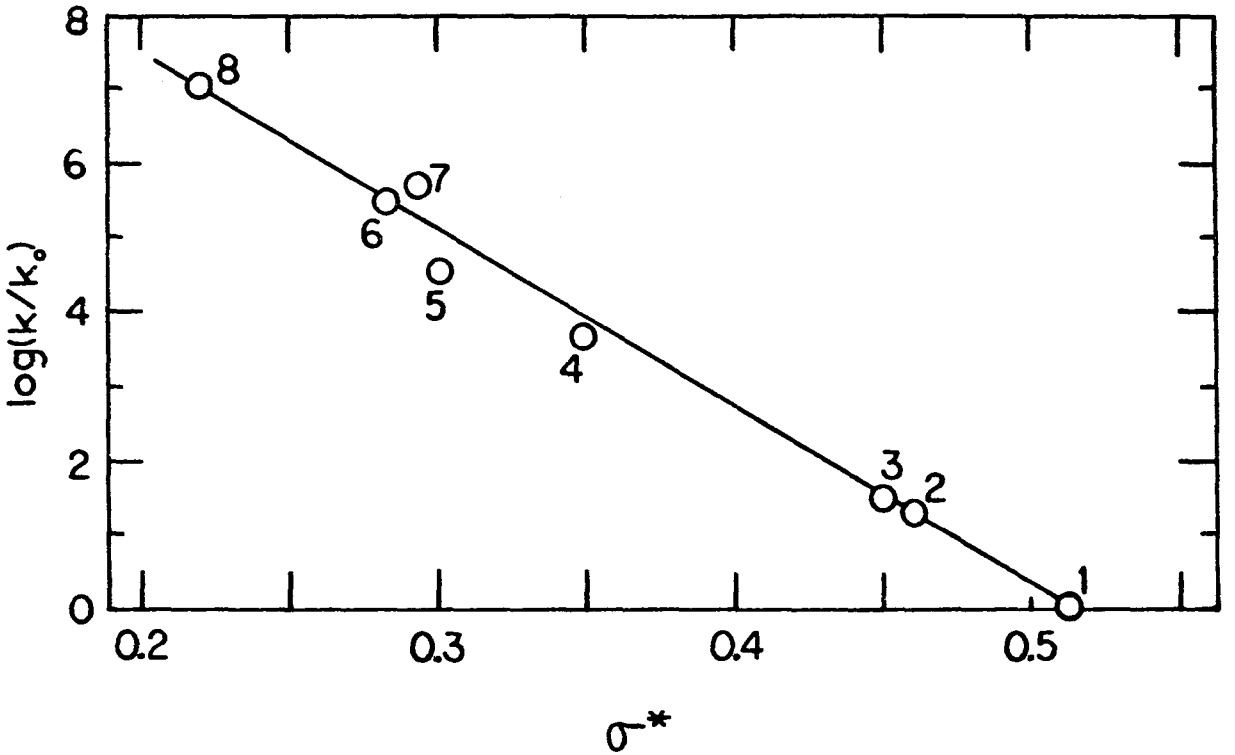

Figure I-24. Plot of attempted Taft correlation of homolysis rate constants. The numbering scheme is from Table I-21

really due to the steric effect once again. Others have commented on the general applicability of the Taft relation and the use of σ* values (93,94). It may well be that the Taft relation is simply not a good model for the reaction at hand. To test this idea, we considered homolysis of $CrCH(CH_3)_2^{2+}$, σ* for 2-propyl being -0.19 (84,92). If the electronic effects were dominant, one would expect to be able to plot the homolysis rate for $CrCH(CH_3)_2^{2+}$ in Figure I-24, and presumably it would be somewhere near the line. Actually, from Figure I-24 $CrCH(CH_3)_2^{2+}$ would be expected to have an extremely high homolysis rate, (as would $CrCH_3^{2+}$ and $CrC_2H_5^{2+}$), but $CrCH(CH_3)_2^{2+}$ has a known homolysis rate of 1.78×10^{-4} sec^{-1} (95) and $CrCH_3^{2+}$ and $CrC_2H_5^{2+}$ presumably homolyze so slowly that homolysis has not been detected as an important reaction. These "tests" of the applicability of the Taft relationship to this case seem to indicate that the correlation observed most probably exists due to the aforementioned parallel between steric and electronic factors in this reaction.

Having applied these "tests" to the attempted Taft correlation, it seems only fair that a similar test should be applied to the steric relationship already presented based upon the correlation between $\Delta G^{\ddagger}$ and $\sqrt{H_{sp}}$. Using a value of 1.6 for the $\sqrt{H_{sp}}$ for $CrCH(CH_3)_2^{2+}$, from Rüchardt's and Beckhaus' data (87), one would predict the homolysis rate from Figure I-25 to be between $\sim 10^{-3}$ and $\sim 10^{-4}$ sec^{-1}, in excellent agreement with the experimental value already quoted. One also would predict $CrCH_3^{2+}$ and $CrCH_2CH_3^{2+}$ to be <u>very</u> stable towards homolysis as they indeed are. In fact, although the exact H_{sp} values for a $-CH_2Ø$

substituent are not available in reference 87, one may estimate from the data available that H_{sp} for $-CH_2\emptyset$ would be $\sim$3, and therefore the $\sqrt{H_{sp}}$ for this substituent would be $\sim$1.7, once again predicting a homolysis rate of $\sim 10^{-3}$ sec^{-1} from Figure I-26, again in very good agreement with the experimentally determined value of 2.6×10^{-3} sec^{-1} (17).

In conclusion, we have examined the cleavage of the chromium-carbon bond by two modes, heterolytic and homolytic. The heterolytic mode, acidolysis, indicated that the bulky organic ligands were more susceptible to acidolysis than the smaller, less substituted organic groups. A similar finding was made for the homolytic reactions of the α-hydroxyalkylchromium(III) and α-alkoxyalkylchromium(III) complexes. We have found a correlation between the rate of homolysis and the degree of strain induced in the ground state by steric interactions between the substituents on C_α and, presumably, the water molecules in the cis positions on the chromium(III) center. Space-filling models show a particularly strong degree of interaction when isopropyl or tert-butyl groups are substituted on C_α in conjunction with a methyl group. These are also the two complexes which are the least stable towards homolysis. More studies of this kind are needed to generate sufficient data to further separate both steric and electronic effects in regard to the metal-alkyl bond.

B. REACTIONS WITH Cu^{2+} OR Fe^{3+}

INTRODUCTION

This section of the thesis deals with the reactions of Cu^{2+} and Fe^{3+} with the α-hydroxyalkylchromium(III) complexes which were introduced in the preceding section. Bakač and Espenson have recently reported the reactions of Cu^{2+} and Fe^{3+} with a number of α-hydroxyalkylchromium(III) complexes (16,42). Some of their findings will be introduced to lay a foundation for a discussion of the results found here. Because the scope of this investigation was limited to a kinetic study, the reaction stoichiometry and products were presumed to be analogous to what was found in the prior study (42).

The following stoichiometry, Equation I-33, was previously determined for the reaction of Fe^{3+} with $CrCH_2OH^{2+}$ (16,42). It was

$$2\ Fe^{3+} + CrCH_2OH^{2+} \longrightarrow 2\ Fe^{2+} + Cr^{3+} + H^+ + HCHO \quad (I\text{-}33)$$

also shown that Cr^{2+} is formed as an intermediate which quickly reacts with Fe^{3+} in a redox reaction. A 2:1 stoichiometry was also found for Cu^{2+} reactions.

These reactions of Cu^{2+} and Fe^{3+} with α-hydroxyalkylchromium(III) complexes are unique among organochromium chemistry. Simple alkylchromium(III) complexes do not react with oxidants. (It should be noted, however, that isopropylchromium does react with oxygen (96)). Even the aralkylchromium(III) complexes only react with oxidants indirectly <u>via</u> homolysis (17-23).

An attempt will be made to explain these differences in reactivity for organochromium complexes. Mechanisms will also be presented in an attempt to adequately describe the Cu^{2+} and Fe^{3+} reactions with α-hydroxyalkylchromium(III) complexes.

EXPERIMENTAL

Materials

Reagents

Organochromium complexes The organochromium complexes used in this study: $CrCH(C_2H_5)OH^{2+}$, $CrC(CH_3)(C_2H_5)OH^{2+}$, $CrC(CH_3)(i\text{-}C_3H_7)OH^{2+}$ and $CrC(C_2H_5)_2OH^{2+}$ were prepared by the modified Fenton's reagent method as described in Part I.A. The characterization of these complexes has also been treated in the first section.

Inorganic reagents Most of the inorganic reagents used were introduced in the first section. Those reagents which were not previously introduced are cited here.

Copper(II) perchlorate solutions A stock solution of $Cu(ClO_4)_{2\,aq}$ was prepared by dissolving CuO wire (Fisher Scientific Co.), containing a solid copper metal core, in $HClO_4$ ($\sim$3 M) over a period of several days. After the CuO had dissolved, the remaining metal residue was filtered off and the mother liquor, $Cu(ClO_4)_{2\,aq}$ solution, collected. The solution was then clarified with diatomaceous earth which was subsequently removed by filtration. Alternatively, $Cu(ClO_4)_{2\,aq}$ solutions were prepared by dissolving the solid hydrate in perchloric acid (G. F. Smith), with identical results being obtained regardless of the method of preparation.

Iron(III) perchlorate solutions Solutions of $Fe(ClO_4)_3$ in $HClO_4$ were prepared and analyzed by a standard literature procedure (97). Alternatively, solutions were prepared by dissolving the

$Fe(ClO_4)_3$ hydrate (G. F. Smith Co.) with identical results obtained.

Methods

Analyses

The concentrations of organochromium species were usually estimated from absorbance measurements. The Cu^{2+} concentration was determined iodometrically and the $[H^+]$ in Cu^{2+} solutions was determined directly using standard base and bromphenol blue indicator. All other routine analyses were described in the first section.

Kinetics

The Cu^{2+} or Fe^{3+} reactions with the α-hydroxyalkylchromium(III) complexes were followed spectrophotometrically at a convenient wavelength, usually near 400 nm. The experiments were carried out under an atmosphere of Cr^{2+}-scrubbed nitrogen. Standard syringe techniques were used for transferring solutions anaerobically.

Kinetic data were obtained with Cu^{2+} or Fe^{3+} in at least a twenty-fold excess. Under these conditions, pseudo-first-order plots of ln (D_t-D_∞) *versus* time were typically linear for three half-lives. For most stopped-flow experiments, the data were automatically digitized and transferred to a PDP-15 computer for a least-squares treatment. Kinetic data for each complex were collected at 1.00 M ionic strength using $LiClO_4$. Rate constants were evaluated as a function of $[Cu^{2+}]$ or $[Fe^{3+}]$ at several acidities.

RESULTS

The kinetic data, which were collected as pseudo-first-order rate constants, were manipulated in the following manner. Data were collected at three or more acid concentrations for a given complex. At a particular acid concentration, the excess reagent, Cu^{2+} or Fe^{3+}, was also varied over a range limited by ionic strength. Plots of k_{obs} *versus* [oxidant] at a given $[H^+]$ were linear, and the slopes of these plots yielded second-order rate constants. Plots of second-order rate constants *versus* $1/[H^+]$ were also linear. The following general rate law is thus obeyed:

$$\frac{-d[CrC(R^1R^2)OH^{2+}]}{dt} = (k_o + \frac{k'}{[H^+]}) [CrC(R^1R^2)OH^{2+}][Ox] \qquad (I\text{-}34)$$

This is the same rate law which was previously found for the less substituted α-hydroxyalkylchromium(III) complexes (42). All of the data were routinely treated by least-squares analysis. The values of k and k' were determined from the plots of second-order rate constants *versus* $1/[H^+]$. Invariably, the acid-dependent pathway was found to be dominant. The kinetic data for each complex are summarized in Tables I-24 through I-31. A final summary of the values of k_o and k' for each complex is presented in Table I-32.

The slowest reacting species was $CrCH(C_2H_5)OH^{2+}$, which was also the only complex prepared from a primary alcohol. Both the Cu^{2+} and Fe^{3+} rate constants for this complex were in the range of what was previously found for other members of this series (see Table I-32). The remaining complexes studied show a steady increase in the

Table I-24. Kinetic data for the reaction of Cu^{2+} with $CrCH(C_2H_5)OH^{2+}$[a]

$[H^+]$/M	$[Cu^{2+}]$/M	k_{obs}/s^{-1}	$k_{Cu^{2+}}/M^{-1}s^{-1}$[b]
0.10 M	0.10	1.210±0.013(5)	11.9±0.4
	0.05	0.643±0.003(5)	
	0.04	0.511±0.003(5)	
	0.02	0.245±0.004(5)	
0.20 M	0.10	0.691±0.005(5)	6.7±0.2
	0.05	0.349±0.006(5)	
	0.04	0.299±0.006(5)	
	0.02	0.148±0.002(5)	
0.40 M	0.10	0.421±0.002(5)	3.96±0.3
	0.075	0.336±0.003(6)	
	0.05	0.223±0.003(5)	

[a]Experiments at 1.00 M ionic strength ($LiClO_4$); $[Cr^{2+}]_o$ = $\sim 1 \times 10^{-3}$ M.

[b]Second-order rate constants calculated from the slope of k_{obs} versus $[Cu^{2+}]$. Values in parentheses represent the number of replicate determinations.

Table I-25. Kinetic data for the reaction of Fe^{3+} with $CrCH(C_2H_5)OH^{2+}$[a]

$[H^+]$/M	$[Fe^{3+}]$/M	k_{obs}/s^{-1}[b]	$k_{Fe^{3+}}/M^{-1}s^{-1}$
0.50	0.018	0.232±0.003(3)	
	0.028	0.294±0.01(3)	
	0.038	0.385±0.02(4)	
	0.048	0.458±0.01(4)	9.3±0.7
0.10	0.018	0.110±0.005(4)	
	0.028	0.161±0.002(6)	
	0.038	0.222±0.003(4)	
	0.048	0.254±0.001(4)	
	0.058	0.337±0.017(4)	5.5±0.2
0.20	0.018	0.067±0.002(6)	
	0.028	0.0938±0.0015(4)	
	0.048	0.148±0.003(6)	2.96±0.15

[a]At 25.0°C and 1.0 M ionic strength; all values in 1 M 2-propanol.

[b]Values in parentheses represent the number of replicate determinations.

Table I-26. Kinetic data for the reaction of Cu^{2+} with $CrC(CH_3)(C_2H_5)OH^{2+}$[a]

$[H^+]$/M	$[Cu^{2+}]$/M	k_{obs}/s^{-1}[b]	$k/M^{-1}s^{-1}$
0.090	0.10	2.58±0.04(7)	
	0.080	2.33±0.03(8)	
	0.040	1.68±0.04(8)	
	0.020	1.33±0.05(8)	15.9
0.10	0.10	2.36±0.06(11)	
	0.080	2.16±0.03(8)	
	0.040	1.54±0.04(7)	
	0.020	1.20±0.02(8)	14.9
0.12	0.10	2.09±0.03(7)	
	0.080	1.96±0.02(7)	
	0.040	1.42±0.01(7)	
	0.20	1.18±0.02(6)	11.9
0.15	0.10	2.02±0.04(16)	
	0.080	1.83±0.02(14)	
	0.40	1.46±0.02(14)	
	0.020	1.24±0.01(8)	9.8
0.30	0.10	1.32±0.02(10)	
	0.089	1.27±0.03(11)	
	0.075	1.22±0.01(5)	
	0.040	1.06±0.01(8)	
	0.020	0.98±0.01(8)	4.3
0.50	0.080	1.29±0.05(11)	
	0.050	1.21±0.03(6)	
	0.020	1.09±0.03(7)	3.25

[a]At 25.0°C and 1.0 M ionic strength; all values in 1 M 2-butanol.

[b]Values in parentheses represent the number of replicate determinations.

Table I-27. Kinetic data for the reaction of Fe^{3+} with $CrC(CH_3)(C_2H_5)OH^{2+}$[a]

$[H^+]$/M	10^2 $[Fe^{3+}]$/M	k_{obs}/s^{-1}[b]	$k_{Fe^{3+}}/M^{-1}s^{-1}$
0.10 M	6.9	10.03±0.07(6)	
	4.9	7.27±0.04(7)	
	2.4	4.08±0.03(7)	132±3
0.20 M	5.9	5.01±0.14(8)	
	3.9	3.67±0.01(7)	
	2.4	2.66±0.03(7)	67±0.1
0.30 M	4.4	3.09±0.01(7)	
	2.9	2.43±0.02(8)	
	1.4	1.75±0.01(7)	44.7±0.4

[a]At 25.0°C and 1.0 M ionic strength; all values in 1 M 2-butanol.

[b]Values in parentheses represent the number of replicate determinations.

Table I-28. Kinetic data for the reaction of Cu^{2+} with $CrC(C_2H_5)_2OH^{2+}$[a]

$[H^+]$/M	10^2 $[Cu^{2+}]$/M	k_{obs}/s^{-1}[b]	$k_{Cu^{2+}}/M^{-1}s^{-1}$
0.115	3.9	9.58±0.1(6)	
	7.4	10.64±0.06(8)	
	14.9	12.90±0.3(7)	30.17±0.04
0.15	3.9	9.63±0.05(5)	
	7.4	10.35±0.12(7)	
	14.3	11.94±0.15(5)	22.3±0.6
0.30	2.4	8.90±0.05(8)	
	5.9	9.37±0.09(7)	
	9.9	9.71±0.08(7)	10.80±1.4

[a]At 25.0°C and 1.0 M ionic strength; solvent was saturated with 3-pentanol (∿0.05 - 0.1 M).

[b]Values in parentheses represent the number of replicate determinations.

Table I-29. Kinetic data for the reaction of Fe^{3+} with $CrC(C_2H_5)_2OH^{2+a}$

$[H^+]$/M	$[Fe^{3+}]$/M	k_{obs}/s^{-1}[b]	$k_{Fe^{3+}}/M^{-1}s^{-1}$
0.125	0.073	33.4±0.7(7)	
	0.073	31.5±0.5(5)	
	0.048	24.6±0.3(5)	
	0.038	21.9±0.3(5)	
	0.023	17.1±0.2(4)	306±18
0.20	0.063	21.8±0.5(8)	
	0.038	17.2±0.2(6)	
	0.023	13.8±0.2(7)	198±11
0.30	0.048	16.4±0.3(6)	
	0.038	14.1±0.2(7)	
	0.023	12.1±0.3(5)	169±26

[a]At 25.0°C and 1.0 M ionic strength; solvent was saturated with 3-pentanol (∿0.05 - 1.0 M).

[b]Values in parentheses represent the number of replicate determinations.

Table I-30. Kinetic data for the reaction of Cu^{2+} with $CrC(CH_3)(i\text{-}C_3H_7)OH^{2+a}$

$[H^+]$/M	$[Cu^{2+}]$/M	k_{obs}/s^{-1}[b]	$k_{Cu^{2+}}/M^{-1}s^{-1}$
0.05	0.158	57.0±2.0(12)	
	0.08	38.6±0.4(7)	
	0.04	28.9±0.3(6)	
	0.02	24.2±0.1(7)	240.9±0.6
0.10	0.149	39.3±0.8(6)	
	0.074	30.1±0.3(7)	
	0.029	24.3±0.3(7)	
	0.019	22.2±0.1(7)	126.3±1.9
0.25	0.099	26.3±0.4(8)	
	0.059	24.33±0.07(6)	
	0.024	22.2±0.1(7)	58.6±0.7
0.30	0.079	24.92±0.09(6)	
	0.039	23.06±0.10(8)	
	0.019	21.74±0.06(7)	52.1±6.2

[a]At 25.0°C and 1.0 M ionic strength; solvent was saturated with 3-methyl-2-butanol.

[b]Values in parentheses represent the number of replicate determinations.

Table I-31. Kinetic data for the reaction of Fe^{3+} with $CrC(CH_3)(i\text{-}C_3H_7)OH^{2+a}$

$[H^+]/M$	$[Fe^{3+}]/M$	k_{obs}/s^{-1}[b]	$k_{Fe^{3+}}/M^{-1}s^{-1}$
0.10	0.039	102.1±1.5(8)	
	0.019	62.6±1.0(8)	
	0.014	51.2±0.5(7)	2018.6
0.20	0.05	70.8±0.7(6)	
	0.04	61.5±0.7(3)	
	0.02	42.3±0.8(4)	951.4
0.40	0.035	38.5±0.5(7)	
	0.0215	32.5±0.3(7)	
	0.014	28.7±0.21(7)	464.0

[a]At 25.0°C and 1.0 M ionic strength; solvent was saturated with 3-methyl-2-butanol.

[b]Values in parentheses represent the number of replicate determinations.

Table I-32. Parameters for the dependence of oxidation rate constants on $[H^+]$

Complex	$k_{Cu}/M^{-1}\ s^{-1}$ =		$k_{Fe}/M^{-1}\ s^{-1}$ =	
	k_o	k'/H^+	k_o	k'/H^+
$CrCH_2OH^{2+}$ [a]	0.036(7)	0.251(3)	0.22(1)	0.496(6)
$CrCH(CH_3)OH^{2+}$ [a]	0.68(12)	1.46(5)	0.71(2)	0.481(5)
$CrC(CH_3)_2OH^{2+}$ [a]	0.77(4)	0.574(13)	3.79(34)	1.90(8)
$CrCH(CF_3)OH^{2+}$ [a]	2×10^{-4}		0	0.127(1)
$CrCH(CH_3)OC_2H_5^{2+}$ [a]	n.r.		0.082(7)	0.040(21)
$CrCH_2OCH_3^{2+}$ [a]	n.r.		0.0062(18)	0.0127(5)
$CrC(CH_3)_2OCH(CH_3)_2^{2+*}$ [b]	n.r.		n.r.	
$CrCH(C_2H_5)OH^{2+}$ [b]	1.36(9)	1.06(1)	1.1(5)	0.42(3)
$CrC(CH_3)(C_2H_5)OH^{2+}$ [b]	0.0(4)	1.46(10)	1.4(6)	13.07(6)
$CrC(C_2H_5)_2OH^{2+*}$ [b]	0.0(7)	3.3(1)	60(28)	30(5)
$CrC(CH_3)(i\text{-}C_3H_7)OH^{2+*}$ [b]	13.5(7)	11.36(6)	0.0(12)	193(8)

[a] At 24.8°C and 1.0 M ionic strength; References 16 and 42.

[b] This work, at 25.0 ± 0.1°C; 1.0 M ionic strength and 1.0 M alcohol, complexes denoted by (*) were in aqueous solutions saturated with alcohol or ether. Values in parentheses represent the uncertainty (standard deviations) in the last significant digit.

acid-dependent term, especially the Fe^{3+} reactions, which parallel the increase in substitution at the α-carbon. Thus, the acid-dependent term increases almost 500 fold going from $CrCH(C_2H_5)OH^{2+}$ to $CrC(CH_3)(i\text{-}C_3H_7)OH^{2+}$. The experiments with $CrC(CH_3)_2OCH(CH_3)_2^{2+}$ showed no direct reaction with either Cu^{2+} or Fe^{3+}. The homolysis reaction observed upon reaction with Cu^{2+} or Fe^{3+} has been dealt with in the first section. This is similar to the type of reactivity found for other ether-derived complexes (Table I-32).

Some representative plots of k_{obs} versus [oxidant] are shown (Figures I-25 and I-26) for reactions of Fe^{3+} with $CrC(CH_3)(C_2H_5)OH^{2+}$ and $CrC(CH_3)(i\text{-}C_3H_7)OH^{2+}$. Similar plots were made from the other complexes and for reactions with Cu^{2+}. The linear dependence of the second order rate constants with $[H^+]^{-1}$ is also shown for the same two complexes reacting with Fe^{3+} (Figures I-27 and I-28). The intercepts of the plots of k_{obs} versus [oxidant] approximate the first order homolysis rate constants (see Homolysis, in the previous section). Since the values of the homolysis rate constants are characteristic of a particular complex, these intercepts further substantiate that the reactions which were followed were those of the α-hydroxalkylchromium-(III) species and not of some other species.

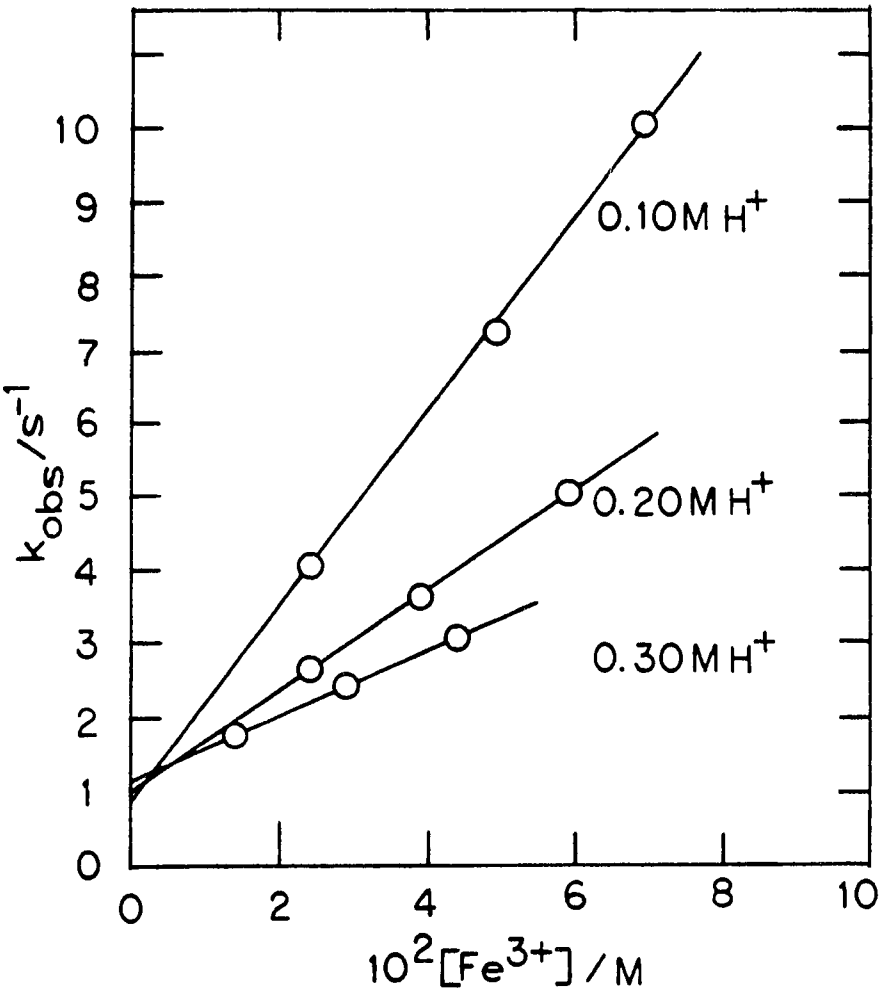

Figure I-25. Plot of k_{obs} versus $[Fe^{3+}]$ for reactions with $CrC(CH_3)(C_2H_5)OH^{2+}$ at 0.10, 0.20, and 0.30 M $HClO_4$; at 25.0°C and μ = 1.00 M ($LiClO_4$)

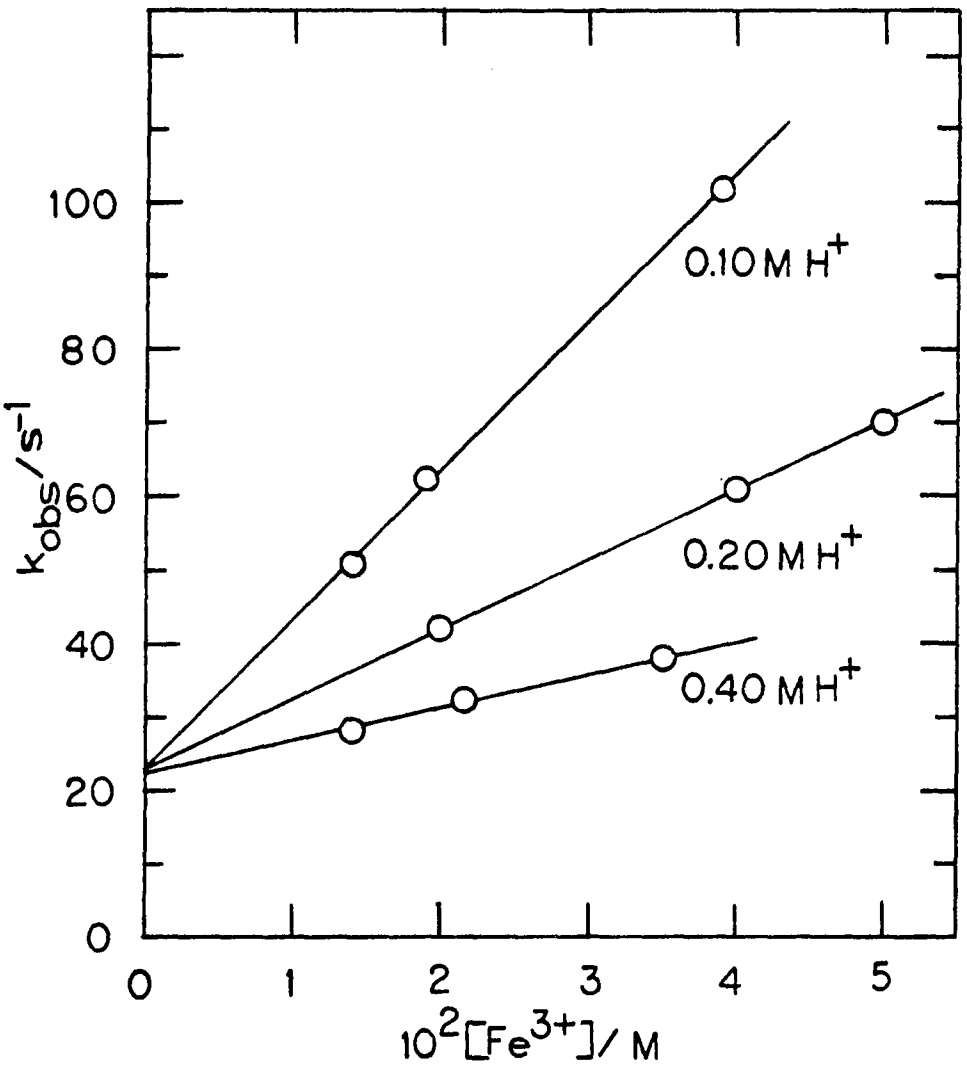

Figure I-26. Plot of k_{obs} versus $[Fe^{3+}]$ for reactions with $CrC(CH_3)(i\text{-}C_3H_7)OH^{2+}$ at 0.10, 0.20, and 0.40 M $HClO_4$; at 25.0°C and μ = 1.00 M ($LiClO_4$)

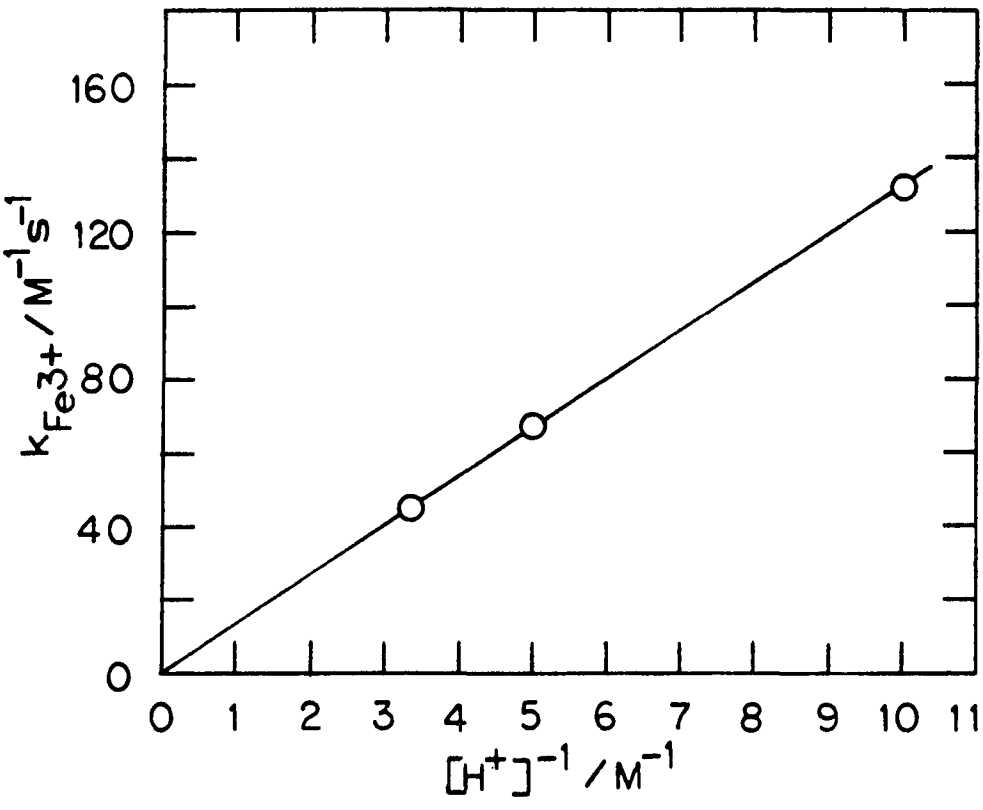

Figure I-27. Plot of $k_{Fe^{3+}}$ <u>versus</u> $[H^+]^{-1}$ for reactions of Fe^{3+} with $CrC(CH_3)(C_2H_5)OH^{2+}$ at 25.0°C and μ = 1.00 M ($LiClO_4$)

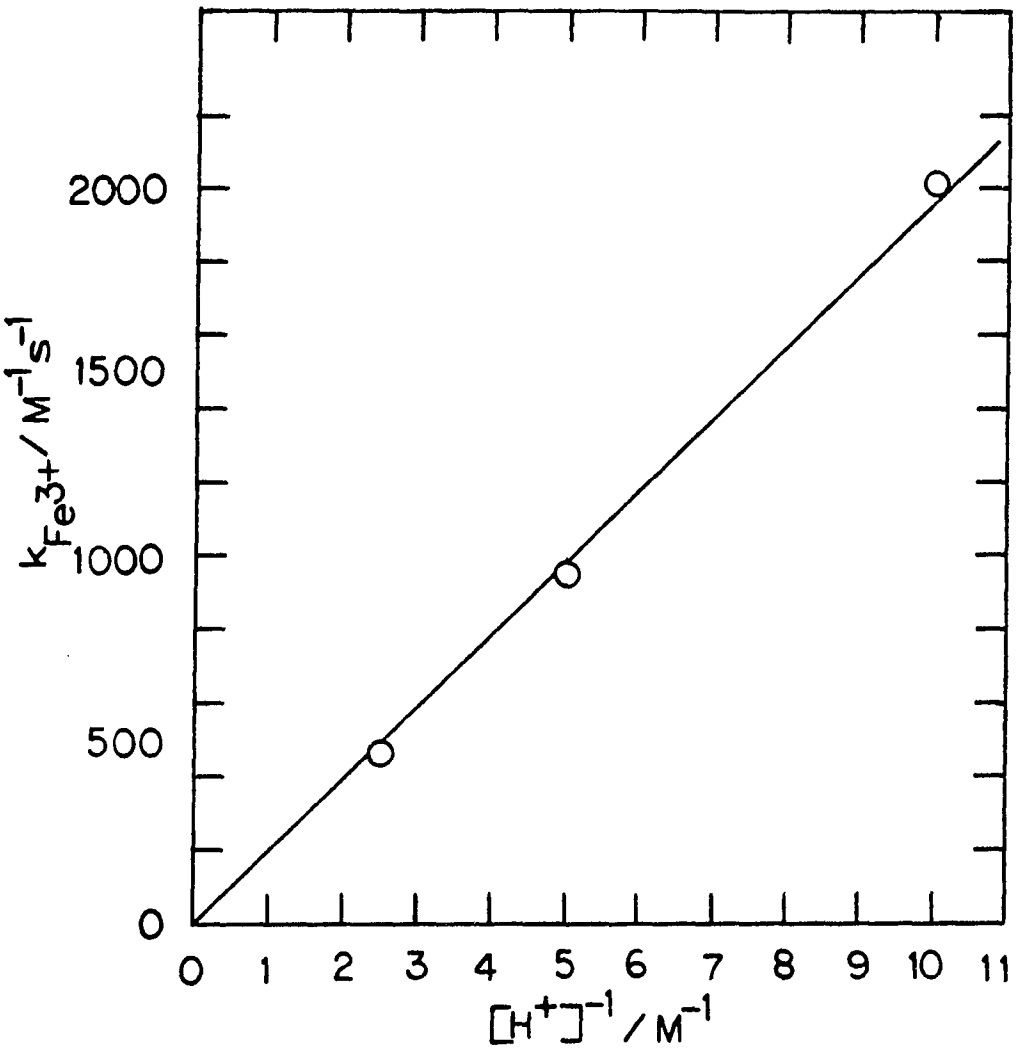

Figure I-28. Plot of $k_{Fe^{3+}}$ <u>versus</u> $[H^+]^{-1}$ for reactions of Fe^{3+} with $CrC(CH_3)(i\text{-}C_3H_7)OH^{2+}$ at 25.0°C and μ = 1.00 M ($LiClO_4$)

DISCUSSION

Earlier work with the Fe^{3+}_{aq} and Cu^{2+}_{aq} oxidation of α-hydroxyalkylchromium(III) complexes has clearly established the stoichiometry, products and general course of the reaction. With the added kinetic information gained from this study, an attempt will be made to present mechanisms for these oxidation reactions. Because of the transient nature of the species studied here, an assumption has been made that the products formed are analogous to those found in earlier studies.

The mechanisms proposed here are an attempt to explain the facts presently known for Cu^{2+}_{aq} and Fe^{3+}_{aq} oxidations of $CrC(R^1R^2)OH^{2+}$ complexes. The two most probable mechanisms are presented along with some alternative schemes. The possibility that Cu^{2+} and Fe^{3+} react by different pathways is also explored. However, like any proposed mechanism, these cannot be proven to be correct and are open to future revision when and if new findings are made.

One of the more striking mechanistic clues available in this study is the predominant pathway which is dependent on $[H^+]^{-1}$. This pathway requires ionization of a proton from one of the reactive species in forming the transition state. Unfortunately, there are several sites on the reactive species from which a proton may ionize. The most logical possibilities would seem to be: (1) a water molecule coordinated to Cu^{2+}_{aq} or Fe^{3+}_{aq}, (2) a water molecule coordinated to the organochromium species, or (3) the proton on the -OH group of the α-hydroxyalkyl ligand.

The first possibility would seem quite reasonable for Fe^{3+} which has a pK_a of 2.78 under the conditions used here (98). For Cu^{2+}, which has a pK_a ~8, ionization of a proton would be much less favorable. Also, the value of K_a is part of the rate expression if a water molecule on Cu^{2+}_{aq} is ionized, placing constraints on the values of other rate constants which seem to be unreasonable. Ionization of a proton from a water molecule coordinated to the Cr^{III} center would also be a possibility, and will also be considered in discussing the possible mechanisms. Finally, an additional site for proton ionization exists in these complexes and that is the -OH group of the α-hydroxyalkylchromium(III) complexes. The pK_a values for some α-hydroxyalkyl radicals are known to be ~10-14 (Ref. 12, p. 211). The ligation to a Cr^{III} center would be expected to lower the pK_a for these groups markedly (Ref. 75, pp. 316-319). Therefore, the -OH group must also be considered as a possible site for the proton ionization.

As we have just seen, there are several sites which all seem to be possible sites of the proton ionization which would account for the $[H^+]^{-1}$ term in the rate expression. The ambiguity associated with the site of proton ionization is the main stumbling block to establishing the reaction mechanisms for the Cu^{2+} and Fe^{3+} reactions. The vexing problem of several sites which may account for a $[H^+]^{-1}$ term in the rate expression has been recognized by many investigators (Ref. 75, pp. 69-71, and references cited).

Let us explore the third possibility first. If the site of proton ionization were the hydroxyl group of the hydroxyalkyl ligand,

then presumably the metal ion oxidants (Cu^{2+}, Fe^{3+}) may bind at this site. A possible scheme for this pathway is shown below for the case with Cu^{2+} as the oxidant. The rate law for this scheme, using the

Scheme I-8

$$Cu^{2+}_{aq} + (H_2O)_5CrC(R^1R^2)OH^{2+} \underset{k_{-1}}{\overset{k_1}{\rightleftharpoons}} [(H_2O)_5CrC(R^1R^2)OCu^{3+}] + H^+ \quad (I\text{-}35)$$

$$[(H_2O)_5CrC(R^1R^2)OCu^{3+}] \xrightarrow{k_2} Cr^{2+} + Cu^+_{aq} + (R^1R^2)C{=}O \quad (I\text{-}36)$$

steady-state approximation for the intermediate, is

$$\frac{-d[CrC(R^1R^2)OH^{2+}]}{dt} = \frac{k_1k_2[CrC(R^1R^2)OH^{2+}][Cu^{2+}]}{k_{-1}[H^+] + k_2} \quad (I\text{-}37)$$

If $k_{-1}[H^+] >> k_2$, then this rate law has the same form as the apparent rate constant obtained from experimentation. This mechanism seems quite reasonable for Cu^{2+}_{aq} which has very labile waters and fast substitution rates which are nearly diffusion-controlled ($t_{\frac{1}{2}} \sim 10^{-8}$ sec (99)). This mechanism is the same one proposed earlier by Bakac and Espenson (16,42). It should be noted that there are other mechanisms which also seem plausible for the Cu^{2+} reactions. Briefly, one could envision reaction of Cu^{2+}_{aq} with a $HOCr(H_2O)_4C(R^1R^2)OH^{2+}$ species, in which the transition state could resemble that shown below. The rate law would have the same form as the kinetic data and must be considered a possible pathway. The mechanism shown in Scheme I-8 is tentatively favored for the Cu^{2+} reactions on the grounds that the range of rate

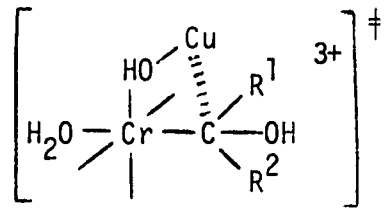

constants is rather narrow. In addition, the α-alkoxyalkyl complexes do not react at all with Cu^{2+}. These are just what this mechanism would predict. These are admittedly not conclusive arguments for that assignment, however, and proton ionization from another site cannot be ruled out.

On the other hand, Scheme I-8 can be ruled out for the Fe^{3+} reaction because of the slow substitution rates of water molecules coordinated to Fe^{3+}. This can be shown by rearranging Equation I-37 to the form (with Fe^{3+} substituted for Cu^{2+}):

$$k_{obs} = \frac{k_1 k_2 [Fe^{3+}]}{k_{-1}[H^+] + k_2}$$

In order to agree with the experimental kinetic data $k_{-1}[H^+]$ must be $>> k_2$ or $\frac{k_{-1}[H^+]}{k_2} >> 1$. Using values from Table I-31 for the reaction of Fe^{3+} with $CrC(CH_3)(i\text{-}C_3H_7)OH^{2+}$: $k_{obs} = 102\ s^{-1}$ and $[Fe^{3+}] = 0.039$ M, the assumption that $\frac{k_{-1}[H^+]}{k_2} >> 1$ may be tested. If this assumption is not valid, then the form of the rate law does not fit the experimental data and the mechanism may be discarded. Using a value of 90 $M^{-1}\ s^{-1}$ for k_1 (Ref. 100, p. 59), which is the value for the reaction of Fe^{3+}

and SCN^-, we may test the assumption.

$$\frac{k_{-1}}{k_2}[H^+] = \frac{[Fe^{3+}]k_1}{k_{obs}} = 0.034$$

Clearly, 0.034 is not much greater than one! Furthermore, we may also calculate that for the example used; k_1 for Fe^{3+} substitution would have to be $\sim 6 \times 10^4$ M^{-1} s^{-1} to fit the observed kinetic data, this is far outside of the range of the fastest Fe^{3+} substitution rate constants. Even if substitution on Fe^{3+} was fast enough in this case, the kinetic data indicate that bulky alkyl groups on the α-carbon show no rate-retardation whatever. In fact, the trend observed for values of k' indicate that the rate constant increases with increasing bulkiness at the α-carbon. The insensitivity of k' to the steric bulk around the -OH group can be exemplified by considering the following three complexes: $CrCH(C_2H_5)OH^{2+}$, $CrC(CH_3)(C_2H_5)OH^{2+}$ and $CrC(CH_3)(i\text{-}C_3H_7)OH^{2+}$. The apparent rate constants for the inverse acid pathway are 0.42, 13.07 and 193 s^{-1}, respectively. Indeed, the trend observed is in the opposite direction of what one would expect based upon steric considerations, but seemingly k' is quite responsive to substitution at the α-carbon.

To explain the Fe^{3+}_{aq} mechanism, consider the first site proposed as a possible site for proton ionization, the metal ion itself. This implies that $FeOH^{2+}_{aq}$ would be the reactive species. A possible mechanism based upon this site for proton ionization is shown in Scheme I-9.

Scheme I-9

$$(H_2O)Cr(H_2O)_4C(R^1R^2)OH^{2+} \underset{k_{-38}}{\overset{k_{38}}{\rightleftharpoons}} Cr(H_2O)_4C(R^1R^2)OH^{2+} + H_2O \qquad \text{(I-38)}$$

$$Fe(H_2O)_6^{3+} + Cr(H_2O)_4C(R^1R^2)OH^{2+} \underset{k_{-39}}{\overset{k_{39}}{\rightleftharpoons}} H^+ + [(H_2O)_5Fe(OH)Cr(H_2O)_4C(R^1R^2)OH^{4+}] \qquad \text{(I-39)}$$

$$[(H_2O)_5Fe(OH)Cr(H_2O)_4C(R^1R^2)OH^{4+}] \xrightarrow{k_{et}} FeOH^+ + Cr^{2+} + (R^1R^2)C{=}O + H^+ \qquad \text{(I-40)}$$

Making the steady-state approximation for the concentration of the bimetallic intermediate, the rate law has the form shown:

$$\frac{-d[CrC(R^1R^2)OH^{2+}]}{dt} = \frac{k_{38}k_{39}k_{et}[Fe^{3+}][CrC(R^1R^2)OH^{2+}]}{k_{-38}k_{-39}[H^+] + k_{-38}k_{et}} \qquad \text{(I-41)}$$

If $k_{-39}[H^+] >> k_{et}$, then the limiting form of the rate law is:

$$\frac{-d[CrC(R^1R^2)OH^{2+}]}{dt} = \frac{k_{38}k_{39}k_{et}[Fe^{3+}][CrC(R^1R^2)OH^{2+}]}{k_{-38}k_{-39}[H^+]} \qquad \text{(I-42)}$$

which is the same as the form found for the predominant inverse acid-dependent pathway. (In this case, k' would be equal to $(k_{38}k_{39}k_{et}/k_{-38}k_{-39}$, as can be seen in Equation I-42.)

The most critical step in this mechanism is the substitution into the inner sphere of the Cr^{III} complex. Although most Cr^{III} complexes are considered to be substitution inert, alkyl groups are known to labilize the water coordinated <u>trans</u> to the alkyl group (101). Recent

evidence has shown that $CrCH_2OCH_3^{2+}$ and $CrCH_2OH^{2+}$ (48) are much more labile than $CrCH_2Cl^{2+}$ and $CrCHCl_2^{2+}$ for which ligand substitution rates are known (101). If the substitution on the complexes studied here are even faster, this would help explain the trend in rate constants observed.

In order to get an idea of the magnitude of the substitution rates on various Cr^{III} complexes, the half-times for the following complexes are compared at 25° and 0.1 M NCS^-: Cr^{3+}, $CrCHCl_2^{2+}$, $CrCH_2Cl^{2+}$, $CrCH_2OCH_3^{2+}$ and $CrCH_2OH^{2+}$. The calculated half-times for the anation reaction with NCS^- are: 9.3×10^6 s, 128 s, 42 s, 9.9×10^{-2} s, and 1.3×10^{-2} s, respectively. These values show the tremendous labilizing effect the alkyl groups have on substitution reactions of Cr^{III}. They also show that within the series of alkylchromium complexes for which substitution rates are known, there is a large variation depending upon the nature of the alkyl group. For the series of α-hydroxyalkylchromium(III) complexes, it seems reasonable that substitution of groups on the α-carbon which are electron-donating should inductively "push" more electron-density to the Cr^{III} center, thus increasing the lability of the trans water. If this premise is true, one would expect complexes such as $(H_2O)_5CrC(CH_3)(C_2H_5)OH^{2+}$, $CrC(C_2H_5)_2OH^{2+}$, and the other highly substituted analogs studied would be even more substitution labile than $CrCH_2OH^{2+}$. This increased lability would presumably manifest itself in the form of higher apparent rate constants for the Fe^{3+}_{aq} reactions (since the

value of $k_{38}k_{39}/k_{-38}$ would be expected to be higher) which is exactly the trend observed.

This mechanism is similar in many ways to the mechanism proposed for reaction of Cr^{2+} with Fe^{3+} which also has a predominant pathway which is inverse acid dependent (102,103). The k' value for the Fe^{3+} reaction with Cr^{2+} is larger than the k' values found in this study, which certainly seems reasonable. (Compare 7.3×10^3 sec^{-1} for k' at 25° for the Fe^{3+} + Cr^{2+} reaction (103) with 1.9×10^2 sec^{-1} for $CrC(CH_3)(i\text{-}C_3H_7)OH^{2+}$, the largest value of k' measured here.) If this analogy is valid, one may argue that the increasingly more powerful reducing radicals, such as $\cdot C(CH_3)(C_2H_5)OH$ and $\cdot C(C_2H_5)_2OH$, cause the chromium center to be more electron rich, such that it approaches the level of reactivity of Cr^{2+} with Fe^{3+}.

One may also note that Fe^{3+} does not appear to react with $CrC(CH_3)_2OCH(CH_3)_2^{2+}$ at all and only slightly with the other two ether-derived complexes (Table I-32). (Copper(II) does not react directly with any of the ether complexes.) Two very different interpretations of the meaning of this result are possible. The alkyl group bound to the oxygen atom may be a blocking group (Cu^{2+} mechanism), or it may simply serve as a site which renders the two electron oxidation of the alkyl ligand much less thermodynamically accessible (104). The latter interpretation would be applicable to the Fe^{3+}_{aq} mechanism.

In summary, <u>different</u> mechanisms are required to explain the reactions of Cu^{2+}_{aq} and Fe^{3+}_{aq} with α-hydroxyalkylchromium(III)

complexes. One must conclude that for those complexes which have similar apparent rate constants for Cu^{2+}_{aq} and Fe^{3+} (the first few entries in Table I-32) that the similarity is simply due to a cancelling effect of a number of parameters such as pK_a, substitution rate and redox potential. Finally, with the more highly substituted complexes, the stronger driving force of Fe^{3+} over Cu^{2+} (more powerful oxidizing strength) seems to begin to dominate the k' values. One may conclude that as the chromium center becomes more strongly reducing, due to increased electron density from the alkyl ligand, the differences in reactivity toward Cu^{2+} and Fe^{3+} become more distinct.

PART II. BINUCLEAR COBALT COMPLEXES OF SCHIFF BASE MACROCYCLIC LIGANDS

INTRODUCTION

The study of bimetallic complexes has grown extensively in recent years and has been the subject of several review articles (105-106). There are three major areas of interest in the study of binuclear complexes. First, there is a question whether the metal ions interact in such a way to exhibit chemical reactivity which is different from mononuclear analogs. This type of interaction is known for metalloenzymes such as nitrogenase which has coupled metal centers and is able to reduce nitrogen under mild conditions. Second, it is important to investigate these complexes to see if interactions between the metal centers change the electronic properties of the metals such that they behave differently than the mononuclear analogs (107). Third, these complexes are interesting examples for the study of magnetic exchange interactions (108).

This thesis is concerned with the preparation and characterization of dicobalt complexes of binucleating Schiff base ligands. The complexes may be viewed as two cobalt atoms held a fixed distance apart in space by a rigid coplanar macrocyclic ligand containing an extended π bonding system. The coplanarity of the ligand system is expected to be maintained so that the π-bonding may be delocalized (109-111). The structures of the complexes are shown in Figure II-1. Space-filling models indicate that the cobalt centers are $\sim$8Å apart. In this study, the group in the fifth position of the salicylaldehyde ring was varied (Complexes I-III) to study the effect of substitution on the properties

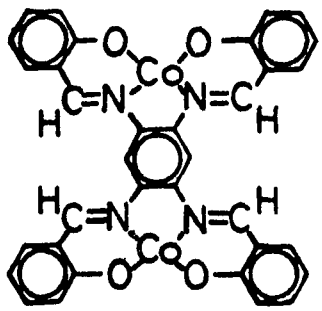

I

$Co_2(sal_4bz)$

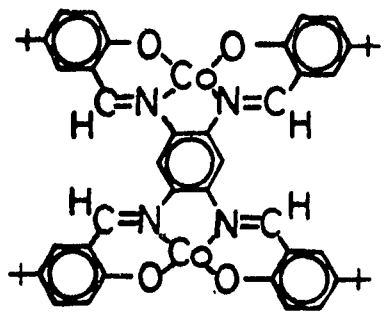

II

$Co_2(5\text{-}Bu^t sal_4bz)$

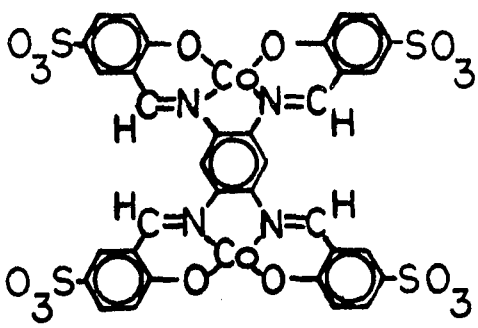

III

$Co_2(5\text{-}SO_3 sal_4bz)$

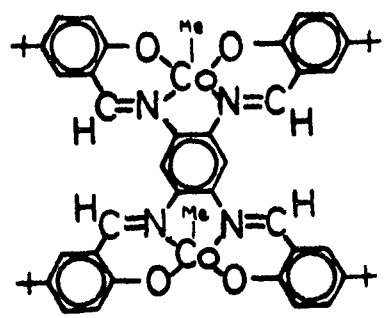

IV

$(CH_3Co)_2(5\text{-}Bu^t sal_4bz)$

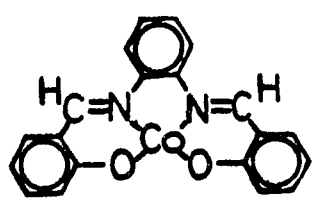

V

$Co(sal_2phen)$

Figure II-1. Structures of cobalt complexes

of the complexes. One organometallic derivative was also prepared (Complex IV) and its reactivity was examined.

The fifth complex, mononuclear Co(sal_2phen) was used as a guide to the possible reactivity of the binuclear complexes since it has a similar ligand system and coordination environment. With regard to the coordination number, V forms five coordinate species quite readily when it is coordinated to a strong axial ligand. The spin state of V has also been determined to be low spin, thus with a very similar ligand field environment, one might consider the binuclear complexes to also be low spin.

Another feature of mononuclear complex V is its ability to form 1:1 oxygen adducts in aprotic solvents. These adducts are formed reversibly in aprotic solvents, but in protogenic solvents the action of air on the Co^{II} complex causes oxidation to the Co^{III} complex (112). The implication of these findings on the conclusions made in the study at hand will be dealt with in more detail in a following section.

Most extensive studies based on binuclear complexes of this type have focused on the solid complexes (108,113). Undoubtedly, this has been due, in part, to the slight solubility of the complexes in solution. The approach usually has been to probe the magnetic coupling interactions of the two metals (usually Cu) held by the chelate. Some of these magnetic studies have indicated that the 1,2,4,5-tetraamino-benzene unit can be effective in promoting metal-metal interactions (113,114). These magnetic studies are, of course, indicative of solid state interactions, but the effect of solvolysis would not be expected

to greatly disrupt the intramolecular interactions in these binuclear complexes. EPR studies have shown that the metal-metal interaction is an intramolecular one and not intermolecular (113). The 1,2,4,5-tetraaminobenzene bridging moiety provides a pathway for a superexchange mechanism and this could thereby provide metal-metal interaction. In terms of redox chemistry, this exchange mechanism could manifest itself in several ways. For a Co^{III}-Co^{III} to Co^{III}-Co^{II} process, the possibility of nonadiabatic electron transfer exists due to the large spin change required (115). One might also hope to detect the mixed-valence state by the production of a near IR absorption band (116). These complexes hold a certain promise for the possibility of expanding our understanding of the factors governing the reactivity of metal complexes. By varying the nature of the binucleating ligands, one might hope to systematically probe steric effects, electronic effects and other parameters relevant to the reactivity of metal complexes. Some of the factors which might be varied in a series of complexes are the metal-to-metal distance, the degree of conjugation in the binucleating ligand itself, and substituents on the ligand. In this way, the extent to which one parameter dominates over another could be examined by varying them one at a time. The possibilities seem almost limitless; for instance, for a given ligand system, one might choose to see the effect of electron-donating groups <u>versus</u> electron-withdrawing groups located at the periphery of the ligand. Thus, despite the known difficulties associated with such bulky ligands and complexes, the rewards possible seem to justify their preparation.

EXPERIMENTAL

Materials

Substituted salicylaldehydes

5-tert-Butylsalicylaldehyde Anhydrous glycerol (160 g; 1.63 mol) and boric acid (35 g; 0.566 mol) were placed in a 1 L, 3-neck round bottom flask for the preparation of anhydrous glyceroboric acid (117). The viscous solution was heated to 170°C and kept at that temperature for at least 1 hour. The solution was then cooled to 160°C and 25 g each of p-tert-butylphenol and hexamethylenetetramine were added rapidly in alternating portions. The reaction was very exothermic and the flask had to be externally cooled very soon after the reaction began or the temperature would rise above 190°C. The solution was stirred for ∿5 - 7 min., but not any longer. After the 5 - 7 min. reaction time, the flask was cooled to 100-110°C and ∿4 M H_2SO_4 (100 mL) was added. The viscous, dark brown solution was then subjected to a steam distillation and 1-2 L of distillate was collected. The distillate was extracted with ether and the ether layer was allowed to stand overnight over anhydrous $CaCl_2$. Finally, the ether layer was filtered to remove the $CaCl_2$ and evaporated leaving a yellow oil. The yellow oil was vacuum distilled with the desired product obtained water free at 57-58.5°C/0.1 mm Hg. ^1H nmr δ 1.35 (9H), 6.9-7.1 m (1H), 7.5-7.7 m (2H), 9.9 s (1H), 10.955 (1H).

Sodium salicylaldehyde-5-sulfonate Sulfuric acid (95%, 250 ml) was slowly added to a 500 mL round bottom flask containing salicylaldehyde (Aldrich 98%, 29 g). The temperature was kept at 40° or lower to prevent oxidation of the aldehyde. The reaction mixture was stirred for 18-24 hrs at 35° and then cooled in an ice bath prior to being poured very slowly over 500 g of distilled water ice. The solution was diluted with water (500 mL), sodium carbonate (250 g) was added to neutralize the acid, and the volume was reduced by about one-half on a rotary evaporator at 40°. The gray precipitate of sodium salicylaldehyde-5-sulfonate one-sixth hydrate was recrystallized from hot water and dried at 100° in vacuo. The isolated yield of feathery white needles was 14.5 g (27%). The solid was found to be hygroscopic and was protected from moisture. A smaller scale experiment with 5 g of salicylaldehyde gave a yield of 45%, mp. > 304°; ν_{max} KBr 3530, 3440, 2900, 1660, 1180, 1035; ^{1}H NMR (D_2O):[1] δ 9.98 (s, aldehydic), 8.12 (d, J = 2.3 Hz), 7.94 (q, J = 8.7, 2.3 Hz), 7.08 (d, 1.0 H, J = 8.7 Hz); ^{13}C NMR (D_2O):[2] δ 198.5, 163.2, 136.3, 135.4, 131.8, 121.3, 118.9. Anal. Calcd for $C_7H_5O_5SNa \cdot \frac{1}{6} H_2O$: C, 37.01; H, 2.37. Found: C, 37.00; H, 2.20.

---

[1]Proton chemical shifts are relative to Tiers' salt (sodium-2,2-dimethyl-2-silapentane-5-sulfonate).

[2]The ^{13}C chemical shifts were measured in D_2O relative to p-dioxane and calculated relative to TMS by adding a constant of 66.99 ppm.

The phenylhydrazone was prepared by addition of phenylhydrazine hydrochloride (1.0 g; 6.9 mmol) to an aqueous solution of 5-sulfosalicylaldehyde sodium salt (0.5 g; 2.2 mmol). The solution was warmed to 60-70° and stirred for ∿2 hrs. The golden-yellow precipitate was filtered and washed with ethanol and ether and was recrystallized from hot water in which it was only slightly soluble. The solid was dried in vacuo at 100°. The product was found to be the phenylhydrazinium salt of the phenylhydrazone derivative as described by Blau (118). Anal. Calcd for $C_{19}H_{20}N_4O_4S$: C, 56.99; H, 5.03; N, 13.99. Found: C, 56.70; H, 5.09; N, 14.00.

Ligands

1,2,4,5-Tetrasalicylalideneaminobenzene [$(salH)_4bz$] To a stirred suspension of 1,2,4,5-tetraminobenzene tetrahydrochloride (0.95 g; 3.3 mmol) in ∿100 mL of dry methanol under dry nitrogen, a solution of sodium methoxide was added until the benzenetetramine was completely dehydrohalogenated. This process was followed by a series of striking color changes, a final yellow color marking the endpoint. Salicylaldehyde (1.61 g; 13.2 mmol) was slowly added dropwise into the warmed solution of the benzenetetramine with an immediate color change being noted toward a darker orange-brown. Orange solids precipitated out of the solution within ∿1 hour and the solution was cooled. The precipitate was filtered and washed several times with methanol and ether and air dried. (Yield: 90%, mp 270-290° decomp.) Due to the low solubility of the ligand, a small portion was recrystallized from

$CHCl_3$ and used for microanalysis. Anal. Calcd for $C_{34}H_{26}N_4O_4 \cdot (1.5CHCl_3)$: C, 55.66; H, 3.57; N, 7.64. Found: C, 56.18; H, 3.69; N, 8.08.

1,2,4,5-Tetra(5-tert-butylsalicylalideneamino)benzene $(5\text{-}Bu^tsalH)_4bz$ Freshly prepared sodium methoxide was added to a suspension of 1,2,4,5-tetraaminobenzenetetrahydrochloride (1.73 g; 6.1 mmoles) until the cloudy-gray suspension went through a series of color changes including a brilliant pink to a bright green and finally a pale yellow. This dehydrohalogenation step was carried out in a 250 mL round bottom flask containing dry methanol (100 mL) which was under a constant stream of dry nitrogen. The tetraamine thus produced in situ was reacted as quickly as possible because it has been found to be somewhat unstable (perhaps simply air-sensitive). The substituted aldehyde[1] (5-Bu^{t}salicylaldehyde) (4.47 g; mmol) was added dropwise with constant stirring to the benzenetetramine solution. As the drops of the 5-tert-butylsalicylaldehyde were added, the solution turned a rich oxblood color. The solution was refluxed for ∿24 hr during which time an orange precipitate fell out of the solution. After filtration, the ligand was recrystallized from boiling $CHCl_3$. (Yield: 40-75%.) Mass spectrum m/e 779 ± 1. ^1H NMR ($CDCl_3$): δ 1.3 s, 6.9-7.6 m, 8.8 s,

[1]The corresponding sulfonated ligand prepared from 5-sulfosalicylaldehyde and 1,2,4,5-tetraaminobenzene was not isolated as a solid, but prepared in situ and reacted immediately with the cobalt(II) solution. Therefore, its preparation is fully described in the metal complex section.

12.6 s (no integration due to low S/N). Anal. Calcd for $C_{50}H_{58}N_4O_4$: C, 77.09; H, 7.50; N, 7.19. Found: C, 76.23; H, 7.56; N, 7.62.

Cobalt complexes

General synthetic route All of the binucleating ligands were prepared from the same central moiety, 1,2,4,5-tetraaminobenzene. The 1,2,4,5-tetraaminobenzene tetrahydrochloride was purchased (Aldrich 98%) and used without further purification. Commercial sodium methoxide was not found to be satisfactory for the dehydrohalogenation of 1,2,4,5-tetraaminobenzene so it was freshly prepared from cut sodium metal in methanol immediately prior to its use (119). The Duff reaction was used to prepare 5-tert-butylsalicylaldehyde (117). A new, direct synthesis of 5-sulfosalicylaldehyde from sulfuric acid and salicylaldehyde was used to prepare the water soluble sodium salt of 5-sulfosalicylaldehyde (120). In all cases, reagent grade solvents were used without further purification except for drying over 4A molecular sieves, unless otherwise specified. The general synthetic route can be represented as:

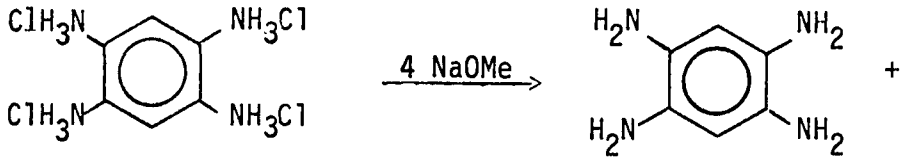

+ 4 NaCl + 4 MeOH

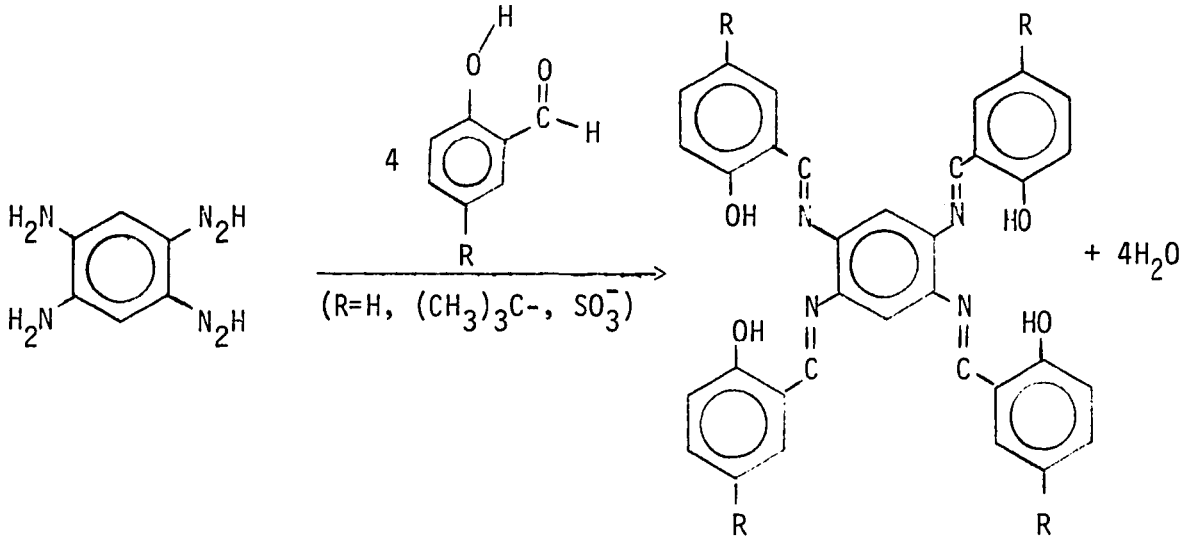

$$H_4(5\text{-Rsal}_4\text{bz}) \xrightarrow[N_2 \text{ atmosphere}]{2\ Co(OAc)_2 \cdot 4\ H_2O} Co_2^{II}(5\text{-Rsal}_4\text{bz}) + 4\ HOAc + 8\ H_2O$$

In the preparation of the cobalt complexes, it was found that it was not necessary to rigorously exclude air during their filtration. Ultimately, the 5°C solutions in methanol were filtered in air and washed with cold, deaerated methanol which purified the brown Co_2^{II} solids from any small amounts of Co_2^{III} which may have been produced. The solids, once dried, showed no tendency to convert to the Co_2^{III} form over a period of months.

1,2,4,5-tetra(Salicylideneaminobenzene)dicobalt(II) ($Co_2(sal_4bz)$)

Freshly vacuum dried (100°C) (sal_4bzH_4) ligand (0.22 g; 0.39 mmol) was placed in a glass fritted extraction thimble which in turn was placed in a Soxhlet apparatus. Deaerated, dry THF was used as the solvent to extract the ligand into solution and wash it down into the reaction

vessels containing $Co(OAc)_2 \cdot 4H_2O$ (0.23 g; 0.92 mmol). The system was kept under N_2 for the duration of the experiment. After several days of extractions, a dark, brown powder was filtered from the collection flask in an inert atmosphere frit (mp >300°C).

1,2,4,5-tetra(5-tert-Butylsalicylidene)aminobenzenedicobalt(II) ($Co_2(5\text{-}Bu^tsal)_4bz$) Chloroform (800 mL) was deaerated with prepurified nitrogen. The 5-Bu^tsalicylidenebenzenetetramine ligand whose preparation was previously described was added to the warmed chloroform solution (1.23 g; 1.0 mmol). Then, $Co(OAc)_2 \cdot 4H_2O$ (3.2 mmol) was added dropwise in an ethanol solution (∿100 mL) which had also been deaerated. Immediately, as the ethanol solution was added, the ligand solution changed color from an orange-yellow to a deep brown color. After several hours of stirring the warm ethanol-chloroform solution, a brown precipitate began to be noticeable. After being stirred overnight, the solution was cooled in an ice bath, the brown precipitate was filtered and dried in the vacuum oven at 100°C for 10-12 hr. Anal. Calcd for $C_{50}H_{62}N_4O_8Co_2$: C, 62.36; H, 6.34; N, 5.82; Co, 12.2. Found: C, 62.65; H, 6.00; N, 6.32; Co, 12.3.

1,2,4,5-tetra(5-Sulfosalicylidene)aminobenzenedicobalt(II) sodium salt ($[Co_2(5\text{-}SO_3sal)_4bz]Na_4$) In a 3-neck, 150 mL round bottom flask, a solution of 30 mL of DMSO and 30 ml dry methanol was deaerated with prepurified N_2. 1,2,4,5-Tetraaminobenzene tetrahydrochloride (0.31 g; 1.09 mmol) (Aldrich) was added to the DMSO/methanol and a purple-gray suspension was formed. The suspension was warmed and with

vigorous stirring a purple solution was obtained. A solution of freshly prepared NaOMe was slowly added until the purple solution gradually changed to a yellow color. Then, 5-sulfosalicylaldehyde sodium salt (1.01 g; 4.5 mmol) in ∿20 mL of DMSO was added dropwise and a brilliant deep red solution was obtained. Finally, with the reaction at reflux temperature, $Co(OAc)_2 \cdot 4H_2O$ (0.541 g; 2.2 mmol) in ∿25 mL of DMSO was added dropwise. After addition of the diacetatocobalt(II) tetrahydrate, the solution became very dark, with a small amount of precipitation noticeable. After ∿18 hr reaction time, the precipitate was filtered from a cooled solution in air with some difficulty by vacuum filtration. The precipitate was washed with ethanol and ether and air dried, a black solid being obtained. The solid obtained was very water soluble and when dissolved in aerated water, an orange-brown solution was obtained.

Dimethyl(1,2,4,5-tetra(5-tert-butylsalicylidene)aminobenzene)-dicobalt(III) ($CH_3Co(5\text{-}Bu^t sal_4 bz)CoCH_3$) Solid sodium borohydride (5 mgs; 0.13 mmol) was added under a stream of N_2 to a deaerated solution of $Co_2^{III}(5\text{-}Bu^t sal_5 bz)$ (30 mg; 0.03 mmol) dissolved in methanol (250 mL). The excess borohydride produced an immediate color change from red to light straw-yellow. An excess of methyl iodide (0.1 ml; 1.6 mmol) was added to the vessel using a Teflon needle and the flask was subsequently sealed under a positive N_2 pressure. After several hours in the dark, the solution had become a darker brown. From this point on, exposure of the solution to light was avoided as much as possible. The methanol solution was extracted with CH_2Cl_2

(100 mL), with water added to the methanol to cause separation of the aqueous methanol from the CH_2Cl_2. After this extraction, the methanol layer was colorless and the CH_2Cl_2 layer a very dark brown. The CH_2Cl_2 was removed on a rotary evaporator with gentle warming (35°C). A dark brown solid was obtained by taking the solution to dryness. (Yield 85-90%.) The dimethyl complex was purified by column chromatography using LH-20 Sephadex resin and eluting with CH_2Cl_2/MeOH (10:1). Any Co_2^{III} which was not methylated remained at the top of the column as a pink-red band, while the dimethyl moved down the column as a brown band. ^1H NMR (CD_2Cl_2): δ 1.3 s, 7.0-7.6 m, 8.9 s (no integration was obtained due to very low S/N).

Inorganic reagents

Preparation of $CrCl_2$ solutions Chromium(II) solutions were prepared by dissolving chromium metal pellets (99.999%; Apache Chemicals Inc.) in 6 M HCl (49). In a typical preparation, two pellets ($\sim$2 g) were placed in an argon purged test tube with a 24/40 T joint equipped with gas inlet and outlet tubes. After careful deaeration, HCl ($\sim$15 ml, 6 M) was added to the test tube. With warming, the solution began to turn blue as the pellets dissolved. Eventually, all of the metal dissolved and the volume of the solution was reduced with heating. Upon cooling, a blue solid was obtained which was rinsed with several aliquots of deaerated acetone until the acetone rinse was nearly colorless. The acetone removed $CrCl_3 \cdot 6H_2O$ and excess HCl. $CrCl_2$ stock solutions were made from this solid with the desired amount

of dilute perchloric acid solution. The concentrations of the stock solutions were usually determined from an absorption maximum at 713 nm (ε = 4.9).

Preparation of bromopentaamminecobalt(III) A stock sample of $(Co(NH_3)_5Br)Br_2$ was used as the starting material for the preparation of the perchlorate salt. The $(Co(NH_3)_5Br)Br_2$ (5 g; 13 mmol) was dissolved in ~0.2 M $HClO_4$ (1.5 L) and warmed to 35°C for 10 minutes. The solution was filtered through a glass frit to remove any undissolved material. Concentrated $HClO_4$ (~250 mL) was added to the solution and it was cooled in an ice bath. A fine purple precipitate was obtained by filtration and was washed with cold ethanol and three washings of ether. The product was air-dried. The absorption spectrum in 0.1 M $HClO_4$ matched the literature (53).

Methods

Analyses

The cobalt content of the complexes was determined by a standard spectrophotometric method. An accurately weighed sample of the complex was digested in fuming $HClO_4$ to yield a Co^{2+} solution. This solution was diluted to a known volume with 50% acetone/water in the presence of excess NH_4SCN to produce $Co(SCN)_4^{2-}$. The absorbance at λ_{max} for $Co(SCN)_4^{2-}$ (623 nm; ε 1842 M^{-1} cm^{-1}) was used to calculate the percentage of cobalt in the samples.

Stoichiometries

The stoichiometry of several reactions was determined, including the reactions of Hg^{2+}, with $(CH_3Co)_2(5\text{-}Bu^t sal_4 bz)$, $CrCl_2$ with $Co_2^{III}(5\text{-}Bu^t sal_4 bz)$ and $Co(NH_3)_5Br^{2+}$ with $Co_2^{II}(5\text{-}SO_3 sal_4 bz)$. In all cases, the stoichiometries were determined by spectrophotometric titrations. The general procedure used was as follows. A stock solution of the dicobalt complex to be titrated would be prepared and its concentration determined by the absorbance of a characteristic visible peak which had a previously determined ε value (Table II-1). A known volume of this solution would be transferred to a 1 or 2 cm cell, as appropriate, and aliquots of the reagent with which the compound was to be titrated would be added using microliter syringes. After each addition, once a constant absorbance reading was obtained, the absorbance was recorded. These readings were used to make a stoichiometry plot. Alternately, 5 identical cells were filled with a known volume of the cobalt complex solution and various amounts of the titrant solution were added to each cell. The absorbance of each cell was recorded before and after the titrant was added. When necessary, volume corrections were calculated; however, these were usually so small that they could be neglected.

Kinetics

Owing to the solubility problems and purification difficulties discussed earlier, none of the kinetic studies was of a substantial nature. All of them should be classified as preliminary experiments

Table II-1. Electronic spectra of the ligands and cobalt complexes[a]

Compound	Solvent	λ_{max}/nm (Log_{10} ε/M^{-1} cm^{-1})
sal_4bzH_4	DMSO	396(4.44), 353(4.48)
$(Co^{II})_2(sal_4bz)$	DMSO	475(4.78), 322(4.78)
$(Co_2^{III})_2(sal_4bz)$	DMSO	520(---), 491(---), 331
5-$Bu^t$$sal_4bzH_4$	THF	398(4.57), 366(4.58), 277(4.49)
$(Co^{II})_2$(5-$Bu^t$$sal_4bz$)	Methanol	∿450(∿4.5), 328(∿4.6)
$(Co^{III})_2$(5-$Bu^t$$sal_4bz$)	Methanol	525(4.52), 491(4.53), 344(4.54), 258(4.85)
$(CH_3Co)_2$(5-$Bu^t$$sal_4bz$)	Methanol	620(sh), 462(4.43), 330(4.46)
$(Co^{II})_2$(5-$SO_3$$sal_4bz$)	Water	416(4.69), 310(4.56)
$(Co^{III})_2$(5-$SO_3$$sal_4bz$)	Water	498(4.63), 467(4.62), 334(4.56), 262(5.04)

[a]Values were determined at room temperature.

and any conclusions drawn from these experiments should bear this in mind. Fast reactions were followed using a Durrum 110 stopped-flow spectrophotometer. For single-stage reactions under pseudo-first-order conditions, the absorbance *versus* time data were recorded on a Biomation 802 Transient Recorder and rate constants were obtained from a least squares routine using a PDP-15 computer. For reactions with longer half-lives, a Cary 219 recording spectrophotometer was used and the data were treated by conventional pseudo-first-order plots of $\log(D_t - D_\infty)$ *versus* time.

Because of experimental factors, some reactions had to be studied under second-order conditions. The expression used for these experiments was:

$$\ln \frac{[B]}{[A]} = \ln \frac{[B_o]}{[A_o]} + \{a[B_o] - b[A_o]\}kt$$

The kinetic data were plotted as $\ln \frac{[B]}{[A]}$ *versus* time. The concentrations of species [A] and [B] were determined by absorbance maxima and checked with the total absorbance change.

Instrumentation

Reactions were studied using Cary Model 14 or 219 spectrophotometers and a Durrum Model D-110 instrument. Nmr data were obtained on a Varian HA-100 spectrometer or a JEOL Model FX-90Q instrument; ir spectra were determined using a Beckman 4820 instrument.

RESULTS

In general, prior to solution studies, all of the complexes were purified by column chromatography. Gel filtration using Sephadex LH-20 was found to separate $Co_2^{III}(5\text{-}Bu^t sal_4 bz)^{2+}$ nicely from the dimethyl derivative and from the Co_2^{III} in methanol solvent. Surprisingly, LH-20 was also found to be useful for the purification of the anionic complex $Co_2^{II}(5\text{-}SO_3 sal_4 bz)^{4-}$. Spectral analysis of the fractions collected in any particular chromatogram was used to decide which fractions were suitable for use. The spectra of the various fractions showed conclusively that the purification process was definitely required to obtain a "spectrally" pure fraction. It should be noted, however, that in many cases most of the impurity was simply an undesired oxidation state of the complex. (For instance, if the Co_2^{III} product was desired, a small amount of Co_2^{II} would often be found.)

Reactions of the Binuclear Complexes

Reaction of $Co_2^{III}(5\text{-}Bu^t sal_4 bz)^{2+}$ with $CrCl_2$

$Co_2^{III}(5\text{-}Bu^t sal_4 bz)^{2+}$ which was prepared by air oxidation of the Co_2^{II} solid dissolved in methanol, was reacted with $CrCl_2$. The $CrCl_2$ reduction was qualitatively observed to be a very fast reaction, apparently complete in the time of mixing in a spectrophotometer cell. As can be seen in Figure II-2, a 2:1 stoichiometry of reaction between $CrCl_2$ and Co_2^{III} was obtained (Equation II-1).

$$2CrCl_2 + Co_2^{III} \longrightarrow 2CrCl_2^{+} + Co_2^{II} \qquad \text{(II-1)}$$

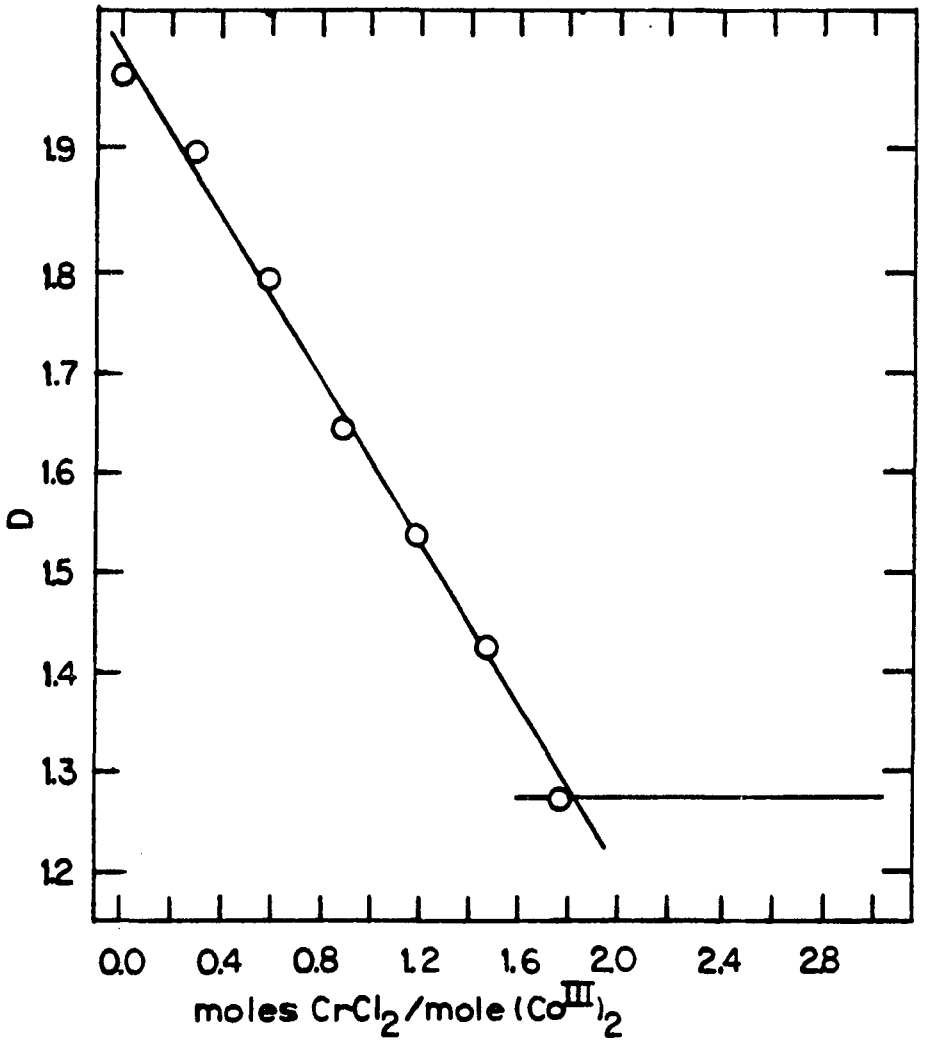

Figure II-2. Spectrophotometric titration for the reaction of $CrCl_2$ with $Co_2^{III}(5\text{-}Bu^t sal_4 bz)^{2+}$ (ℓ = 1 cm)

(This stoichiometry was obtained with the endpoint taken as that point at which the 440-450 nm peak of Co_2^{II} was maximized, beyond that point the 450 nm peak was reduced in absorbance by additional $CrCl_2$.) The spectral changes observed when $CrCl_2$ was added to Co_2^{III} are shown in Figure II-3. Isosbestic points at 377 and 479 nm were maintained prior to the addition of excess $CrCl_2$; however, after an excess of $CrCl_2$ was added, the isosbestic points were lost.

The reaction was studied by the stopped-flow method at 25 ± 0.2°C and was found to be a very fast reaction under conditions of excess $CrCl_2$ (∿10 msec). The reaction, however, was not studied because of difficulties with the solvent conditions, i.e., keeping dilute Cr(II) in methanol solution at a pH > 3 to keep the Co_2^{II} from decomposing once it was reduced by Cr(II). Finally, an additional problem was found under conditions of a large excess of Cr(II) which was attributed to ligand reduction by Cr(II).

Reduction of $Co_2^{III}(5\text{-}Bu^t sal_4 bz)^{2+}$ with $CrCl_2$ in methanol with pyridine present as a base added in excess, yielded similar results to those in the absence of pyridine (Figure II-4) except that the initial Co_2^{III} spectrum was altered somewhat by the added pyridine. Still, as can be seen in Figure II-4, isosbestic points at 380 and 478 nm appear to be maintained.

Another reductant for Co_2^{III} was found to be hydrogen using PtO_2 as a catalyst. This reduction resulted in the production of a species which has a spectrum that matches the spectrum produced by Cr(II) reduction. Owing to the very fine particle size of the catalyst, it

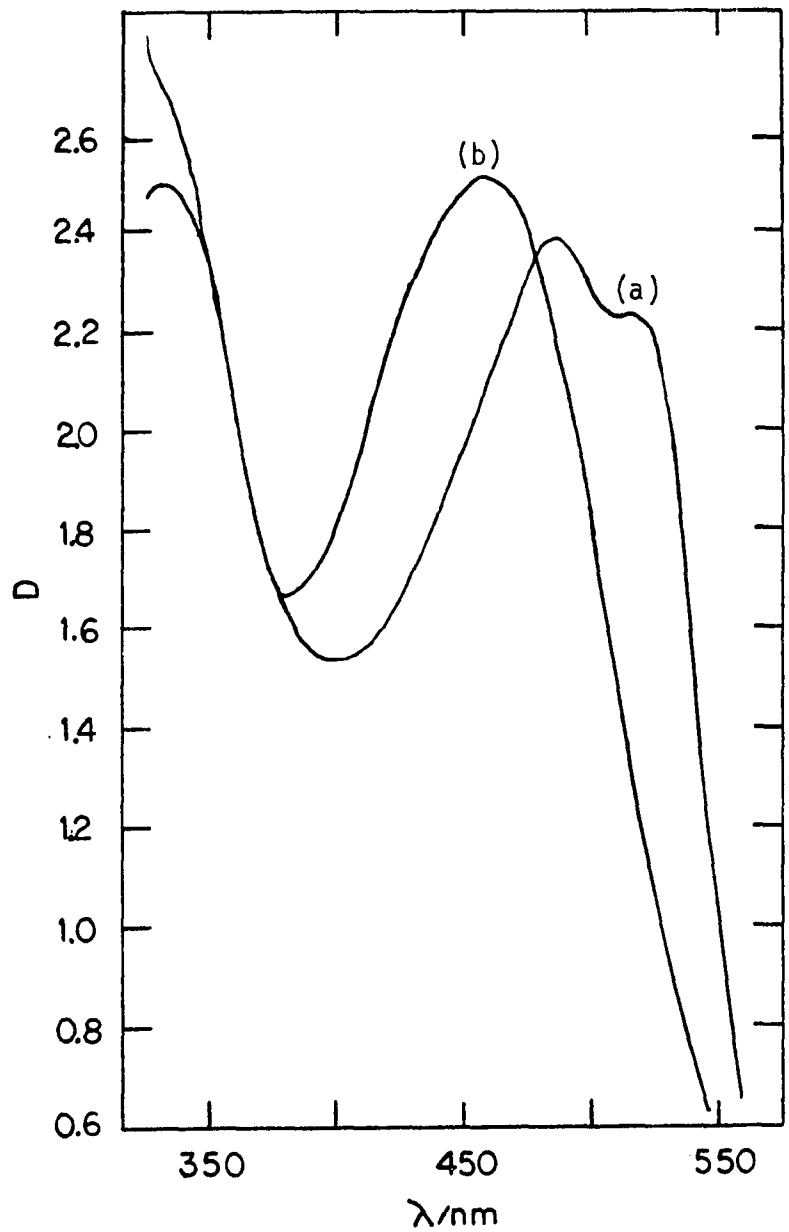

Figure II-3. Electronic spectrum of $Co_2^{III}(5\text{-}Bu^t sal_4 bz)$ before (a) and after (b) addition of 2 equivalents of $CrCl_2$ (ℓ = 1 cm)

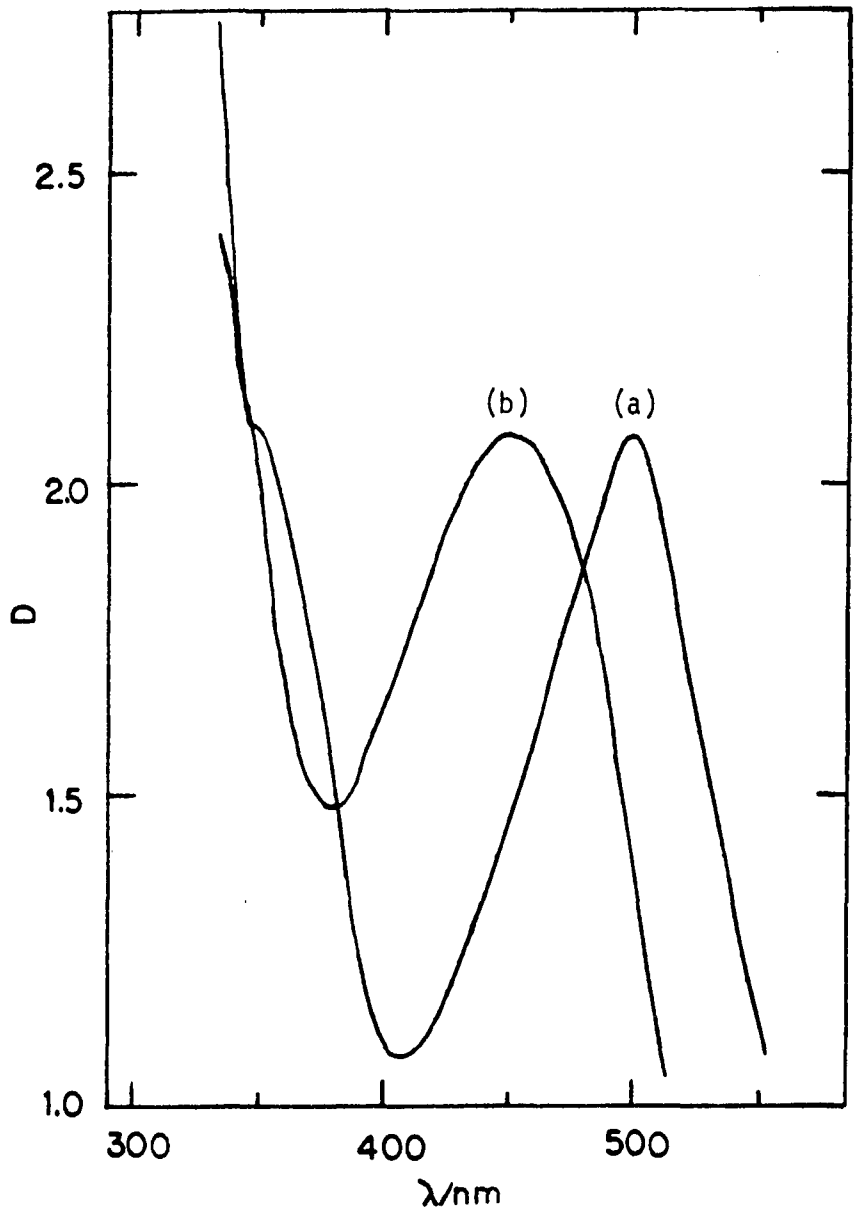

Figure II-4. Electronic spectrum of $Co_2^{III}(5\text{-}Bu^t sal_4 bz)$ before (a) and after (b) addition of 2 equivalents of $CrCl_2$ with pyridine present (10^{-3} M) (ℓ = 1 cm)

was necessary to filter it off under air-free conditions using a millipore filter prior to using the solutions. The reduction typically required 2 hours to reach completion.

Reaction of $Co_2^{III}(5\text{-}SO_3sal_4bz)^{2-}$ with $CrCl_2$

The stoichiometry for the reaction of $CrCl_2$ with $Co_2^{III}(5\text{-}SO_3sal_4bz)^{2-}$, Equation II-2, was established by spectrophotometric titration as 2:1 (Figure II-5). Despite some complications with

$$2CrCl_2 + Co_2^{III}(5\text{-}SO_3sal_4bz) \longrightarrow 2CrCl_2^{+} + Co_2^{II} \qquad \text{(II-2)}$$

pH, the Co_2^{III} complex of the sulfonated ligand was considered to be a good one for kinetics investigations because of its water solubility. This opened the way for the study of the Cr(II) reaction without trying to work in mixed solvents. Unfortunately, the sensitivity of the sulfonated complex to high acid required working with buffered solutions in a pH range of ∿3-6. Side reactions were another complication if $CrCl_2$ was used in large excess, so second order conditions were employed. Under second order conditions with Co_2^{III} always in slight excess, there was no evidence of a ligand reduction reaction. In acetate buffer solution, the $CrCl_2$ reduction reaction was found to be $\sim 10^6$ $M^{-1}s^{-1}$ and varied inversely with $[H^+]$ (Table II-2).

In an effort to obtain the Co^I state in $Co_2(5\text{-}Bu^tsal)_4bz$, a solution of $Co_2^{III}(5\text{-}Bu^tsal)_4bz^{2+}$ in methanol was treated with $NaBH_4$. The red solution quickly became a pale yellow, but its visible spectrum, as shown in Figure III-5, was quite different from the

Table II-2. Rate constants for the reaction of $CrCl_2$ with $(Co_2^{III})(5\text{-}SO_3sal_4)bz^a$

pH	10^{-6} k/M^{-1} s^{-1}
1.3	0.004
4.3	1.2 ± 0.1 (4)
4.3	1.1 (1)
6.0	9.8 (1)

[a] μ = 0.11 M ($NaClO_4$); aqueous solutions were used with acetate buffer unless otherwise indicated; T = 25°C.

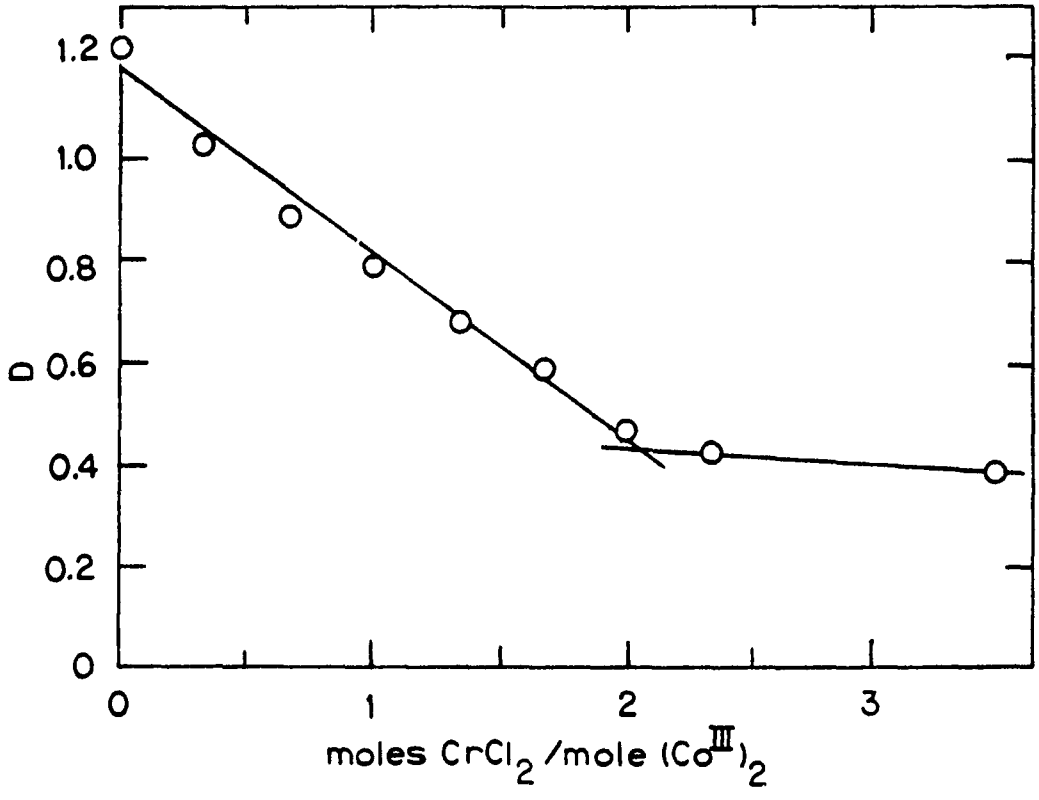

Figure II-5. Spectrophotometric titration for the reaction of $CrCl_2$ with $Co_2^{III}(5\text{-}SO_3sal_4bz)^{2+}$ (ℓ = 1 cm)

spectrum of Co_2^{II} (either from the solid or by Cr(II) reduction. Furthermore, this borohydride reduced species reacted quite cleanly with Cu^{2+} to give a spectrum very similar to the Co_2^{II} spectrum. Several attempts to obtain a stoichiometric value for oxidation of this highly reduced species always yielded highly irreproducible results. Nevertheless, it would seem that this reduced species required at least four or more equivalents of Cu^{2+} to reach what could be considered similar to the Co_2^{II} state by comparison with the Cr(II) reduced spectrum (Figure II-6). The problem in obtaining good stoichiometries may have been due to incomplete quenching of the borohydride present in the solutions, although even when acetone was added in excess to quench the borohydride prior to the titration with the Cu^{2+} solution, variable stoichiometries were obtained.

Reaction of $Co_2^{II}(5\text{-}Bu^t sal_4 bz)$ with oxidants

Several oxidants, including H_2O_2, O_2, $Co(NH_3)_5Cl^{2+}$, $Co(NH_3)_5Br^{2+}$, and Ce^{IV} were found to oxidize $Co_2^{II}(5\text{-}Bu^t sal_4 bz)$ to a species which had a spectrum very similar to the initial Co_2^{III} spectrum. However, complete resolution of the longer wavelength (500 nm) double-peak feature was usually not obtained. Clearly, one of the best oxidants for this reaction was found to be $Co(NH_3)_5Br^{2+}$ (Table II-3). Although it reacted somewhat sluggishly, it produced a good Co_2^{III} spectrum (Figure II-7). The reaction typically took 10-30 minutes to reach completion under second-order conditions, but was faster than the reaction of $Co(NH_3)_5Cl^{2+}$.

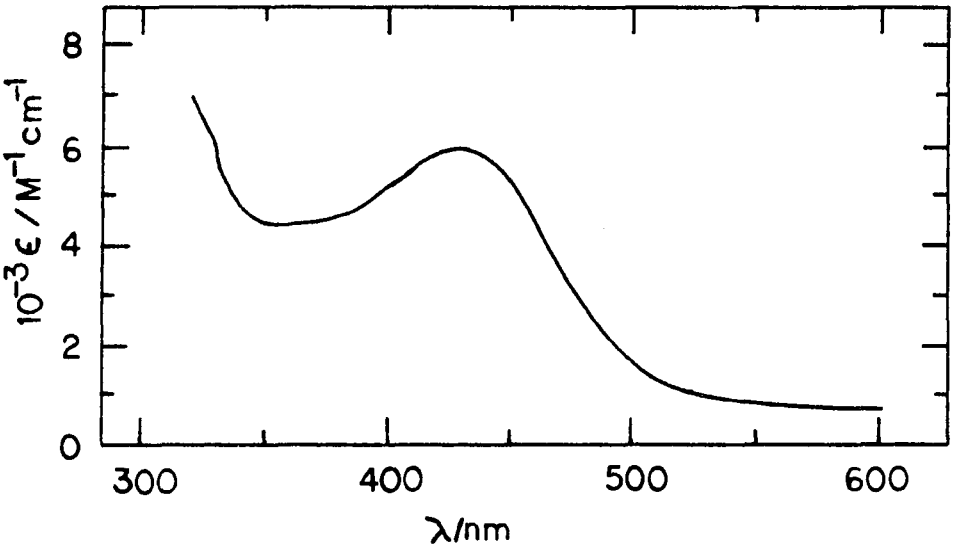

Figure II-6. Electronic spectrum of $Co_2(5\text{-}Bu^t sal_4 bz)$ in methanol after reduction with $NaBH_4$

Table II-3. Rate constants for the reaction of oxidants with $(Co^{III})_2(5\text{-}Bu^t sal_4 bz)$ at 25°[a]

Oxidant	Concentration/M	$[(Co^{II})_2(5\text{-}Bu^t sal_4 bz)]$/M	$k/M^{-1}\ s^{-1}$
$Co(NH_3)_5Br^{2+}$	1.1×10^{-3}	$<2 \times 10^{-5}$	9.7×10^4[b]
	5×10^{-4}	$<2 \times 10^{-5}$	9.1×10^4[b]
	8×10^{-4}	$\sim 10^{-5}$	10 ± 3[c]
H_2O_2	5×10^{-4}	$\sim 10^{-5}$	1.7×10^4[b]
	5×10^{-4}	$\sim 10^{-5}$	~ 80[b]

[a] $(Co^{II})_2(5\text{-}Bu^t sal_4 bz)$ was prepared by reduction of $(Co^{III})_2(5\text{-}Bu^t sal_4 bz)$ with H_2 over PtO_2.

[b] Unbuffered methanol solutions; ionic strength not adjusted.

[c] At pH 7.5 with THAM/HCl buffered 10% aqueous methanol.

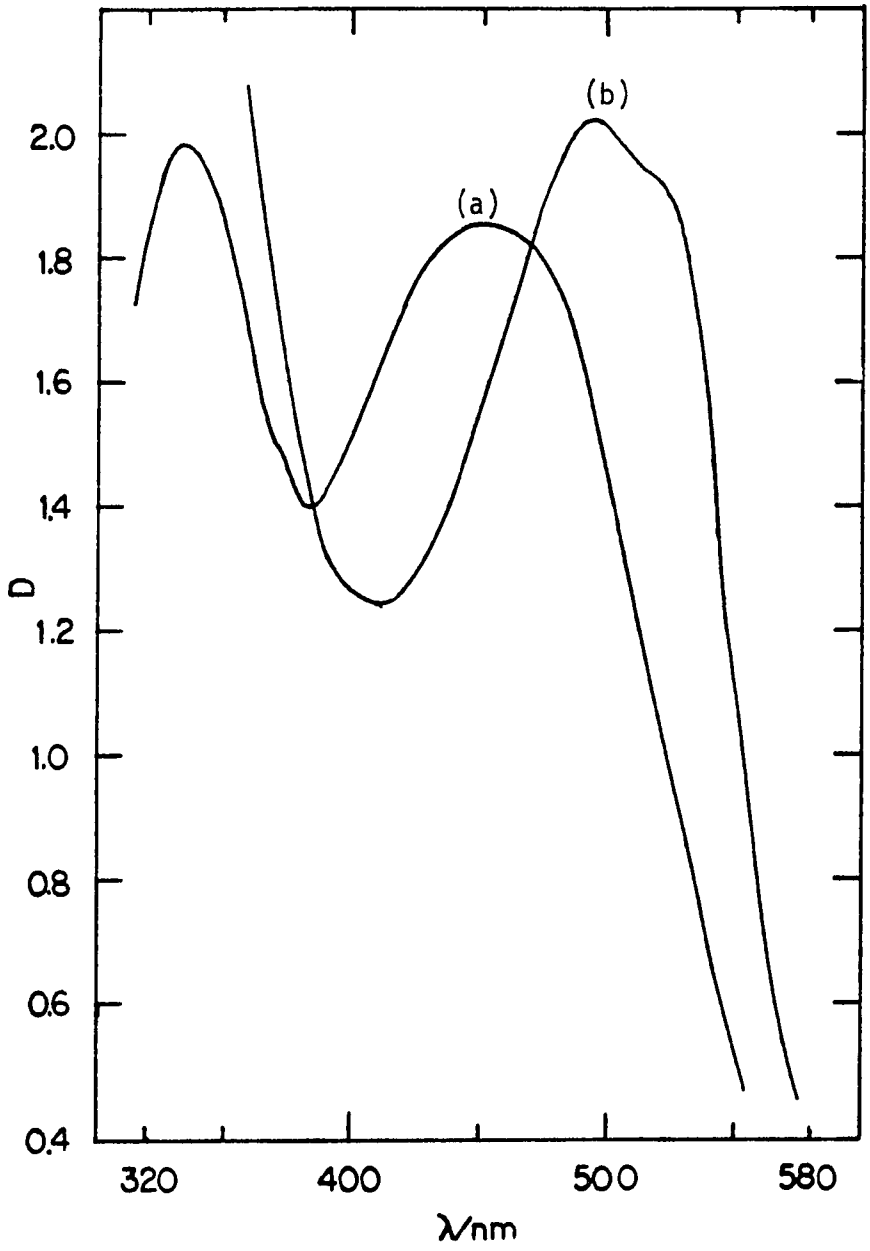

Figure II-7. Electronic spectrum of $Co_2^{II}(5\text{-}Bu^t sal_4 bz)$ before (a) and after (b) reaction with $Co(NH_3)_5Br^{2+}$ (ℓ = 1 cm)

For the reaction of $Co_2^{II}(5\text{-}Bu^t sal_4 bz)$ with H_2O_2, some preliminary kinetic experiments were performed spectrophotometrically (Table II-3). The absorbance was monitored at 500 nm which is an absorbance maximum for the Co_2^{III} complex. Hydrogen peroxide was always used in excess over Co_2^{II} because in experiments with Co_2^{II} in excess, the reaction appeared to be autocatalytic. All of the plots of $\ln|D_t - D_\infty|$ versus time were found to be curved with the initial points lying above the "best fit" line. The last oxidant, Ce^{IV}, was not found to be very useful because the high acid needed to keep Ce^{IV} from polymerizing was too high for the Co_2^{II} complex and caused considerable decomposition. The spectral changes were consistent with the oxidation of the Co_2^{II}, however.

The reaction of $Co(NH_3)_5Br^{2+}$ with $Co_2^{II}(5\text{-}SO_3 sal_4 bz)^{4-}$ was very similar to its reaction with $Co_2^{II}(5\text{-}Bu^t sal_4 bz)$ except that it was much faster and therefore much easier to titrate spectrophotometrically. The spectrophotometric titrations once again revealed a 2:1 stoichiometry for the reaction between $Co(NH_3)_5Br^{2+}$ and $Co_2^{II}(5\text{-}SO_3 sal_4 bz)^{4-}$ (Figure II-8).

Organometallic compound formation and reactivity

Reaction of "$NaBH_4$-reduced $Co_2(5\text{-}Bu^t sal_4 bz)$" with CH_3I in methanol was found to occur relatively slowly, requiring 20-30 minutes to reach completion. The reaction was carried out under an inert atmosphere of Cr^{2+}-scrubbed N_2; the product solution was found to be light-sensitive, but not air-sensitive. By diluting the methanol solution with water

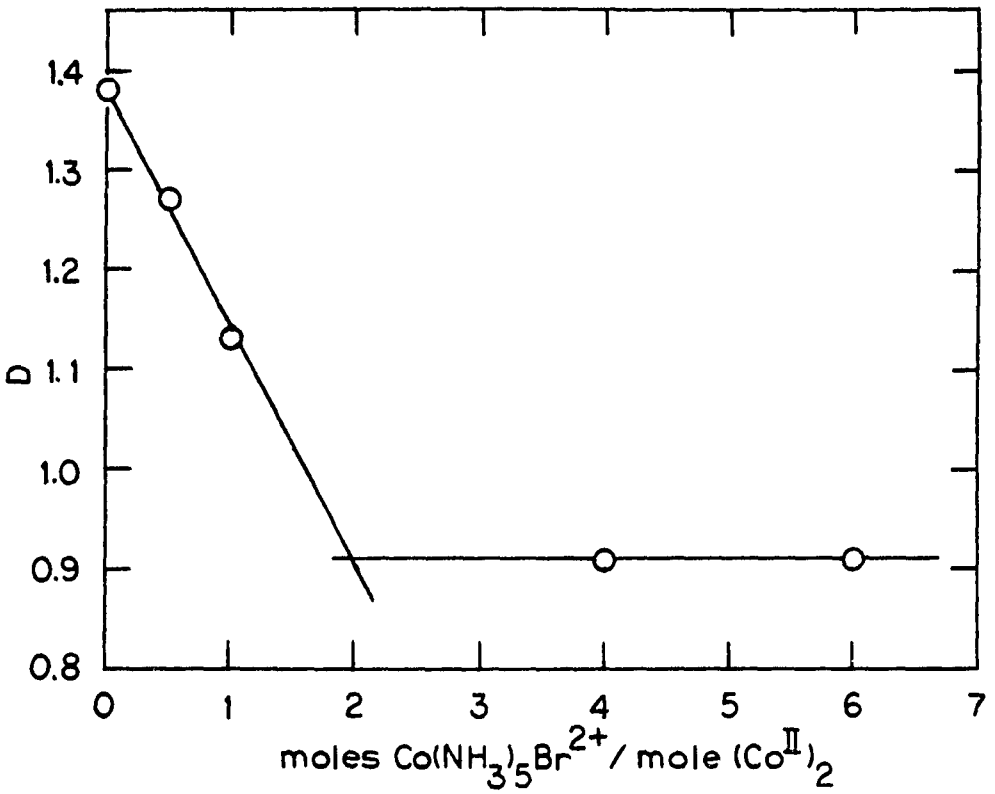

Figure II-8. Spectrophotometric titration for the reaction of $Co(NH_3)Br^{2+}$ with $Co_2^{II}(5\text{-}SO_3sal_4bz)^{4-}$ (ℓ = 1 cm)

and extracting the aqueous methanol with CH_2Cl_2, a dark brown CH_2Cl_2 solution was obtained. Because of the relatively low solubility of Co_2^{II}(5-Bu^{t}sal$_4$bz), only small quantities of this dark brown complex could be prepared (10-20 mgs). Because of this, the complex was identified as being a dimethyl complex by its chemical reactivity. Based upon mononuclear analogs such as $CH_3Co(sal_2phen)$, Hg^{2+} would be expected to cleave the cobalt-carbon bond in a relatively fast reaction (121). Also, the spectrophotometric titrations between Hg^{2+} and $(CH_3Co)_2$(5-Bu^{t}sal$_4$bz) revealed a 2:1 stoichiometry and the reaction was qualitatively noted to be a fast one. Although the CH_3Hg^+ product was not checked, by analogy with mononuclear complexes it is written as

$$2Hg^{2+} + (CH_3Co)_2 \xrightarrow{fast} 2HgCH_3^+ + Co_2^{III} \qquad (II\text{-}3)$$

the other product of this electrophilic cleavage reaction. In any event, the Co_2 product was clearly Co_2^{III} (Figure II-9), even under anaerobic conditions. The 2:1 stoichiometry and the rate of the Hg^{2+} reaction clearly indicate that a dimethyl cobalt complex has been formed.

Some kinetic experiments were performed to examine the Hg^{2+} reaction more closely (Table II-4). The rate constant determined was similar to that observed for the mononuclear analog (2.4×10^3 versus 3.3×10^4 M^{-1} s^{-1} (120). The rate law may be written as:

$$\frac{-d[(CH_3Co)_2]}{dt} = k[Hg^{2+}][(CH_3Co)_2]$$

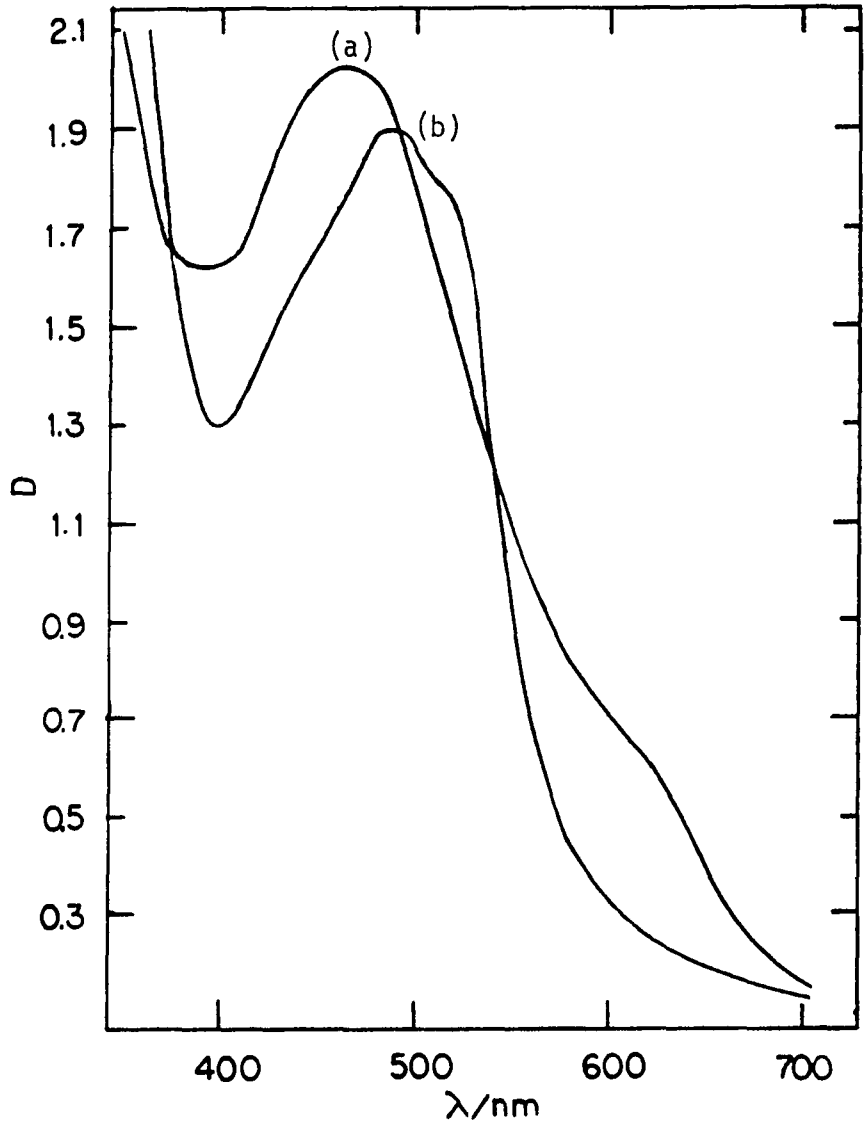

Figure II-9. Electronic spectrum of $(CH_3Co)_2(5\text{-}Bu^tsal_4bz)$ before (a) and after (b) reaction with Hg^{2+} (ℓ = 1 cm)

Table II-4. Rate constants for the reaction of Hg^{2+} with $(CH_3Co)_2(5\text{-}Bu^t sal_4 bz)$

10^4 $[Hg^{2+}]$/M	k_{obs}/s^{-1}	10^3 k/M^{-1} s^{-1}
1.05	0.29(2)	2.7
2.1	0.52(3)	2.5
4.2	0.86(7)	2.1

[a]Solvent was 0.1 HNO_3 in methanol; $[(CH_3Co)_2] = 1.4 \times 10^{-5}$ M; T = 25 ± 0.2°C.

Therefore, this provides another bit of chemical evidence consistent with its identification. There was no evidence for two different rate constants for the two methyl groups of each molecule. The implications of this would appear to be that both methyl groups are cleaved by Hg^{2+} independent of one another. The dimethyl complex was also characterized by its photosensitivity (Figure II-10) as shown in Equation II-4, and its stability in the absence of light, Equation II-5. It was also

$$(CH_3Co)_2(5\text{-}Bu^t sal_4 bz) \xrightarrow[O_2]{light} Co_2^{III}(5\text{-}Bu^t sal_4 bz) + CH_3\text{-products} \quad (II\text{-}4)$$

$$(CH_3Co)_2(5\text{-}Bu^t sal_4 bz) \xrightarrow[dark]{O_2} N.R. \quad (II\text{-}5)$$

observed that reaction II-4 was substantially retarded if the system was purged with N_2 prior to exposing it to the light (122). The spectral changes in the absence of O_2 were also quite different with very little evidence for Co_2^{III} formation.

Several attempts were made to prepare the corresponding diethyl complex from ethyl iodide, but in each attempt it appeared that no reaction took place. The reason for this lack of reaction will be discussed later. In any case, no other alkyl derivatives were prepared.

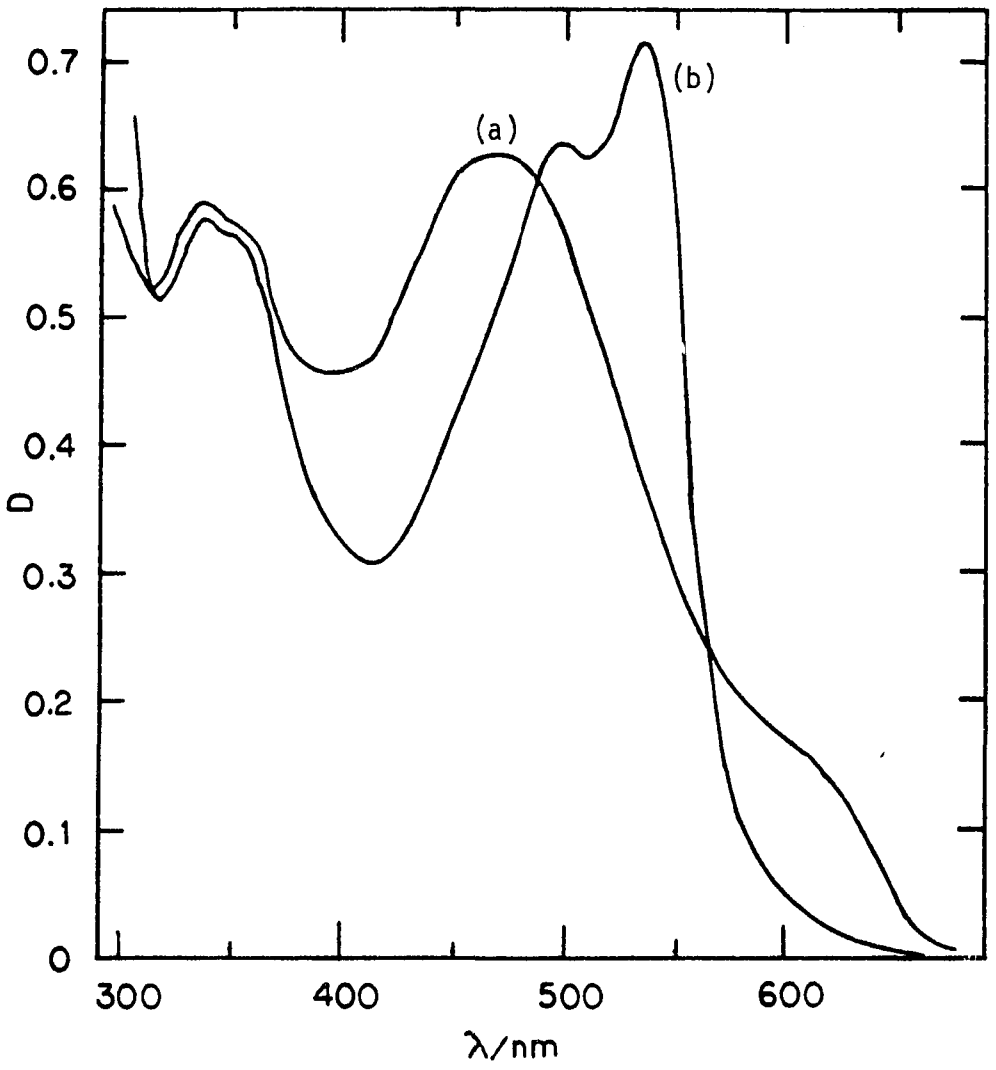

Figure II-10. Electronic spectrum of $(CH_3Co)_2(5\text{-}Bu^tsal_4bz)$ before (a) and after (b) ∿1 hr exposure to room lights (ℓ = 1 cm)

DISCUSSION

In the reactions studied, the presence of two cobalt atoms which might be able to interact electronically did not seem to impart special reactivity to these complexes. Even in a complex which would appear to be ideally set-up to show neighboring group effects such as the dimethyl complex (IV), no evidence of a monomethyl intermediate with unique properties was detected.

One might expect to observe two kinetic steps if the monomethyl complex reacted at a different rate than the dialkyl. This would be equivalent to A→B→C, where A = dialkyl and B = monoalkyl. One chemical reason for observing only one step could be that both metal centers react as separate transition metal complexes and can be treated as separate entities. This would imply that the bridging group does not allow a significant amount of interaction between the two metal centers. The observation of single-stage kinetics for A→B→C has been recently reviewed (123). In another instance, the $CrCl_2$ reduction of $Co_2^{III}(5\text{-}SO_3sal_4bz)$ under second order conditions was found to give straight-line plots, implying that no neighboring group effects were being observed. Therefore, these two reactions which were operating under entirely different conditions both showed no evidence of neighboring group participation. Again, simply stated, these reactions of the binuclear complexes were kinetically indistinguishable from the mononuclear analogs.

The situation was not as clear-cut with regard to the oxidation reactions of $Co_2^{II}(5\text{-}Bu^tsal_4bz)$ and $Co_2^{II}(5\text{-}SO_3sal_4bz)^{4-}$. In the former

case, both H_2O_2 and $Co(NH_3)_5Br^{2+}$ gave curved first-order plots under pseudo-first-order conditions. Although in some cases, two-stage kinetics might have been used to rationalize the results, more than two steps were sometimes observed. The sorting-out of further information seems unreasonably difficult at this time. It was observed, however, that two rate constants were quite reproducible for this reaction. The problem which developed was, again they were not the only two steps observed.

The trends which can be ascertained from the chemistry of $Co_2^{II,III}(sal_4bz)^{0,2+}$, $Co_2^{II,III}(5\text{-}Bu^t sal_4bz)^{0,2+}$ and $Co_2^{II,III}(5\text{-}SO_3 sal_4bz)^{4,2-}$ are somewhat limited because of several factors. Owing to the extremely low solubility of $Co_2^{II}(sal_4bz)$, very little of its solution chemistry was studied. The approach taken was to characterize as well as possible its UV-visible spectrum and observe some solution properties as a function of the metal oxidation state and solvent. Unfortunately, both the ligand and the cobalt complex were too insoluble for nmr studies. The second and third members of the series were studied in two different solvents and thus comparisons between these two are also somewhat strained. What can be confidently stated is that the addition of the 5-tert-butyl groups to $Co_2(sal_4bz)$ greatly increased its solubility, perhaps by as much as 2 or 3 orders of magnitude in some solvents. Despite this increase in solubility, the 5-tert-butyl complex was still not soluble enough for nmr studies. However, the dimethyl derivative $(CH_3Co)_2(5\text{-}Bu^t sal_4bz)$ was sufficiently more soluble to allow for nmr data acquisition (see Experimental).

Also, the (5-Bu^{t}sal$_4$bzH$_4$) ligand was quite a bit more soluble in CH_2Cl_2 and $CHCl_3$ than (sal$_4$bzH$_4$), and its nmr spectrum was also obtained (see Experimental). The peak positions for the free ligand were assigned based on their chemical shifts. Unfortunately, the peak positions for the complex did not allow an unambiguous assignment of the methyl groups bonded to cobalt. Their existence was already established, however, by the stoichiometry of the reaction with Hg^{2+}. Because the dimethyl complex was always prepared on a small scale, no elemental analysis was obtained for it. The small scale preparation was necessitated by the low solubility of the starting material. Despite this, chromatographic separations revealed that the only impurity which could be separated was a small amount of unmethylated complex in the form of Co_2^{III}(5-Bu^{t}sal$_4$bz)$^{2+}$.

The fact that the dimethyl complex was prepared from a $NaBH_4$ reduced solution reveals that the reduction must be reversible by some pathway during the course of reaction with CH_3I or the subsequent work-up. This may be claimed because the ultimate dimethyl product yields Co_2^{III} when exposed to air and light or reacted with Hg^{2+}. Although the $NaBH_4$ reduction clearly does not produce a Co_2^{I} solution, there is a possibility that a small amount of cobalt-hydride species are formed and ultimately react with CH_3I. Another possibility would be that the reaction takes place by an activation of CH_3I. Perhaps one Co center could activate the CH_3I forming an activated precursor complex and a second Co react with the activated complex to give a methylated Co. For a binuclear complex, this could be an

intramolecular or an intermolecular process. This type of scheme bears some resemblance to a reaction of B_{12r} with several alkyl iodides including methyl iodide. Halpern has proposed that one molecule of B_{12r} could activate RX and a second molecule of B_{12r} would then react with the activated methyl iodide (124). Perhaps this type of activation would account for the somewhat slow reaction of $Co_2^{II}(5\text{-}Bu^t sal_4 bz)$ with methyl iodide.

$$B_{12r} + RX \rightleftharpoons B_{12r}\cdot RX$$

$$B_{12r}\cdot RX + B_{12r} \rightarrow R\text{-}B_{12} + B_{12a} + X^-$$

$$2B_{12r} + RX \longrightarrow R\text{-}B_{12} + B_{12a} + X^-$$

The third member of the series $Co_2^{II}(5\text{-}SO_3 sal_4 bz)^{4-}$ is of about the same solubility as the 5-tert-butyl complex, perhaps slightly more soluble, but now, of course, the solubility is in water in which the other two complexes were insoluble. Its chemistry is similar to the other two in several respects. All three complexes show similar changes when air-oxidized in the presence of some type of coordinating base, namely a double-absorbance peak at longer wavelength (∿500 nm) and another peak at 330 nm. (Another even stronger peak ∿260 nm was not fully explored.) All three complexes show similar changes when reduced with $NaBH_4$ and a tendency to be reduced beyond the Co_2^{II} state. This further reduced state does not show the reactivity which would be expected for a Co^I center and, indeed, is not considered to be Co^I. As previously mentioned, this state is considered to be likely to be

due to some ligand reduction, which $NaBH_4$ is known to be suitable for in methanol (125,126). Because of the stated intent of this work, a further reduced ligand system was not considered to be of interest for further study. For this reason, $NaBH_4$ was typically avoided for reducing Co_2^{III} solutions to Co_2^{II}, with milder reductants yielding more suitable results. Even with milder conditions, care had to be exercised to prevent decomposition of the complexes. For example, if $Co_2^{III}(5\text{-}Bu^t sal_4 bz)^{2+}$ was reduced in methanol with H_2 over PtO_2, decomposition would occur unless the solution was buffered around pH ∿6-8. The exact mechanism of this decomposition and the products were not investigated, but from the very large loss in absorbance, it seems likely that the metal was slipping out of the chelate or the ligand was possibly being destroyed.

Owing to the very nature of a Schiff base, i.e., it is formed via a condensation reaction, it might seem contradictory, perhaps even foolhardy, to work with a Schiff base in water. Despite this a priori reasoning, the $Co_2^{III}(5\text{-}SO_3 sal_4 bz)^{2-}$ complex was investigated in water and found to be quite stable at room temperature. Its stability was judged by recording the absorbance spectrum during a 24 hr period and noting <2-3% absorbance change at the maxima and no shift in peak positions. This finding is in good agreement with a recent report of the stability of a $Cu(5\text{-}SO_3 sal_2 en)$ complex in water (127). This finding does contrast, however, with results reported by Merrell and Abrams in which they found the nickel and copper complexes of $(5\text{-}SO_3 sal_4 H_4 bz)$ to be unstable in water (128). Although the

differences may be due to the differences in the labilities of the various metals; it should be noted that $Cu(5\text{-}SO_3sal_2en)$ was stable towards hydrolysis up to 80°C in water and yet $Cu_2(5\text{-}SO_3sal_4bz)$ "readily hydrolyzes". It should be noted, however, that at higher temperatures in water $Co_2(5\text{-}SO_3sal_4bz)$ did decompose to a water-insoluble brown product.

The reaction of $CrCl_2$ with $Co_2^{III}(5\text{-}SO_3sal_4bz)^{2-}$, which was studied kinetically, offers an interesting reaction for speculation. Indirect evidence indicates that the mechanism for reduction is either outer-sphere or if inner-sphere, it probably goes through a halide atom bridge (Ref. 39, p. 501), but most probably not by attack of Cr(II) at the phenolic oxygens with subsequent electron transfer. One might expect the latter type of attack to result in a bound Cr(III) which, being substitutionally inert might remain bound long enough to be detected spectroscopically or by the chromatographic elution pattern. Since this was not observed, electron-transfer most probably occurs by one of the two former pathways.

Careful study of the spectral changes which occur when the Co_2^{II} complexes are reacted with oxygen as opposed to other oxidants, has revealed that the formulation of an oxygen-carrying cobalt species does not seem likely. This conclusion was based on the results obtained when $Co(NH_3)_5Br^{2+}$ in particular was reacted with the Co_2^{II} species of the second and third ligands. By carefully avoiding exposure to air, the effect of the bromopentaaminecobalt(III) alone was investigated. As a comparison of Figures II-11 and II-12 shows, the effect of O_2 and

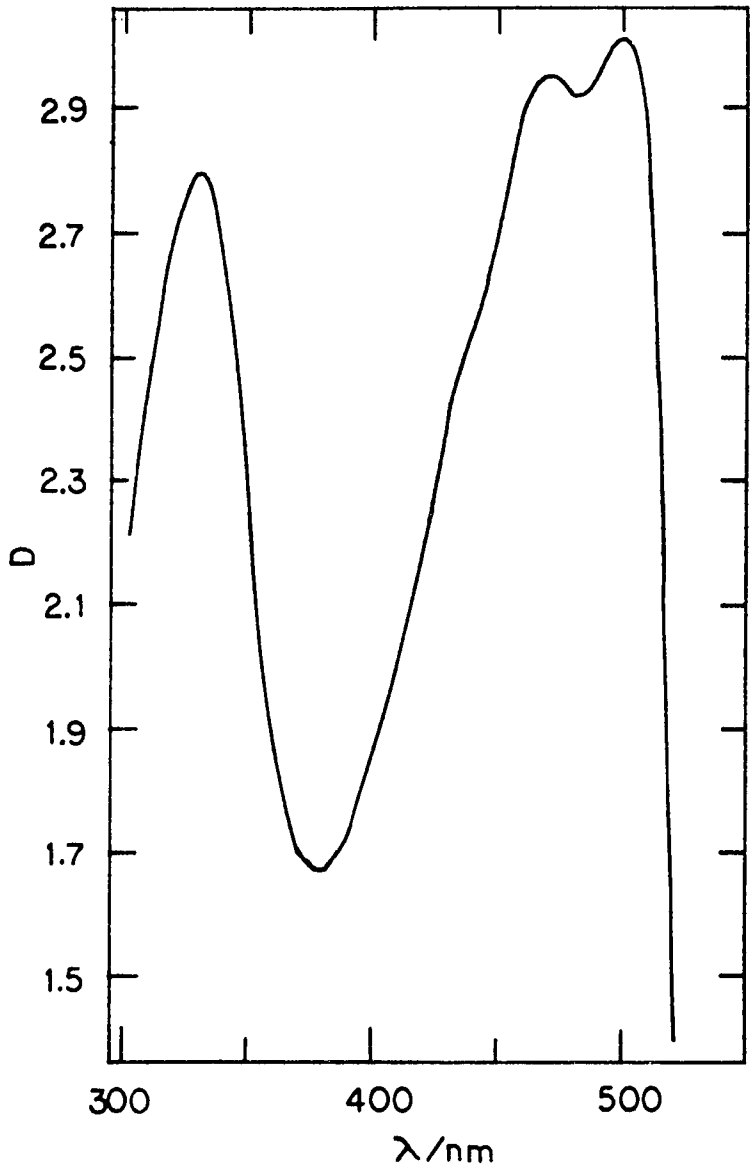

Figure II-11. Electronic spectrum of $Co_2^{III}(5\text{-}SO_3sal_4bz)^{2-}$ produced by reaction of $Co(NH_3)_5Br^{2+}$ with $Co_2^{II}(5\text{-}SO_3sal_4bz)^{4-}$ (ℓ = 1 cm)

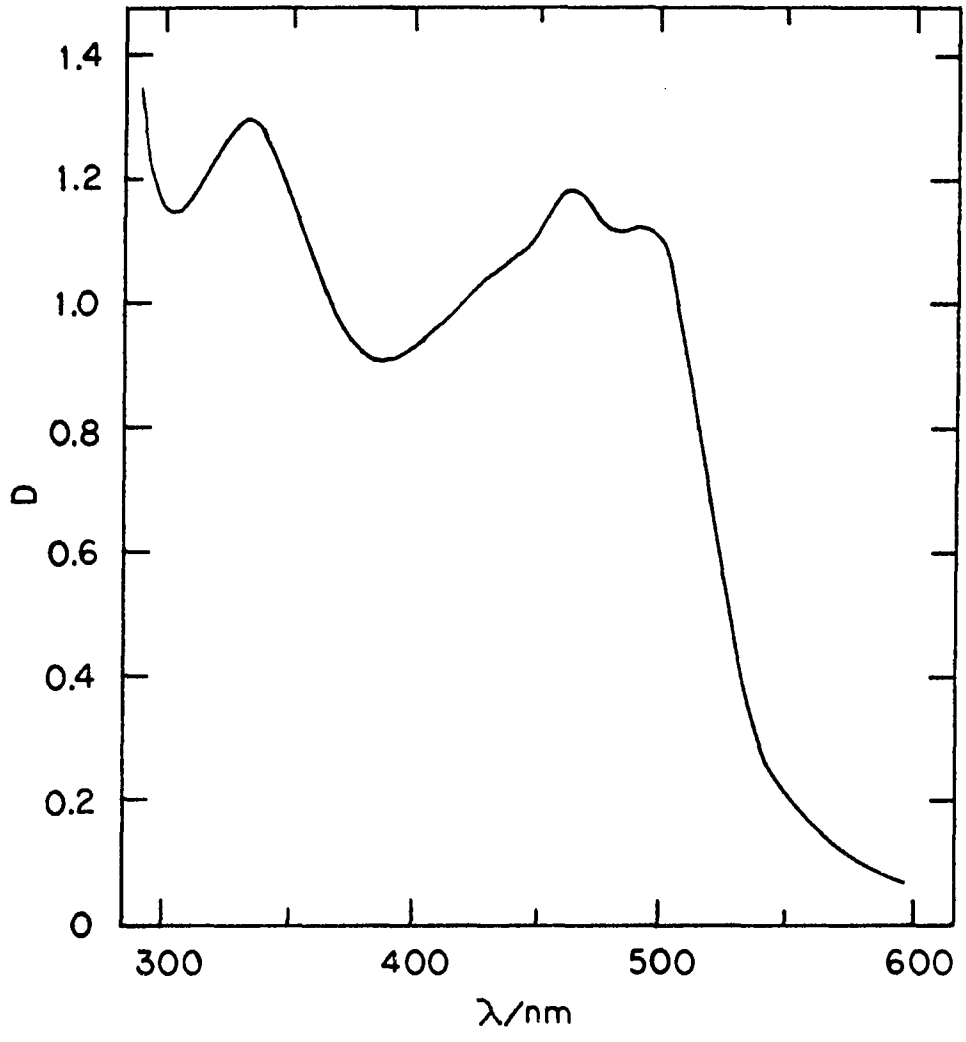

Figure II-12. Electronic spectrum of $Co_2^{II}(5\text{-}SO_3sal_4bz)^{4-}$ partially oxidized with O_2 bubbling to $Co_2^{III}(5\text{-}SO_3sal_4bz)^{2-}$ (ℓ = 1 cm)

$Co(NH_3)_5Br^{2+}$ on the spectrum of $Co_2^{II}(5\text{-}SO_3sal_4bz)^{4-}$ is very similar. The possibility, of course, exists that in the former case a hydroxy-cobalt species forms while in the latter case, a bromo-cobalt species may form.

The $CrCl_2$ reduction of Co_2^{III} (produced initially by air-oxidation) also seems to rule out some sort of oxygen-bound complex because only a 2:1 stoichiometry was obtained for that reaction. An oxygen-bound species would require additional $CrCl_2$.

The first report of a synthetic reversible molecular oxygen carrier which worked in aqueous solution was by Burke and coworkers for a cobalt(II)-histidine complex (129). However, as discussed earlier, the mononuclear model compound, $Co(sal_2phen)$, is not capable of binding oxygen in protogenic solvents. In fact, though there are a large number of cobalt Schiff base type complexes which bind molecular oxygen in solution, it seems that all of them require nonaqueous solvents (130-132). The oxygen binding ability of some of these complexes may be due to the lack of available hydrogen atoms. In this study, protic solvents were used and this lends still further support to the contention that Co_2^{III} species are formed by air oxidation and are not oxygen adducts.

Although these complexes have been difficult to work with in solution studies, some general conclusions seem evident. First, the solubility of these complexes is very dependent upon substitution around the ligand system, but in general the complexes have only slight solubility in most solvents. Second, there appears to be no dramatic

changes in the reactivities of the binuclear analogs as compared with mononuclear models and as far as the results obtained have shown the mixed-valence species appear to have properties which are just intermediate between the Co_2^{II} and Co_2^{III} species. More work is needed in the study of binuclear complexes in solution to probe factors which effect reactivity.

BIBLIOGRAPHY

1. Espenson, J. H.; Kirker, G. W. Inorg. Chim. Acta 1980, 40, 105.
2. Hodgkin, D. C.; Lindsey, J.; Sparks, R. A.; Trueblood, K. N.; White, J. G. Proc. Roy. Soc. 1962, A266, 494.
3. Halpern, J. In "Relations Between Homogeneous and Heterogeneous Catalysis", Basset, J. M., Ed.; Editions du CNRS: Paris, 1978; p. 27.
4. Kochi, J. K. "Organometallic Mechanisms and Catalysis", Academic Press: New York, 1978; p. 573.
5. Parshall, G. W. "Homogeneous Catalysis", Wiley & Sons: New York, 1980; p. 3.
6. Anet, F.A.L.; LeBlanc, E. J. Am. Chem. Soc. 1957, 79, 2649.
7. Kochi, J. K.; Rust, F. F. J. Am. Chem. Soc. 1961, 83, 2017.
8. Ardon, H.; Woolmington, K.; Pernick, A. Inorg. Chem. 1971, 10, 2812.
9. Schmidt, W.; Swinehart, J. H.; Taube, H. J. Am. Chem. Soc. 1971, 93, 1117.
10. Espenson, J. H.; Sheveima, J. S. J. Am. Chem. Soc. 1973, 95, 4469.
11. Leslie, J. P.; Espenson, J. H. J. Am. Chem. Soc. 1976, 98, 4839.
12. Swallow, A. J. Prog. Reaction Kinetics 1978, 9, 274.
13. Cohen, H.; Meyerstein, D. Inorg. Chem. 1974, 13, 2434.
14. Espenson, J. H.; Bakač, A. J. Am. Chem. Soc. 1981, 103, 0000.
15. Bakač, A.; Espenson, J. H. Inorg. Chem. 1981, 20, 0000.
16. Bakač, A.; Espenson, J. H. J. Am. Chem. Soc. 1981, 103, 0000.
17. Nohr, R. S.; Espenson, J. H. J. Am. Chem. Soc. 1975, 97, 3392.
18. Marty, W.; Espenson, J. H. Inorg. Chem. 1979, 18, 1246.
19. Pohl, M. C.; Espenson, J. H. Inorg. Chem. 1980, 19, 235.
20. Espenson, J. H.; Leslie, J. P. J. Am. Chem. Soc. 1974, 96, 1954.

21. Schmidt, A. R.; Swaddle, T. W. J. Chem. Soc. A 1970, 1927.

22. Coombes, R. G.; Johnson, M. D. J. Chem. Soc. A 1966, 177.

23. Coombes, R. G.; Johnson, M. D.; Winterton, N. J. Chem. Soc. 1965, 7029.

24. Walling, C.; Johnson, R. A. J. Am. Chem. Soc. 1975, 97, 363.

25. Walling, C. Acc. Chem. Res. 1975, 8, 125.

26. Dixon, W. T.; Norman, R.O.C. J. Chem. Soc. 1963, 3119.

27. Jefcoate, C. R.; Norman, R.O.C. unpublished observations cited in: Adv. Phys. Org. Chem. 1967, 5, 75.

28. Kelm, M.; Lilie, J.; Henglein, A.; Janata, E. J. Phys. Chem. 1974, 78, 882.

29. Buxton, G. V.; Green, J. C. J. Chem. Soc., Faraday Trans. 1 1978, 74, 697.

30. Freiberg, M.; Meyerstein, D. J. Chem. Soc., Faraday Trans. 1 1977, 73, 62.

31. Bhattacharya, S. N.; Saha, N. C. Radiat. Eff. 1979, 42, 191.

32. Bhattacharya, S. N.; Srisankar, E. V. J. Chem. Soc., Faraday Trans. 1 1978, 74, 622.

33. Asmus, K.-D.; Wigger, A.; Henglein, A. Ber. Bunsenges Phys. Chem. 1966, 70, 862.

34. Neta, P. Adv. Phys. Org. Chem. 1976, 12, 223.

35. Johnson, D. W.; Salmon, G. A. J. Chem. Soc., Faraday Trans. 1 1977, 73, 256.

36. Johnson, D. W.; Salmon, G. A. J. Chem. Soc., Faraday Trans. 1 1979, 75, 446.

37. Eibenberger, J.; Schulte-Frohlinde, D.; Steenken, S. J. Phys. Chem. 1980, 84, 704.

38. Lilie, J.; Beck, G.; Henglein, A. Ber. Bunsenges Phys. Chem. 1971, 75, 458.

39. Basolo, F.; Pearson, R. G. "Mechanisms of Inorganic Reactions", 2nd ed.; Wiley Eastern Ltd.: New Delhi, 1977; Chapter 3.

40. Elroi, H.; Meterstein, D. J. Am. Chem. Soc. 1978, 100, 5540.

41. Blackburn, R.; Kyaw, M.; Phillips, G. O.; Swallow, A. J. J. Chem. Soc., Faraday Trans. 1 1975, 71, 2277.

42. Espenson, J. H.; Bakač, A. J. Am. Chem. Soc. 1980, 102, 2488.

43. Tratchenko I. In "Fundamental Research in Homogeneous Catalysis"; Tsutsui, M. Ed.; Plenum Press: New York, 1979; p. 119.

44. Fahey, D. R. J. Am. Chem. Soc. 1981. 103, 136.

45. Gladysz, J. A.; Selover, J. C.; Strouse, C. E. J. Am. Chem. Soc. 1978, 100, 6766.

46. Casey, C. P.; Andrews, M. A.; McAlister, D. R. J. Am. Chem. Soc. 1979. 101, 3371.

47. Casey, C. P.; Andrews. M. A.; McAlister. D. R.; Rimz, J. E. J. Am. Chem. Soc. 1980, 102, 1927.

48. Bakač, A. Unpublished observations, Ames Laboratory. Iowa State University, Ames, Iowa. 1980-1981.

49. Holah, D. G.; Fackler, J. P. Inorg. Synth. 1967, 10, 26.

50. Diehl, H.; Clark, H.; Willard, H. H. Inorg. Synth. 1939, 1, 86.

51. Moeller, T.; King, G. L. Inorg. Synth. 1957, 5, 185.

52. Schlessinger, G. G. Inorg. Synth. 1967, 9, 160.

53. Parker, O.; Espenson, J. H. J. Am. Chem. Soc. 1969, 91, 1968.

54. Ramsey, J. B.; Aldridge, F. T. J. Am. Chem. Soc. 1955, 77, 2561.

55. For actual spectra see the Aldrich Library of NMR Spectra.

56. Haupt, G. W. J. Res. Natl. Bur. Stand. 1952, 48, 414.

57. Kolthoff, I. M.; Sandell, E. B. "Quantitative Analysis in Inorganic Chemistry". Macmillan: New York, 1958; p. 600.

58. The D-132 accessory was on loan from the ISU Biochemistry Department.

59. The carbon centered radicals may also disproportionate. See: Neta, P. Adv. Phys. Org. Chem. 1976, 12, 275.

60. Candlin, J. P.; Halpern, J. Inorg. Chem. 1965, 4, 766.

61. Cohen, H.; Meyerstein, D. J. Chem. Soc., Dalton Trans. 1977, 1056.

62. Bakač, A.; Espenson, J. H. Inorg. Chem. 1981, 20, 953.

63. Samuni, A.; Meisel, D.; Czapski, G. J. Chem. Soc., Dalton Trans. 1972, 1273.

64. Hyde, M. R.; Espenson, J. H. J. Am. Chem. Soc. 1976, 98, 4463.

65. Zeldes, H.; Livingston, R. J. Chem. Phys. 1966, 45, 1946

66. Zeldes, H.; Livingston, R. J. Chem. Phys. 1970, 53, 2448.

67. Becket, A.: Porter, G. Trans. Faraday Soc. 1963, 59, 2038.

68. Anpo, M.; Kubokawa, Y. Bull. Chem. Soc. Jpn. 1977, 50, 1913.

69. Calvert, J. G.; Pitts, J. N. "Photochemistry". Wiley: New York, 1966; Chapter 5.

70. Kwiatek, J. In "Transition Metals in Homogeneous Catalysis", Schrauzer, G. N., Ed.; Marcel Dekker: New York, 1971; p. 21.

71. Taft, R. W. In "Steric Effects in Organic Chemistry", Newman, M. S., Ed.; Wiley & Sons: New York, 1965; Chapter 5.

72. (a) Burwell, R. L. Chem. Rev. 1954, 54, 615, and references cited.
(b) Stande, E.; Patat, F. In "The Chemistry of the Ether Linkage", Patai, S., Ed.; Interscience Publishers: New York, 1967; Chapter 2.

73. Olah, G. A.; O'Brien, D. H. J. Am. Chem. Soc. 1967, 89, 1725.

74. Olah, G. A.; White, A. M. J. Am. Chem. Soc. 1968, 90, 1884.

75. Wilkins, R. G. "The Study of Kinetics and Mechanisms of Reactions of Transition Metal Complexes", Allyn and Bacon: Boston, 1974; p. 99.

76. Baird, M. C. J. Organomet. Chem. 1974, 64, 289.

77. Braterman, P. S. Top. Curr. Chem. 1980, 92, 165.

78. Martin, J. C. In "Free Radicals", Kochi, J. K., Ed.; Wiley: New York, 1973; Vol. II, p. 493.

79. Langford, C. H. Inorg. Chem. 1965, 4, 265.

80. Hammond, G. S. J. Am. Chem. Soc. 1955, 77, 334.

81. Halpern, J. Pure Appl. Chem. 1979, 51, 2171.

82. Connor, J. A. Top. Curr. Chem. 1977, 71, 94.

83. Endicott, J. F.; Balakrishnan, K. P.; Wong, C.-L. J. Am. Chem. Soc. 1980, 102, 5519.

84. Leffler, J. E.; Grunwald, E. "Rates and Equilibria of Organic Reactions", Wiley: New York, 1963.

85. Chapman, N. B.; Shorter, J. "Advances in Linear Free Energy Relationships", Plenum Press: New York, 1972.

86. Shorter, J. "Correlation Analysis in Chemistry", Plenum Press: New York, 1978.

87. Rüchardt, C.; Beckhaus, H. D. Angew. Chem. Int. Ed. Engl. 1980, 19, 429-436.

88. Kochi, J. K. In "Advances in Free Radical Chemistry"; Williams, G. H., Ed.; Academic Press: New York, 1975; Vol. 5, pp. 219-220.

89. Pavelich, W. A.; Taft, R. W. J. Am. Chem. Soc. 1957, 79, 4935.

90. Hine, J. "Structural Effects on Equilibria in Organic Chemistry"; Wiley: New York, 1965; p. 313.

91. Halpern, J.; Tinker, H. B. J. Am. Chem. Soc. 1967, 89, 6427.

92. Hansch, C.; Leo, A. "Substituent Constants for Correlation Analysis in Chemistry and Biology"; Wiley: New York, 1979.

93. Charton, M. J. Am. Chem. Soc. 1975, 97, 3691.

94. DeTar, D. F. J. Am. Chem. Soc. 1980, 102, 7988.

95. Ryan, D. A. Ph.D. Thesis, Iowa State University, Ames, Iowa, 1981.

96. Ryan, D. A.; Espenson, J. H. J. Am. Chem. Soc. 1979, 101, 2488.

97. Carlyle, D. W.; Espenson, J. H. Inorg. Chem. 1967, 6, 1370.

98. Milburn, R.; Vosburgh, W. C. J. Am. Chem. Soc. 1955, 77, 1352.

99. Swift, T. J.; Connick, R. E. J. Chem. Phys. 1964, 41, 2553.

100. Grant, M.; Jordan, R. B. Inorg. Chem. 1981, 20, 55.

101. Bushey, W. R.; Espenson, J. H. Inorg. Chem. 1977, 16, 2772.

102. Dulz, G.; Sutin, N. J. Am. Chem. Soc. 1964, 86, 829.

103. Carlyle, D. W.; Espenson, J. H. J. Am. Chem. Soc. 1969, 91, 599.

104. Horanyi, G.; Vertes, G.; Konig, P. Naturwiss. 1973, 60, 519.

105. Groh, S. E. Isr. J. Chem. 1977, 15, 277.

106. Casellato, U.; Vigato, P. A.; Vidali, M. Coord. Chem. Rev. 1977, 23, 31.

107. Gagné, R. R.; Spiro, C. L. J. Am. Chem. Soc. 1980, 102, 1443.

108. Mueller-Westerhoff, U. T. Adv. Chem. Ser. 1976, 150, 31.

109. Merrell, P. H.; Osgood, R. A. Inorg. Chim. Acta 1975, 14, L33.

110. Fleischer, E. B.; Jetter, D.; Floriani, R. Inorg. Chem. 1974, 13, 1042.

111. Gluvchinsky, P.; Mochler, G. M.; Healy, P. C.; Sinn, E. J. Chem. Soc. A 1974, 1156.

112. Costa, G.; Puxeddu, L.; Nardin-Stefani, J. Inorg. Nucl. Chem. Lett. 1970, 6, 191.

113. Hasty, E. F.; Colburn, T. L.; Hendrickson, D. N. Inorg. Chem. 1973, 12, 2414.

114. Felthouse, T. R.; Hendrickson, D. N. Inorg. Chem. 1978, 17, 2636.

115. Taube, H. Adv. Chem. Ser. 1977, 162, 127.

116. Gagné, R. R.; Koval, C. A.; Smith, T. J. J. Am. Chem. Soc. 1977, 99, 8367.

117. Duff, J. C. J. Chem. Soc. 1941, 547.

118. Blau, F. Monatsh. Chem. 1897, 18, 123.

119. Burness, D. M. Org. Syn. 1959, 39, 51.

120. Kirker, G. W. Org. Prepr. Proc. Int. 1980, 12, 246.

121. Espenson, J. H.; Bushey, W. R.; Chmielewski, M. E. Inorg. Chem. 1975, 14, 1303.

122. Endicott, J. F.; Ferraudi, G. J. J. Am. Chem. Soc. 1977, 99, 243.

123. Chipperfield, J. R. J. Organomet. Chem. 1977, 137, 355.

124. Halpern, J. Anal. N.Y. Acad. Sci. 1974, 239, 11.

125. Skuratowicz, J. S.; Madden, I. L.; Busch, D. H. Inorg. Chem. 1977, 16, 1721.

126. Dickson, I. E.; Robson, R. Inorg. Chem. 1974, 13, 1301.

127. Elias, H.; Kohler, G. Inorg. Chim. Acta 1979, 34, L215.

128. Merrell, P. H.; Abrams, M. Inorg. Chim. Acta 1979, 32, 93.

129. Burke, D.; Hearon, J. Z.; Caroline, L.; Schade, A. L. J. Biol. Chem. 1946, 165, 723.

130. Vogt, L. H., Jr.; Faigenbaum, H. M.; Wiberley, S. E. Chem. Rev. 1963, 63, 269.

131. Calderazzo, F.; Floriani, C.; Salzmann, J.-J. Inorg. Nucl. Chem. Lett. 1966, 2, 379.

132. Bigotto, A.; Costa, G.; Mestroni, G.; Pellizer, G.; Puxeddu, A.; Reisenhofer, E.; Stefani, L.; Tauzher, G. Inorg. Chim. Acta Rev. 1970, 4, 41.

ACKNOWLEDGEMENTS

I would like to thank Dr. J. H. Espenson for his guidance and understanding throughout the course of this work. His dedication to excellence in scientific endeavors has left a lasting impression on me. I am also indebted to all of the service groups which have assisted me throughout the course of this work. The Analytical Service Group (R. Bachman) provided elemental and g.c. analyses. The assistance of W. J. McGranahan in obtaining ^{13}C nmr spectra is also gratefully acknowledged. I would also like to thank Garry Wells and the members of the Research Shop for fabricating numerous instrument replacement parts, often on short notice. I am also grateful to Dr. H. J. Fromm for the loan of the D-132 multi-mixing apparatus. I would also like to thank the many members of the Espenson Research Group, both past and present, who have provided helpful discussions and lasting friendships. I am especially grateful to Dr. A. Bakač who provided many useful ideas. I must also thank Ms. Sue Musselman for an excellent job typing this thesis. Finally, I would like to thank my wife, Deborah, both for typing the rough draft of this thesis and for her love and support over the years. Our daughter, Stephanie, has also been an inspiration to me and a source of much love.